doi: 10.13133/2280-6148/17999 *Journal of Mediterranean Earth Sciences 15 (2023), xx-xx*

Journal of Mediterranean Earth Sciences

How many hominins walked on the slope of the Foresta ignimbrite deposit (Roccamonfina volcano, central Italy)?

Maria Rita Palombo [1,*], Adolfo Panarello [2]

[1] *CNR - IGAG, Istituto di Geologia Ambientale e Geoingegneria, Area della Ricerca di Roma 1, Roma, Italy*
[2] *Laboratorio di Ricerche Storiche e Archeologiche dell'Anticihità, Dipartimento di Scienze Umane, Sociali e della Salute, Università di Cassino e del Lazio Meridionale, Cassino (FR), Italy*
**Corresponding author: mariarita.palombo46@gmail.com*

ABSTRACT - The footprints left by the Palaeolithic hominins at the ca. 350 ka old Foresta "Devil's Trails" ichnosite (Tora-Piccilli, central Italy) are rather variable, even in a single trackway. The peculiar characteristics of the deposit and the acclivity of the soft, slipping slope the hominins were walking on, which forced trackmakers to change pace and walking direction, likely account for this variability. As a result, determining whether the footprints were left by distinct trackmakers, as it would be logical to hypothesize based on the main settings of the trackways, or by a single individual who descended the slope more than once in a short time span, is difficult. To try to answer the question, we have analysed the Foresta/"Devil's Trails" footprint sample by means of various statistical methods with the double aim of quantitatively defining the minimum number of hominin trackmakers who walked on the ignimbrite deposit's slope and scrutinizing to what extent the acclivity of the substrate and the position of each footprint on the slope may affect their dimensions and proportions. The obtained results suggest that four trackmakers (A, B, C, and E) walked on the ignimbrite slope of the deposit. Individuals A, B, and C most likely had similar foot sizes, whereas individual E had larger one. Conversely, more solid data are needed to support the hypothesis that a fifth individual, smaller in size, left the footprints of short sequence D. Furthermore, the results underline how much the coarse, soft, and slippery substrate, along with the slope acclivity, influenced the direction of walking and its changing, the velocity, the length of the stride, the pace stability, and the way in which the foot rests on the substrate slope and, in turn, the shape and size of the footprints. The synergetic action of these factors influenced the footprint proportions, which differ in dimensions even within the same trackway.

Keywords: *Homo*; footprints; pyroclastic substrate; Middle Pleistocene; MIS 10; statistical analyses.

Submitted: 11 February 2023-Accepted: 2 May 2023

1. INTRODUCTION

The human trackways of the Foresta/"Devil's Trails" (F/DT) ichnosite, first reported in 2003 (Mietto et al., 2003) and here analysed, were impressed by hominins walking on a pyroclastic ignimbrite unit (LS7) (Santello, 2010) of the Roccamonfina volcano (Brown Leucitic Tuff, BLT), which deposited during Plinian eruptions of the second period of the stratovolcano activity (385-230 ka) (Fig. 1).

Several ages have been proposed for the emplacement of the BLT formation, mainly ranging from 385 and 325 ka (e.g., Luhr and Giannetti, 1987; Radicati di Brozolo et al., 1988; Ballini et al., 1990 and references therein; Cole et al., 1992, 1993; De Rita and Giordano, 1996; Rouchon et al., 2008; Santello, 2010; Di Vito, 2022 and references therein). The radiometric dating of LS7 [345±6 ka (Scaillet et al., 2008) and 349±3 ka (Santello, 2010)], and LS8 eruptive events, which occurred at most after 3.24 ka the deposition of LS7 (cf. Santello, 2010, p. 67), indicate that humans and other animals left their footprints during a glacial phase (MIS 10, 374-337 ka), shortly before the Termination IV 8 (Cheng et al., 2009).

The surface on which hominins and other mammals left their tracks likely originated from rapid erosional processes that affected the still-soft pyroclastic flow after it had partially filled a pre-existing valley. The exposed surface of about 2,000 m^2 consists of a narrow sub-planar area at the top and a strongly downward-inclined surface

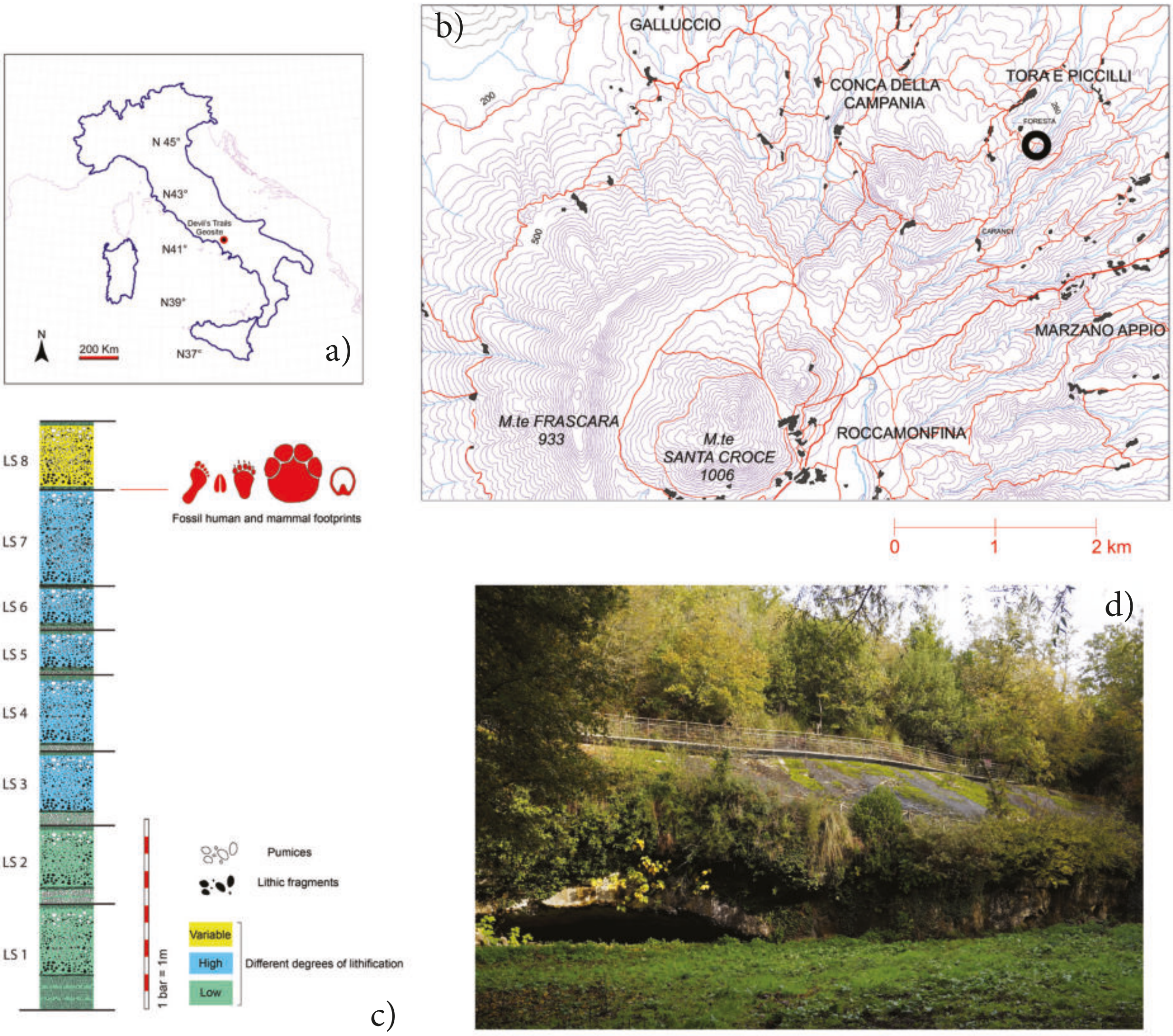

Fig. 1 -The Foresta/"Devil's Trails" ichnosite: a) location; b) geographic map; c) stratigraphic sketch (modified from Santello, 2010); d) south-western view of the trampled slope.

(average slope ~30°, max 80°) (Panarello et al., 2022a, 2022b). The presence of hominin trackways on this slope, as well as the texture and granulometry of the coarse substrate containing about 3-4% of lithic fragments (Santello, 2010), make the F/DT a unique ichnological site. Indeed, most of the hominin footprints known to date open air were impressed on the surface of cineritic deposits, alluvial muddy sediments, or have been found in an aeolian context and rarely on inclined surfaces (e.g., Cape South Coast, South Africa; Helm et al., 2018a, 2018b, 2019a, 2019b).

At the F/DT ichnosite, two different sets of footprints are present. Some are located on the sub-planar surface at the top of the ignimbrite unit LS7 (Figs. 1, 2), while others, which are the only ones analysed in this work, are located on the slope of the ignimbrite deposit (Fig. 3). The arrangement of the numerous bi-directionally oriented footprints impressed on the apical sub-planar surface suggests that hominins walked forth and back time by time in this way. It represents the oldest known prehistoric pathway, more than 50 m long (Panarello, 2016; Panarello and Mietto, 2022 a,b; Panarello et al., 2017 a,b, 2020, 2022a and references therein). From this pathway, two long trackways (Trackway A, which is zeta-shaped, and Trackway B) branch out. Both trackways descend south-eastward along the slope at a minimum distance of about 10.5 m from each other, showing a regular right-to-left succession. A third footprint sequence (Trackway C), also east oriented and divided into two segments by a natural and recent anthropogenic break of the slope, runs along the basal part of the inclined outcrop (Mietto et al., 2003; Avanzini et al., 2008, 2020; Panarello et al., 2017 a,b, 2022a and references therein). A quarry cut in the tuffaceous deposit abruptly interrupted a short sequence, Trackway E, consisting of four west-oriented footprints. Two other couples of footprints were also detected: D01 and D02 (testifying the presence of a trackway then destroyed by a rather recent anthropogenic cut), and F01 and F02,

Fig. 2 - Western view of the prehistoric pathway at the top of the Foresta/"Devil's Trails" ignimbrite deposit slope.

which are close to the long slide of a trackmaker foot (B09 footprint) that characterizes Trackway B (Panarello et al., 2020, 2022 a,b,c,d and references therein). Trackway B is characterised by the presence of a long fossil slip, B09, which has been named following the numbering order of the other footprints, being a step in the regular walking succession created by a long slide of the left foot. Since its length (about 90 cm) largely exceeds that of a footprint, it has been excluded from statistical analyses (Panarello et al., 2022 a,b,c,d).

When humans walked on the ignimbrite flow deposit, the temperature of the substrate had significantly decreased, but it was still soft because the wide circulation of water had soaked the surface in fluids. A neolithization process occurred as the temperature further decreased and was likely completed when the following LS8 pyroclastic unit covered the trampled surface without deforming the tracks and, in turn, permitting their preservation (Santello, 2010).

The soft and slippery substrate and the steepness of the slope affect the direction of walking and its changing, as well as the gait velocity, which influenced stride length, the way in which the foot rests against the substrate slope, and, in turn, the size and morphology of the footprint. As a result, footprints can differ within the same trackway in terms of shape, depth, length, and direction of the steps. Furthermore, it is difficult to establish whether the trackways are penecontemporary or have been left at a short time distance by several individuals, or perhaps by the same individual who descended the slope more than once.

Accordingly, the aim of this research is twofold: i) to quantitatively define the minimum number of hominin trackmakers who walked on the ignimbrite slope deposit; ii) to investigate to what extent the substrate acclivity and the position of each footprint on the slope might have affected the footprint dimensions and proportions.

2. MATERIAL

For the scientific purposes of the present research, we used the last official dimensional and morphometric data published in 2022 (Panarello et al., 2022 a,b,d).

We analysed the footprint morphometry of the three principal trackways (A, B, and C), of the few footprints of the short trackway E, and of the two very short successions of two-step directions of walking D and F. Footprints of the pathway at the top of the slope were excluded from the analysis due to the impossibility of recognizing single trackways as well as taking precise measurements. We analysed the footprints (50), for which it was possible to take both the maximum length and width (Tab. 1) (sample A, including the 23 footprints of Trackway A, the 17 of Trackway B, and the 6 of Trackway C, as well as the footprints D01, E02, E03, and F02), and the sample of the best-preserved traces (21), showing the clearest anatomical features (sample B, including the 9 selected footprints of Trackway A, the 9 ones of Trackway B, and the single selected footprints C05, E03, and F02). For comparison purposes, we also analysed footprints from some Cape South Coast (South African) ichnosites.

3. METHODS

We scrutinized the intra- and inter-trackway variation ranges by means of different statistical analyses [box plots, univariate analysis, bivariate analysis (reduced major axis, RMA), and multivariate analyses (similarity and principal component analysis)] based on the official dimensional and morphometric set of data collected and elaborated by the scientific team working at Foresta ichnosite (cf. Panarello et al., 2023) and published in 2022 (Panarello et al., 2022 a,b,d).

3.1. FOOTPRINT MEASUREMENTS

The F/DT human footprints have been measured and photographed repeatedly at a short distance during several surveys by more than one researcher. The mean value has been retained as the most probable valid measurement. Measurements have been taken using landmarks, which can be easily and quite reliably positioned on the preserved parts of each footprint of F/DT (acropodion, pternion, and most distal points of the lateral and medial metatarsal tubercles), whatever their overall state of preservation (Fig. 4).

We conventionally measured the footprint area (Fa) by

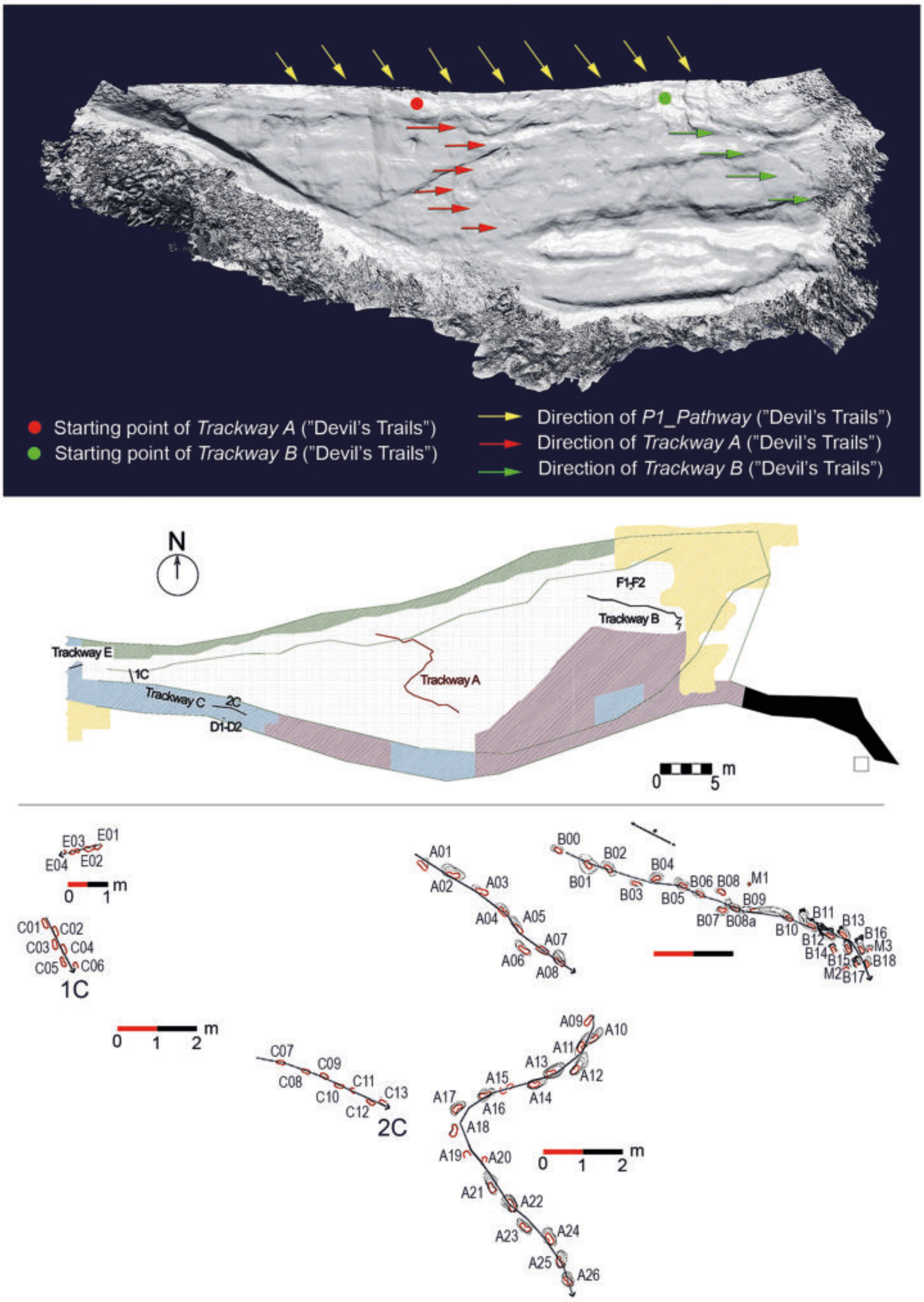

Fig. 3 - General diagram of the Foresta/"Devil's Trails" ichnosite showing the patterns of trackways A, B, C, and E (modified after Panarello et al., 2023).

vectorializing the surface through a geometric polyline never created with less than 40 points, to approximate the actual surface with a percentage that does not affect the last decimal place with respect to the chosen accuracy.

We measured the depth of the footprints in the deepest point of the heel area and in the deeper forefoot area in the following way (Fig. 5):

1) A line parallel to the geographical horizon (HL) has been drawn from the first point of impact of the heel on the slope.

2) The heel depth was measured on the vertical of a plumb line drawn from HL to the deepest point in the heel area.

3) The vertical of a plumb line led from HL to the deepest point of the forefoot area was used to measure the depth to the ball of the foot.

Photogrammetric 3D models, based on detailed footprint images, have been elaborated following Mallison and Wings (2014) by using the software Agisoft Photoscan Pro (version 0.9.0) and then scaled with metal comparators.

Following Falkingham et al. (2018) and Belvedere et

Tab. 1 - Measurements of the hominin footprints impressed on the Foresta/"Devil's Trails" slope of the ignimbrite deposit.

Footprint	Footprint measurements					
	Footprint Length (FI) (mm)	Footprint width (Fw) (mm)	Fw/FI x 100 (Fin)	Footprint area (Fa) (sqmm)	Heel Depth (Hd) (cm)	Ball Depth (Bd) (cm)
A0l-L	25.7	11.1	43.2	240	1.5	3.5
A02-R	25.7	11.2	43.6	229	6.8	6.3
A03-L	24	11.2	46.7	197	2	2.6
A04-R	25.1	11.2	44.6	222	4.4	5.6
A05-L	23.1	10.5	45.4	185	12.6	15.1
A06-R	24.1	10.2	42.3	179	6.8	10.9
A07-L	23	10.3	44.8	173	4	4.4
A08-R	24.5	11.4	46.5	218	26.6	25.5
A09-R	23	10.7	46.5	179	2	7.1
Al0-L	20.9	9	43.1	135	10.7	17.7
A11-R	23.3	10.3	44.2	177	27	29.7
A12-L	22.5	10.4	46.2	184	24.4	25.5
A13-R	23.4	11	47	182	15.7	16.5
A14-L	22.3	11.4	51.1	190	7.3	8.5
A16-L	23.5	11.7	49.8	200	9.4	10.2
A17-R	24.8	11.2	45.2	211	16	16.1
A18-L	24.5	11.5	46.9	217	4.8	7.2
A19R	24.8	-	-	-	4.4	-
A20L	24.5	-	-	-	4.5	-
A21-R	24.5	11.6	46.8	227	18.2	18.6
A22-L	24.7	10.7	43.7	199	11.5	13.5
A23-R	24.5	10.8	44.1	204	9.8	10.9
A24-L	24.5	11.8	47.8	244	15	17.2
A25-R	24.5	11.7	47.7	212	17.4	17.4
A26-L	24.5	10.9	44.5	212	15.2	19.3
B00-L	22	10.3	46.8	197	3.8	4.1
B0l-R	22	11	50	194	3.7	5.7
B02-L	23	10.5	45.6	206	8.7	11.4
B03-R	23	10	43.5	179	4.4	8.5
B04-L	21	l0	47.6	152	4.5	2.8
B05-R	23.2	10.5	45.2	199	12.1	11.6
B06-L	22.5	l0	44.4	173	4.1	5.4
B07-R	23	10.5	45.6	196	4.9	7.8
B0B-L	22	11	50	201	3.5	6.7
B08a-R	22.5	11	48.9	181	19.6	23.2
B09-L	90.1	9.5	-	-	-	-
Bl0-R	21	10.5	50	167	30.2	33
B11-L	23	10	43.5	205	34.5	36
B12-R	23.2	10	43.1	173	15.9	16.4
B13-L	23.1	10.5	45.4	197	18.8	20.6

Tab. 1 - ... Continued

Footprint	Footprint measurements					
	Footprint Length (FI) (mm)	Footprint width (Fw) (mm)	Fw/FI x 100 (Fin)	Footprint area (Fa) (sqmm)	Heel Depth (Hd) (cm)	Ball Depth (Bd) (cm)
B14-R	-	11	-	-	11.8	13
B15-R	23.1	10.6	45.9	162	20.5	22.7
B16-L	23	10.4	45.2	179	23	23.2
B17-R	-	l0	-	-	29.9	-
B18-L	23.1	10.4	45	195	24.3	27
B22-L	-	-	-	-	4.8	-
C05-R	22.6	10.4	46	185	-	-
C07-L	22.6	10.4	46	169	-	-
C08-R	22.1	10.5	47.5	172	7.3	9.3
C09-L	21.4	12	56.1	194	0.1	4.5
Cl0-R	24.6	l0	40.6	194	0.2	2
C11-L	-	l0	-	-	3	7.7
C12-R	24.2	9.5	39.2	176	4.1	8
C13-L	-	l0	-	-	11.5	17.5
001-R	19.3	11.5	59.6	138	3	9.7
002-L	-	12	-	-	2.2	9
E02-L	27	11	40.7	246	-	-
E03-R	27	10.5	38.9	183	12.3	12.8
F02-R	25.9	10.5	40.5	189.5	-	-

al. (2013), depth maps and plans with millimetric level curves have been elaborated using Kitware Paraview software (see Panarello, 2020, 2022; Panarello et al., 2020, 2022 a,b,c,d for data and additional information).

3.2. STATISTICAL ANALYSIS

We analysed the intra-footprint, intra-track, and inter-track relationships among the dimensions of the footprints impressed on the volcanic slope by the Foresta hominins, applying univariate, bivariate, and multivariate statistical analyses to both samples, including all the measured footprints (sample A) and the samples characterised by the most accurate and precise measurements (sample B). We have analysed the dimensional variation ranges considering the four-dimensional variables (i.e., footprints maximum length (Fl), width (Fw), area (Fa), and the ratio of width against maximum length x 100 [(Fw/Fl)x100 in the text, Fin in figures 15-20], as well as the depth of heel (Hd) and ball (Bd)] of all footprints (Sample A) in all trackways and tracks, and in each A, B, and C trackways, and of the best-preserved footprints (Sample B) in all trackways and tracks, and in each A, and B trackways.

Furthermore, we applied the principal component multivariate analysis (PCA) to the human footprints from some Cape South Coast (South African) ichnosites [Brenton-on-Sea, Garden Route National Park, Site 1, Goukamma Tracksite 1, Goukamma Nature Reserve (Tracksite 2) (Helm et al., 2018 a,b, 2019 a,b, 2020 a,b), in which footprints are impressed on inclined aeolian coastal substrates. The explanatory data analysis diagrams (box plots) were used for the visual representation of the dimensional variation in the two sites (Brenton 1 and Goukamma Tracksite 2), counting the richest footprint samples.

Analyses were conducted with the PAST (PAleontological STatistics) 3.16 software (Hammer et al., 2001).

3.2.1. Box Plots

Explanatory data analysis diagrams known as box plots and whisker plots are used to visually represent the distribution of numerical data and its skewness by displaying data quartiles (or percentiles) and medians for the visual representation of variation in the analysed sets of data, as well as to have an effective and easy-to-read statistical summary. A box plot is particularly suitable for comparing distributions because the average value and the overall variation range are immediately clear.

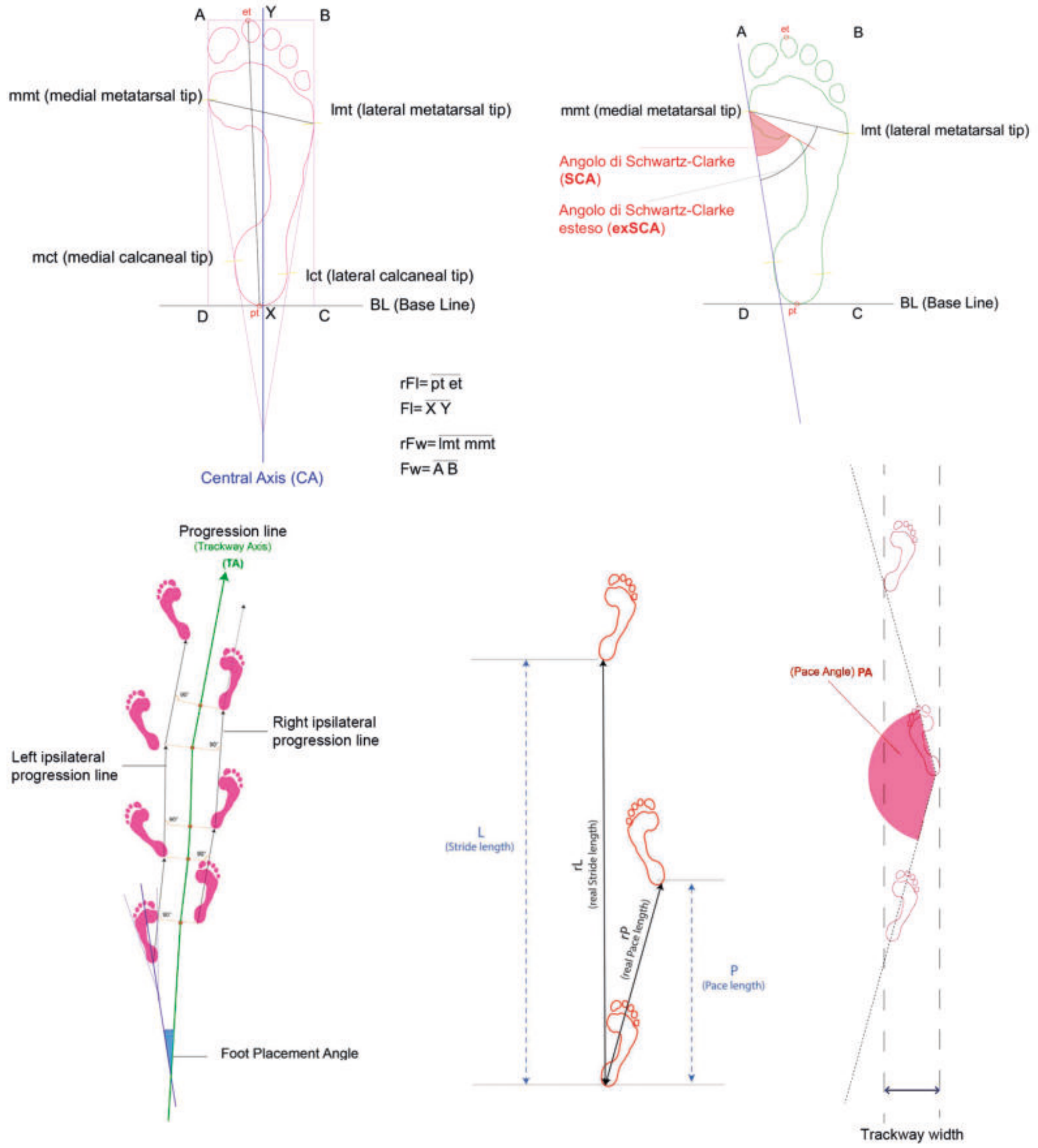

Fig. 4 - Dimensional conventions adopted for the Foresta/"Devil's Trails" human footprints measurements (modified after Panarello et al., 2023).

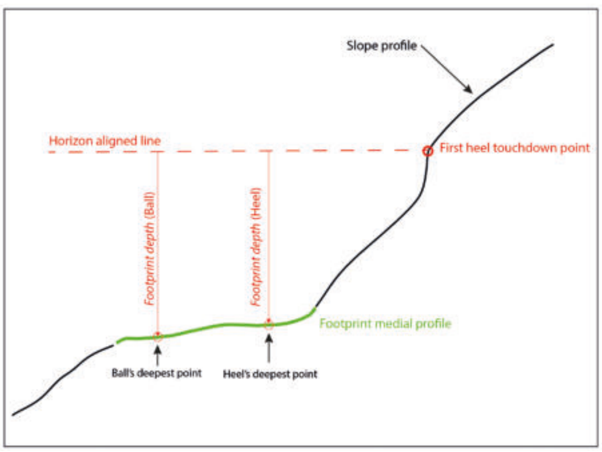

Fig. 5 - A graphic sketch of conventions adopted for measuring footprint depths.

3.2.2. Univariate analysis

We applied four normality tests (Shapiro-Wilk, Anderson-Darling, Lilliefors, and Jarque-Bera tests) to the measurements of the footprints of Trackways A, B (sample A, B), and C (sample A) to verify if the sample was taken from a footprint group with a normal distribution (null hypothesis). Among the applied tests, the Shapiro-Wilk and Anderson-Darling are the most exact, and the Lilliefors and Jarque-Bera are given for reference. A normal distribution is rejected if the given p (normal) is <0.05.

3.2.3. Bivariate analysis

We estimated the relationships between footprint length (dependent variable) and the other footprint parameters (width, area, and length vs. width ratio) (independent variables) by linear bivariate analysis, regressing log-transformed footprint length (dependent/response variable, y-axis) against log-transformed footprint parameters (footprint width, footprint area, and footprint length against footprint width ratio; independent/predictor/explanatory variables, x-axis) of each footprint. We adopted a model II linear bivariate regression (reduced major axis, RMA), which is a common method for handling the problem of natural variability in both x and y, because it tries to reduce the x and y errors by minimizing the sums of squares of the perpendicular distance between each point and the regression line (e.g., Labarbera, 1989; Sokal and Rolf, 1995; Smith, 2009). It is preferable to the least squares method when a considerable variation between the variables is detected, since it is just a ratio of two standard deviations, making no distinction between independent and dependent variables. The RMA method is widely regarded as superior to the MA analysis because it is more likely to produce a significant fit to simulated data samples (e.g., Warton et al., 2006).

The footprint length scales with 'positive allometry' with respect to the focal dependent variable if the allometric exponent AE (slope) is >1, with 'negative allometry' if AE<1, while AE=1 indicates an isometric growth (Huxley and Teissier, 1936). Isometry implies geometric similarity such that no changes in shape with respect to the size occur (Schmidt-Nielsen, 1984).

Estimates of standard errors for slope and intercept imply both a normal distribution of residuals and independence between the variables and the variance of residuals. The RMA fitting, standard error estimation (which assumes a normal distribution of residuals and independence between variables and variance of residuals), slope comparison, and 95%-bootstrapped confidence limits (CIl-CIu = lower and upper limits of the confidence interval) are given for all footprints impressed on the slope following Warton et al. (2006). The r^2 is Pearson's r correlation coefficient squared. The Monte Carlo permutation test (p) on correlation (r^2) uses 9,999 replicates.

Residuals (the distances from each data point to the regression line in the x and y directions) were inspected by means of the Durbin-Watson test for analysing positive autocorrelation and negative autocorrelation of residuals, and the Breusch-Pagan test for verifying the normal distribution and independence between an independent variable and residual variance (homoskedasticity), though log-transformed generally avoids heteroskedasticity.

3.4. MULTIVARIATE ANALYSIS

We evaluated the similarity and differences among footprints by means of clustering (classic cluster analysis) and ordination (principal component analysis-PCA) methods.

3.4.1. Similarity

The hierarchical clustering routine has been successfully used in studies on hominins (e.g., Raichlen et al., 2008) and tetrapod footprints (e.g., Romano and Citton, 2017; Antonelli et al., 2023). We used this method to investigate if the footprint cluster is simply dependent on the putative trackmakers or if any inconsistencies in the footprint clustering might depend on their position on the slope affecting their shape and dimensions.

Cluster analysis is a multivariate technique aimed at grouping cases based on the similarity of their attributes, minimizing the distance within each group, and maximizing the distance between groups. It is commonly used to group a series of samples based on multiple variables (in this case, footprint dimensions) that have been defined for each case (e.g., individual footprints).

We have analysed the clustering of footprints as a whole and on a single trackway by using the unweighted pair-group average method (UPGMA). In UPGMA, the level at which a member (case, i.e., a footprint) joins an existing cluster is based on the average similarity of all the existing members, calculated from the original matrix of coefficients. Each member of a cluster, therefore, has an equal weight at all levels of clustering. Clusters are joined based on the average distance between all the members in the two groups.

3.4.2. Principal Component Analysis

We used PCA as a descriptive and exploratory multivariate technique, being a useful tool for summarising all the information that describes the similarities/differences of a set of cases in a small number of dimensions, regardless of the statistical proprieties of the data (Hammer and Harper, 2006).

According to this method, the positions of cases (footprints) plotted against the two axes (each corresponding to a dimension in space) depict the gradient of greatest variation along the "first" axis and the second largest gradient of variation along the "second" axis. The PCA finds, indeed, new hypothetical variables (linear combinations of the original variables) that account for as much as possible of the variance in multivariate data (e.g., Jolliffe and Cadima, 2016 and references therein). The eigenvalues and eigenvectors of the variance-covariance matrix, or the correlation matrix, are determined with the SVD algorithm, highlighting the factors (variables) that contribute more to join/separate cases (sites) from each other.

This method has frequently been applied also to analysing human footprints (e.g., Hatala, 2014; Citton et al., 2017; Romano and Citton, 2017; Duveau et al., 2018, 2019; Romano et al., 2019; Bennett et al., 2020; Wiseman et al., 2020; Antonelli et al., 2023).

We carried out the Principal Component Analysis (PCA) (a method that maximizes the variance of the projected data) to evaluate the extent of the difference among groups of footprints that belong to each trackway and validate whether the hypothesis that groups of footprints were left by different individuals may be considered or rejected, and whether the position of a footprint on the slope may affect or not affect the extent of its variance.

4. RESULTS

The footprints dimension in the three main trackways' (A, B, and C) are moderately variable within the same track but similar between one track and another, as evidenced by the statistical analyses, while the dimensions of a few footprints in the sequences E and D differ from all the others. Despite the modest dimensional differences and the very small number of footprints E, F, and D, the set of results and the spatial distribution of the footprints suggest that different trackmakers likely walked on the ignimbrite slope deposit, though some probably had a similar foot size, as detailed in the following paragraphs.

4.1. STATISTICAL ANALYSIS

The footprints of trackways A, B, and C are rather similar in length, ranging from 20.9 mm (A09) to 25.7 mm (A01 and A02), with a small difference even within a single trackway. The width variation range is proportionally larger, ranging from 9 mm (A10) to 12 mm (C09) (Tab. 1). As a result, it is not immediate to decide if the three trackways were left by three distinct individuals, as the trackway positions would suggest, or whether they were left by a single individual who walked down the slope several times in a short period of time. We used different statistical methods to answer the question, and to verify to what extent the variations in the dimensions and proportions were influenced by the depth, and in turn by the gait and the position of the foot on the slope.

For a comparative purpose, we conducted PCA on the human footprints from the selected Cape South Coast ichnosites mentioned above and use box plots for the visual representation of size ranges at the richest footprint samples from Brenton 1 and Goukamma Tracksite 2.

4.1.1. Footprint depth

The obtained results show, on the one hand, the significant dissimilarity of footprint depth from one point to another of the slope (Tabs. 1, 2) and, on the other hand, the good correlation of the depth variation shown by heel and ball (Fig. 6). The heel and ball depth vary from a few centimetres, or even millimetres (e.g., A01, A03, A09, C09, and C10 footprints) to about 35 cm (B11) and from 2 cm (C10) to 36 cm (B11), respectively. However, there is a clear prevalence of shallow footprints, as supported by the depth mean (average heel depth = 11.58 cm; average ball depth =13.52 cm), as well as by the values moderately positive of the skewness, indicating that the curve, likely mesokurtic, is right short-tailed. The value of both variation coefficients confirms (heel coefficient = 75.82; ball coefficient = 63.73) is, indeed, much higher not only than 20 (the maximum value for an acceptable standard deviation to the mean), but also than 30, the maximum value to be considered acceptable for a normal data distribution (see e.g., Sheret, 1984; Hammer and Harper, 2005; Mahmoudvand and Hassani, 2009; Shechtman, 2013; Aronhimae et al., 2014; Pélabon et al., 2020 and references therein for a discussion) (Tab. 2).

Tab. 2 - Summary of the univariate analysis statistics' data obtained for the heel and ball of all (samples A) and the best-preserved (Sample B) measured footprints impressed on the Foresta/"Devil's Trails" slope of the ignimbrite deposit.

UNIVARIATE STATISTICS

	Sample A (all footprints)		Sample B (selected footprints)	
	Heel Depth	Ball Depth	Heel Depth	Ball Depth
N	46	46	19	19
Min	0.1	2	4.4	7.2
Max	34.5	36	34.5	36
Sum	532.6	621.7	305.2	332.3
Mean	11.57826	13.51522	16.06316	17.48947
Std. error	1.294354	1.269938	1.776853	1,684985
Variance	77.06618	74.18621	59.9869	53.94433
Stand. dev	8.778735	8.613142	7.745121	7.34468
Median	9.6	11.15	15.9	17.2
25 prcntil	4.1	6.6	11.5	11.6
75 prcntil	17.6	18.775	20.5	22.7
Skewness	0.7677272	0.7815928	0.4790999	0.7358159
Kurtosis	-0.2463639	-0.1048331	0.4772112	0.7470654
Geom. mean	7.55287	10.79536	14.03923	16.04349
Coeff. Var.	75.82084	63.72921	48.21668	41.99486

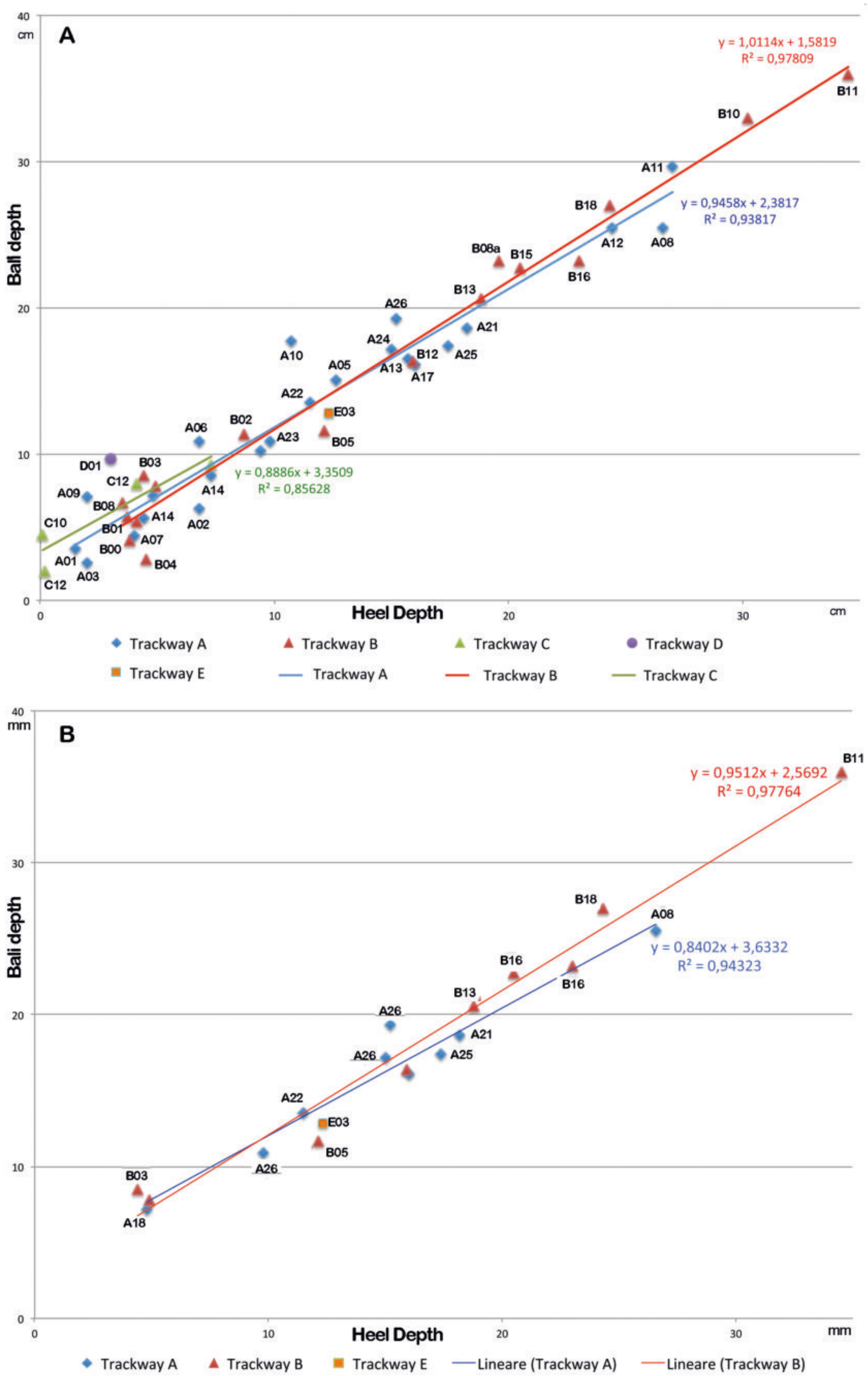

Fig. 6 - Scatter diagram of heel and ball depths of all the measured footprints impressed on the ignimbrite slope surface at the Foresta/"Devil's Trails" ichnosite.

The correlation between heel and ball depth is quite high in the Trackway A footprints (r^2=0.9382), though among the deepest and longest footprints, the heel is deeper than the ball in the A11 one that was impressed during a foot slip and a forward imbalance of body weight. The opposite occurs in the A08 footprint, located at the uppermost part of the slope. Among the medium-length footprints, the heel is deeper than the ball in the A10 footprint, consistently with its position on the slope, which caused the trackmaker's foot to slip forward toward a first lateral and then medial direction. The two less deep and smaller footprints (A01 and A03) are located both in the sub-planar part of the trackway as well as they are the A0, A06, and A05, which are longer and from shallow to medium deep (Fig. 6) (Panarello et al., 2022a). The correlation between footprint length (Fl) and depth, therefore, seems to be only partly conditioned by the footprint position on the trackway.

The heel and ball depths of Trackway B footprints have the maximum correlation value (r^2=0.9781), which is highest in the deepest footprints (B11, B10, and B18) and decreases in the shallowest ones (B00, B01, B03, B07, and B08). Among the latter footprints, there are not only the footprints of the first part of the trackway (B00 and B01, and B03 and B04, which are characterised by a heel deeper than the ball and vice versa, respectively) but also the B07 and B08 footprints. The latter is a footprint marking the beginning of the trackmaker sliding (B09), documented by footprints B10-B11, which are, respectively, the longest and deepest, but with a well-correlated depth of heel and ball (Fig. 6) (Panarello, 2020; Panarello et al., 2022 a,b).

On average, the fluctuation in the depth of the A, B, and C trackways is roughly consistent with the position of the footprints along the trackway and with the trackmaker's gait at that point. Consequently, the depth variability is high (coefficient of variation > 30) even analysing the best-preserved footprints, which show thin anatomical features (Sample B) (Fig. 6). The curve is still right short-tailed but weakly leptokurtic, with a clear prevalence of medium-high depth values, as also indicated by the average values of the heel (16.03 cm) and ball depth (17.49 cm) (Tab. 2). The correlation between heel and ball depth of the footprints of Trackway B (r^2=0.9776) is similar to that obtained for all the Trackway B footprints (Sample A), whereas that of the footprints of Trackway A is a little higher (Fig. 6).

All things considered, the analysis of footprint depth suggests some correlation between heel and ball depth and an occasional correlation between footprint depth and Fl. However, the correlation is always extremely low when the heel and ball depths of each footprint are compared with their length (Fl) and width (Fw) (Figs. 7, 8). Moreover, Fl and Fw have an extremely low correlation (Fig. 9), and their value varies even within the same trackway, regardless of the footprint depth, which can vary significantly even in the case of footprints with very similar Fl and/or Fw.

4.1.2. Footprint dimensions

We analysed the footprint dimension pattern of the four trackways (A, B, C, and E) and of the D and F short series by means of different statistical methods with the double aim of identifying the principal variation factors affecting the observed variations and of objectively confirming the trackmaker minimum number.

4.1.2.1. Box plots

In the box plot obtained considering the 50 footprints for which both the footprints' maximum length (Fl) and width (Fw) and derived values [footprint ara (Fa) and ratio of width against maximum length (Fw/Fl)] were available (Sample A), the length and width of most of the footprints fall within the box of the 25-75% quartiles (Fig. 10a). The main exceptions are the following: the Fl in footprints E02 and E03 (oriented in a direction almost opposite to that of other trackways A, B, and C), and the Fw of footprint A09. In the E02 and E03 footprints, the Fl value is close to the upper inner fence, which corresponds to the data point with a maximum value of less than 1.5 times the box height; the Fw of footprint A09 (a poorly definite footprint located after a Trackway A hiatus), an outliner with a value inferior to 1.5 times the box height; and the Fw and even more Fl of footprint D01, both with values inferior to 1.5 times the box height (lower inner fence).

The footprint distribution is less uniform in the box plot of Fw/Fl, where the footprints C09 and D01 fall well above the upper inner fence, having respectively a value of more than 1.5 and 3 times the height of the box. The variation range reduces, as expected, in Sample B (Fig. 10b), particularly as regards the footprint width, whereas the Fl of most footprints equally divides into two groups, one with a value close to the maximum value of the third quartile, the other to the minimum value of the second quartile. The F02 footprint matches the upper inner fence, whereas the E03 footprint is 1, 5, and 3 times the height of the box. Conversely, the Fw/Fl value of F02 matches that of the lower inner fence, and that of E03 is lower than 1.5 times the box height. In the Fa box plot, the only outliner is E02, with a value slightly higher than the upper inner fence, whereas the values of A24 and B15 match those of the upper and lower inner fences, respectively.

In terms of the box plots obtained for the footprints of each trackway, those obtained for all Trackway A footprints show a very narrow variation range for Fl and especially Fw, whereas A10 falls clearly below the lower inner fence. The range increases in the Fw/Fl box, where the value of the outliner A51 is higher than that of the upper inner fence, and even more in the Fa box plot, where, however, no outliners are present (Fig. 11a). The Fa values are quite variable, also considering only the best-preserved footprints (Fig. 11b), whereas the variation ranges of Fl and Fw are minimal, suggesting that Fl and Fw are not strictly correlated in most trackway A footprints. The box plots obtained for all (Fig. 12a) and the best-preserved footprints (Fig. 12b) of Trackway B provides similar results. The Fa box plot shows the

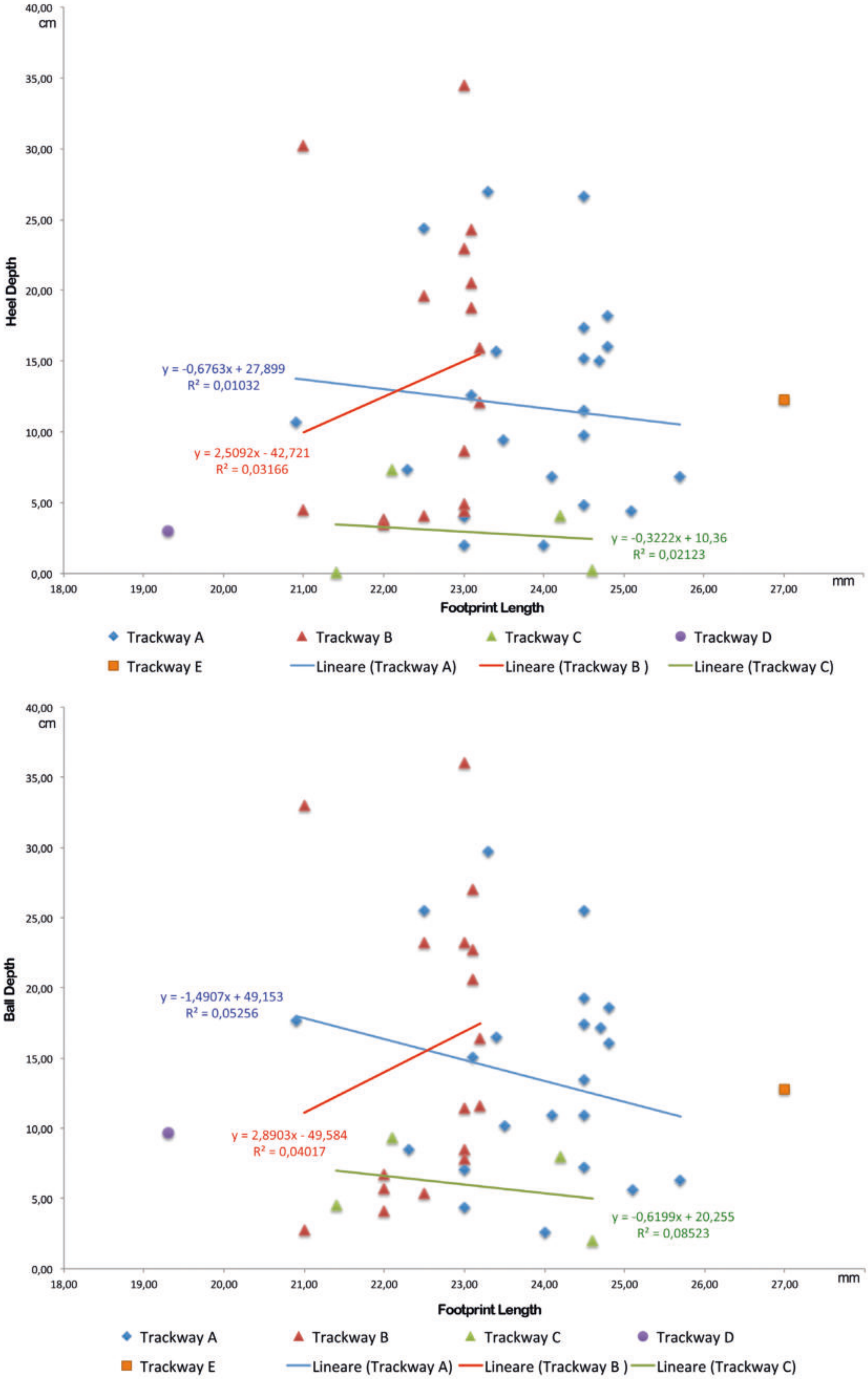

Fig. 7 - Scatter diagram of the heel (above) and ball (below) depth against the footprint lengthin all the measured footprints impressed on the ignimbrite slope surface at the Foresta/"Devil's Trails" ichnosite.

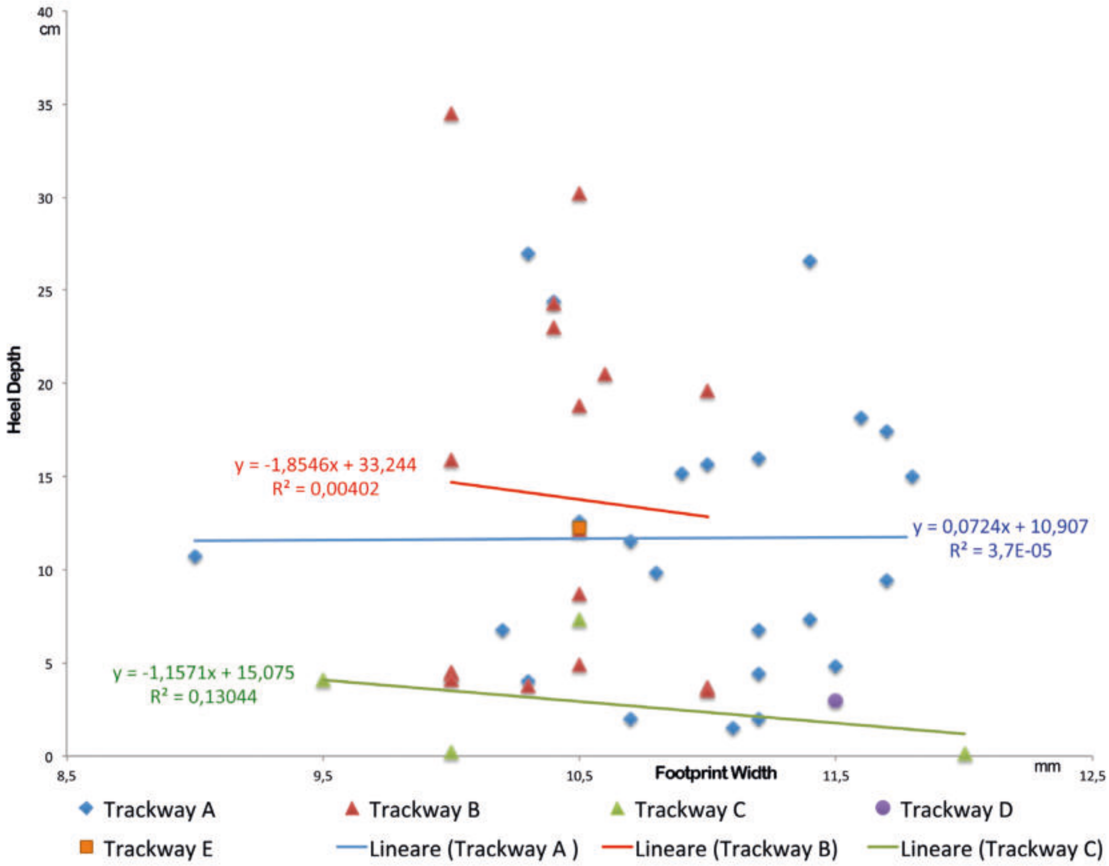

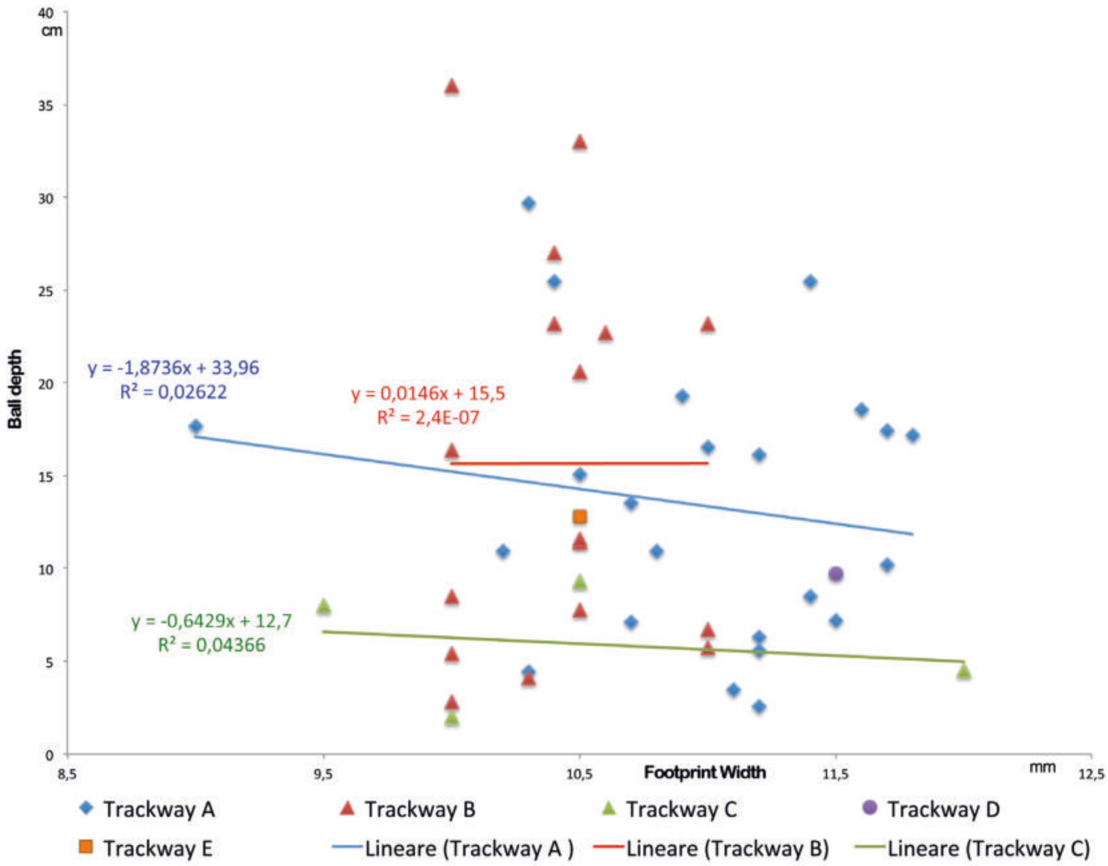

Fig. 8 - Scatter diagram of the heel (above) and ball depth against the footprint width (below) in all the measured footprints impressed on the ignimbrite slope surface at the Foresta/"Devil's Trails" ichnosite.

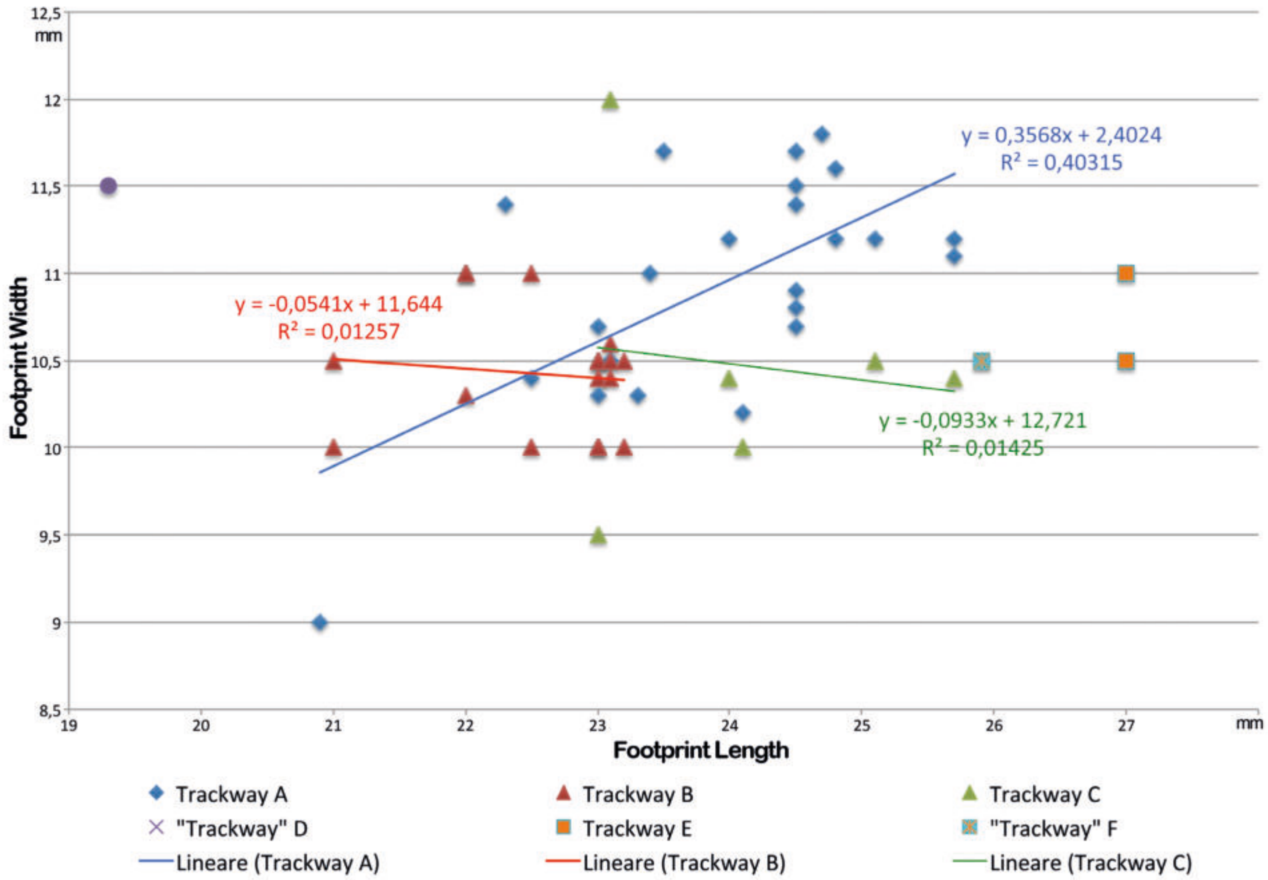

Fig. 9 - Scatter diagram of the length and width of all the measured footprints impressed on the surface of the ignimbrite deposit slope at the Foresta/"Devil's Trails" ichnosite.

largest variation range among the box plots obtained for the dimensions of the few measurable footprints of Trackway C, but the footprint values fall within the 25-75% quartiles, except for C09, whose value matches that of the lower inner fence (Fig. 13). The C09 footprint is confirmed to be proportionally larger than the others, with a value that matches that of the upper inner fence in both the Fw and Fw/Fl box plots (Fig. 10).

4.1.2.2. Univariate analysis

The summary of statistical data highlights the quite restricted range of variation in each of the three trackways A, B, and C. The variation further reduces in the case of sample B, with the average values of the measured dimensions (Fl, Fw, Fa, and Fw/Fl) of trackways A, B, and C being rather similar. The average footprint length, for instance, ranges from 23.95 mm (Trackway A) to 22.57 mm (Trackway B) in sample A and from 24.59 mm (Trackway A) to 23.08 mm (Trackway B), whereas the two measured footprints of sequence E have a length (27 mm) greater than the maximum value of all other footprints (Tabs. 1, 3).

The obtained variation coefficient confirms the moderate variability of footprint dimensions. It is, indeed, always lower than 20, and reaches the maximum values of 12.35 and 13.06 in the case of all footprints' (sample A) Fa of Trackway A and Fw/Fl of Trackway C, respectively (Tab. 3). The values of kurtosis indicate some prevalence of normocurtic or slightly platicurtic distribution of data for most footprint dimensions, with the exception of the leptocurtic distribution shown by Fw/Fl in all footprint samples A and B and by Fw and Fa and Fw and Fw/Fl in the footprint samples of Trackway A and Trackway C, respectively. Most sample skewness values are less than 1 or greater than -1, indicating only moderate if not negligible asymmetry of the Gaussian curves. In particular, the distribution of Fl, Fw, and Fa values of the entire measurable footprints of samples A and B is quasi-symmetric, whereas Fw/Fw values show a moderately positive (1.247) and negative (-1.194) asymmetric distribution in the samples A and B, respectively. Examining the footprints of each trackway, values that are high if compared to the average footprint dimensions (positive asymmetry) are shown by Fl and Fa of Trackway A (sample B), but FL values are moderately tailed to the left, whereas all the footprints of the trackway are analysed (sample A), as it occurs for sample A of the Trackway B footprints. Finally, the Fw value distribution of the totality of Trackway C footprints is right-tailed.

The p values <0.05 resulting in some normality tests

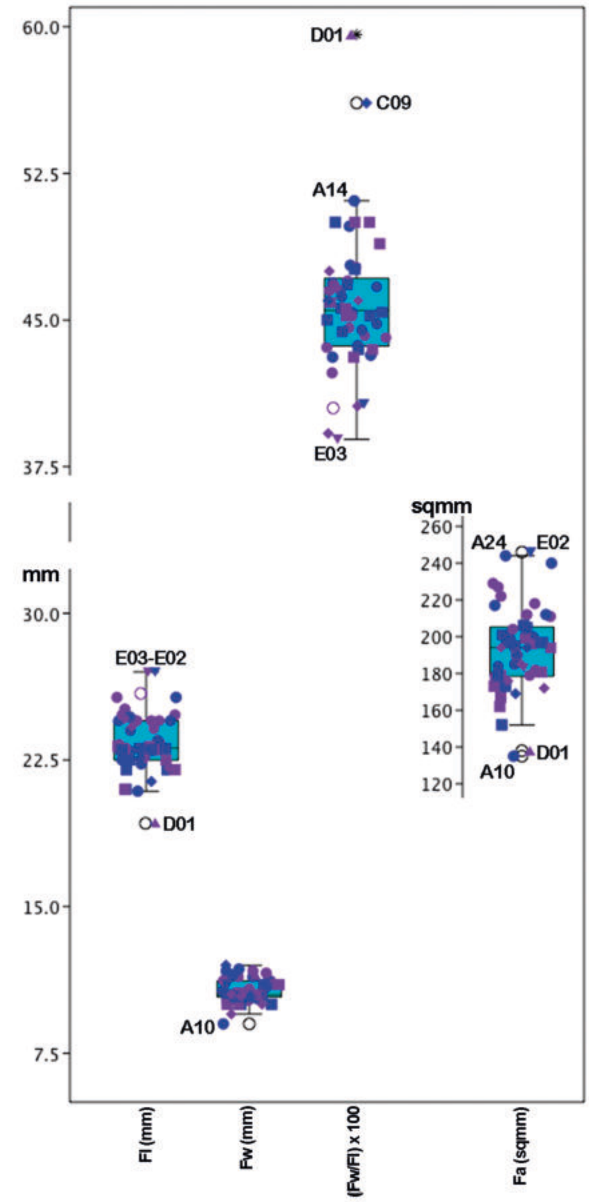

Fig. 10a - Box plot illustrating the variation range of all the measured footprints (Sample A) impressed on the surface of the slope of the ignimbrite deposit at the Foresta/"Devil's Trails" ichnosite.Fl = footprint length; Fw = footprint width; Fa = area. Blue = left footprint; Violet = right footprints; Dot = Trackway A; Fill square = Trackway B; Fill diamond = Trackway C; Fill triangle = Trackway D; Fill inverted triangle = Trackway E; Circle = F footprints.

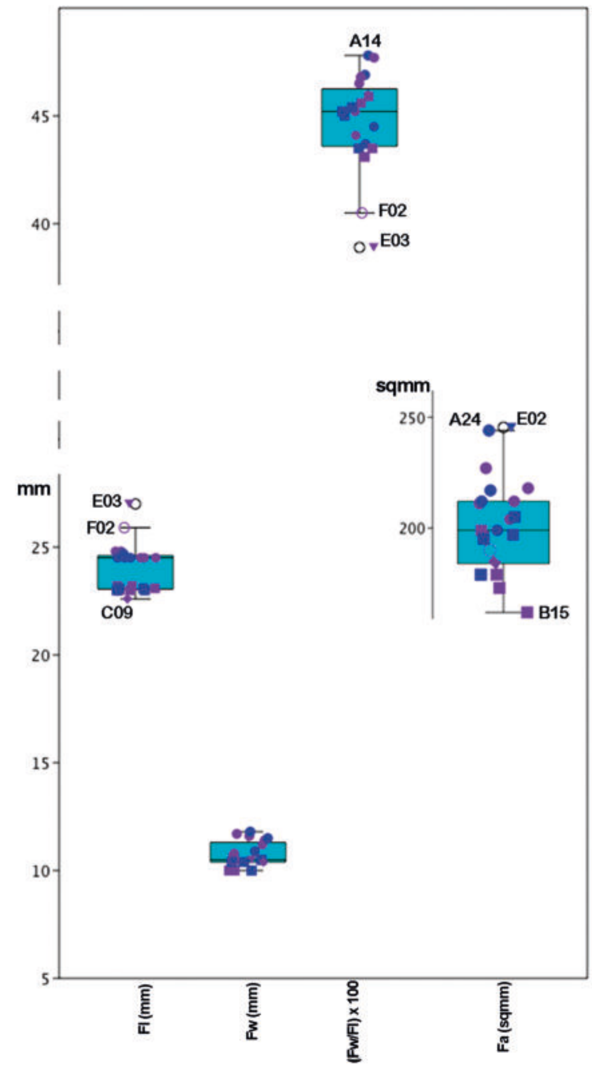

Fig. 10b - Box plot illustrating the variation range of the best-preserved footprints (Sample B) impressed on the surface of the slope of the ignimbrite depositat the Foresta/"Devil's Trails" ichnosite. Abbreviations and symbols as in figure 10a.

(Tab. 4) imply some departures from the data normal distribution, especially as regards to FL of selected footprints (sample B) of Trackway A and to both Fl and Fa of all (sample A) and selected footprints (sample B) of Trackway B. Conversely, the dimensions of Trackway C footprints show a normal distribution.

All things considered, the results of univariate statistical analysis hint at a more random distribution of the footprint dimension in Trackway B than in the other trackways, despite the fact their dimensional ranges are comparable to or inferior to those of Trackways A and C.

4.1.2.3. Bivariate analysis

The reduced major axis (RMA) bivariate linear regression was used to investigate how much the footprint length (FI) (dependent variable) might depend on the other independent variables [footprint width (Fw), area (Fa), and the ratio of Fl against Fw x 100]. The two sets of analysed data, respectively, include all the footprints for which it was possible to measure the four variables considered for the analysis (Sample A) and some selected footprints that allowed sound measurements (Sample B). The sample size ranges from a maximum of 50 (all the measured footprints) to a minimum of 6 cases (all the measured footprints from Trackway C) (Tab. 5, Tab. SI1).

The confidence interval (CI) for slopes is large in the first set of data (Tab. 5). The difference between upper (CIu) and lower (CIl) values ranged from 3.1933 (footprint Fa of Trackway C) to 0.1469 (footprint Fa of Trackway A) (average value of the CIu-CIi interval =

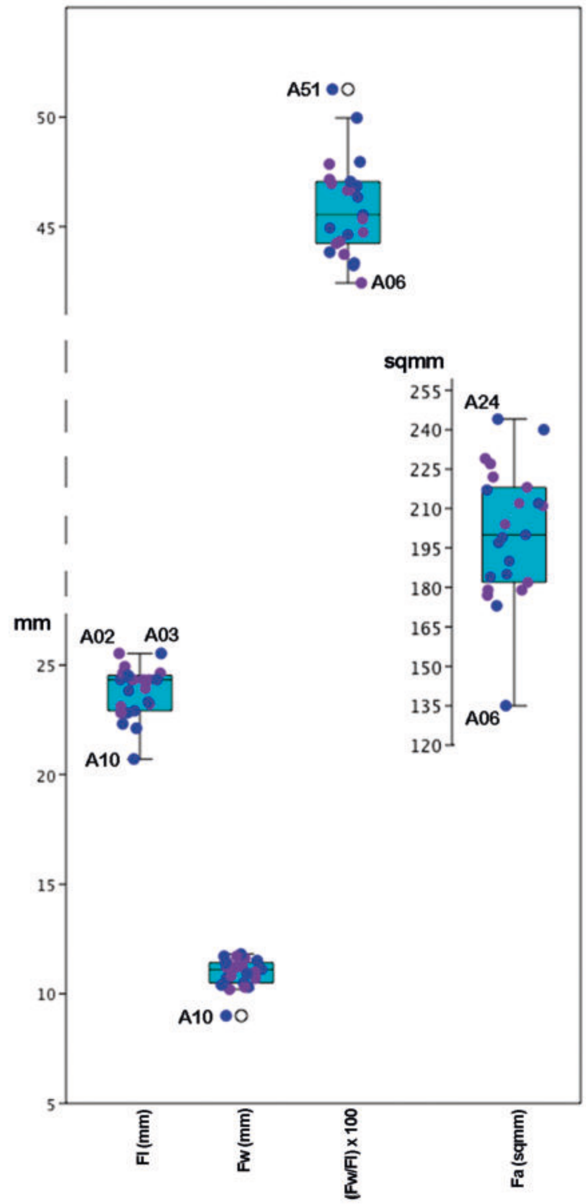

Fig. 11a - Box plot illustrating the variation range in all the measured footprints (Sample A) impressed in the Trackway A on surface of the slope of the ignimbrite deposit at the Foresta/"Devil's Trails" ichnosite. Abbreviations and symbols as in figure 10a.

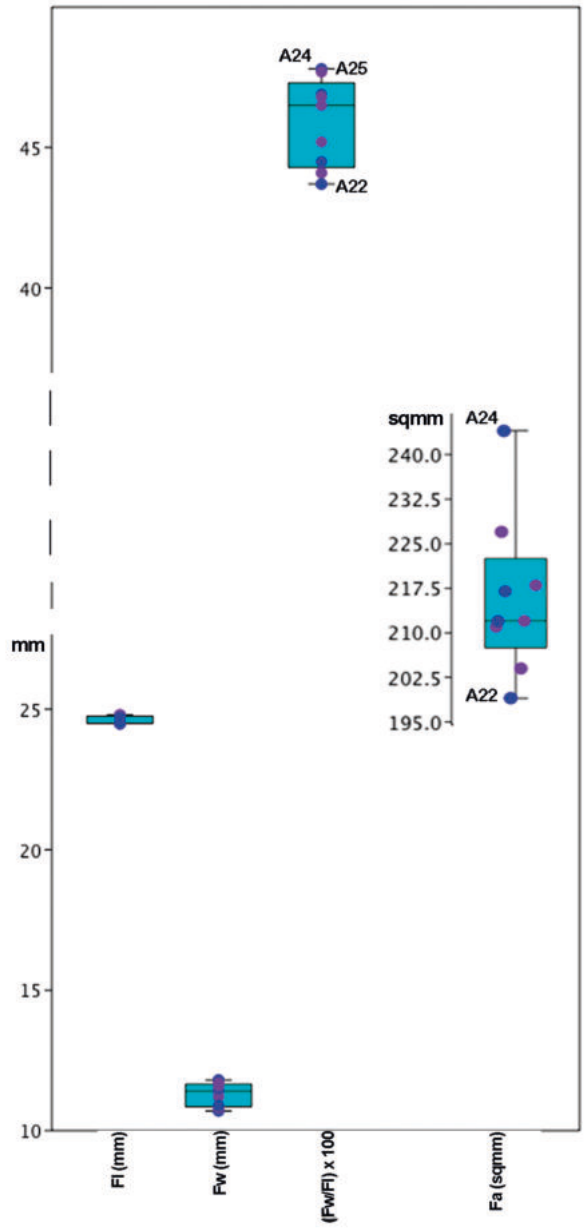

Fig. 11b - Box plot illustrating the variation range in the best-preserved footprints (Sample B) impressed in the Trackway A on the surface of the slope of the ignimbrite deposit at the Foresta/"Devil's Trails" ichnosite. Abbreviations and symbols as in figure 10a.

1.4004). The interval values of Fl of all footprints (2.9649) and Trackway A (2.9208) are also particularly high. In the second set of data (Tab. 5), the confidence intervals (CI) for slopes reduce, ranging from 2.3402 (all footprint Fw/Fl) to 0.1515 (Fa of trackway B footprints), with an average value of 0.7731.

The p-value, which tests the null hypothesis of no correlation and no association between the changes in the independent variable and the shifts in the dependent variable, is <0.05 for most of the independent variables in sample A, with the exception of Fw of all ($p=0.2979$) and Trackway B ($p=0.7017$) footprints, and Fa of Trackway B (0.0781) and Trackway C ($p=0.871$). Conversely, in sample B the p value is >0.05, with an exception given for the Fl of all footprints (0.0233). Moreover, r^2, which explains the extent to which the variance of a variable is related to that of a second variable, is generally low or extremely low in both samples, with exceptions given for Fa (0.7837) and Fw/Fl (0.7837) of all footprints of Trackway A, and Fw (0.7319) and Fw/Fl (0.8995) of all footprints of Trackway C (Tab. 5).

The Breusch-Pagan test provides some support for the robustness of our bivariate analysis. The test results rejected non-stationary variance of residuals nearly for all independent variables in the RMA of both samples. The only exception is Fw/Fl of all footprints (Sample A) for which the test gives a p-value <0.05 (Tab. SI2).

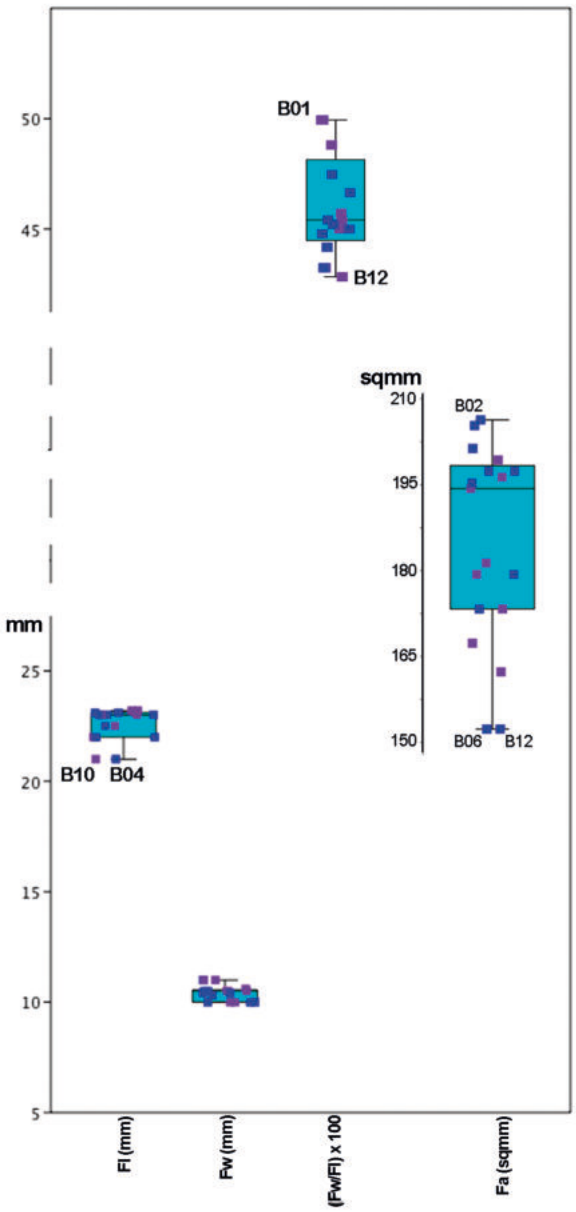

Fig. 12a - Box plot illustrating the variation range of all the measured footprints (Sample A) impressed in the trackway B on the surface of the slope of the ignimbrite deposit at the Foresta/"Devil's Trails" ichnosite. Abbreviations and symbols as in figure 10a.

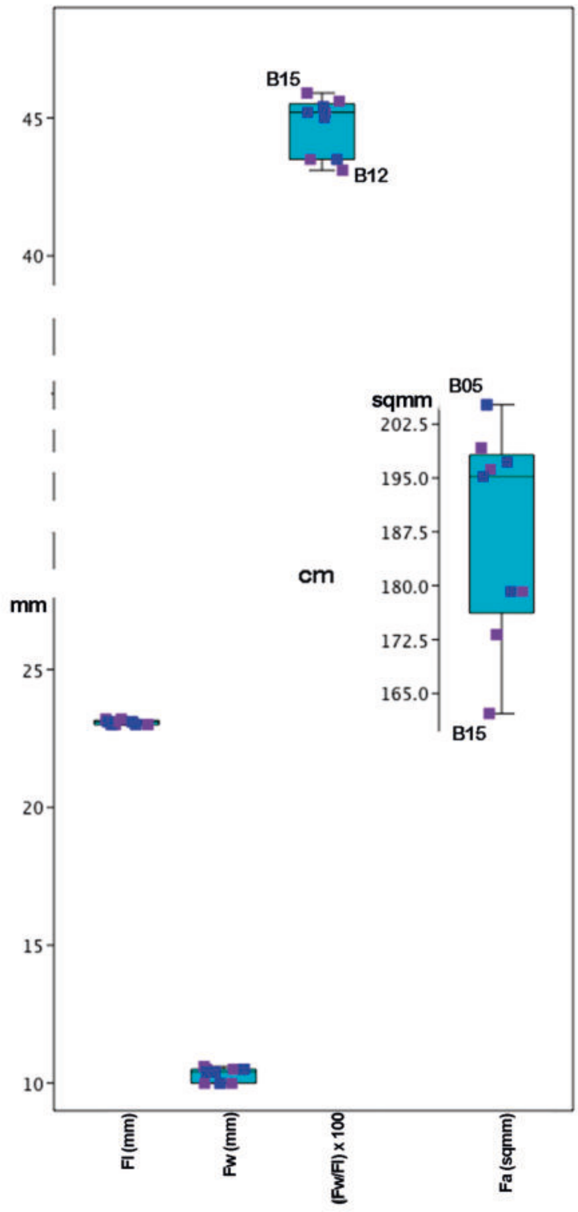

Fig. 12b - Box plot illustrating the variation range of the best-preserved footprints (Sample B) impressed in the trackway B on the surface of the slope of the ignimbrite deposit at the Foresta/"Devil's Trails" ichnosite. Abbreviations and symbols as in figure 10a.

Therefore, the hypothesis of heteroskedasticity (i.e., a non-stationary variance of residuals) could be rejected and homoskedasticity assumed in both samples for all other independent variables. For these variables, the variance of the residuals is equal over the range of measured values, suggesting a normal distribution of residuals.

The Durbin-Waston test for autocorrelation in residuals indicates that for most of the independent variables, there is a moderately positive correlation with the dependent variable (Fl) in the statistical regression analysis of Sample A data, where the test statistic varies from 1.0831 (Fw/Fl of all footprints) to 1.4815 (Fw of all footprints). Fa footprints of Trackway A (2.1468), Fw footprints of Trackway B (2.1119), and Fa footprints of Trackway C (2.3579) show, however, a negative autocorrelation. In general, the p-value was >0.05, except for the Fw and FW/Fl of all footprints, and Trackway A Fl.

The statistic test for Sample B indicates a negative correlation for the independent variables of Trackways A and B footprints, whereas the correlation is positive when the variables of all the selected footprints are analysed. Moreover, the p-value is > 0.05 for the latter variable, but >0.05 in the case of Fw/Fl for all selected footprints.

Overall, the bivariate analysis results indicate a random variation in footprint length and width, which could be due to the synergistic action of the various factors that influenced the trackmakers, who walked with a variable

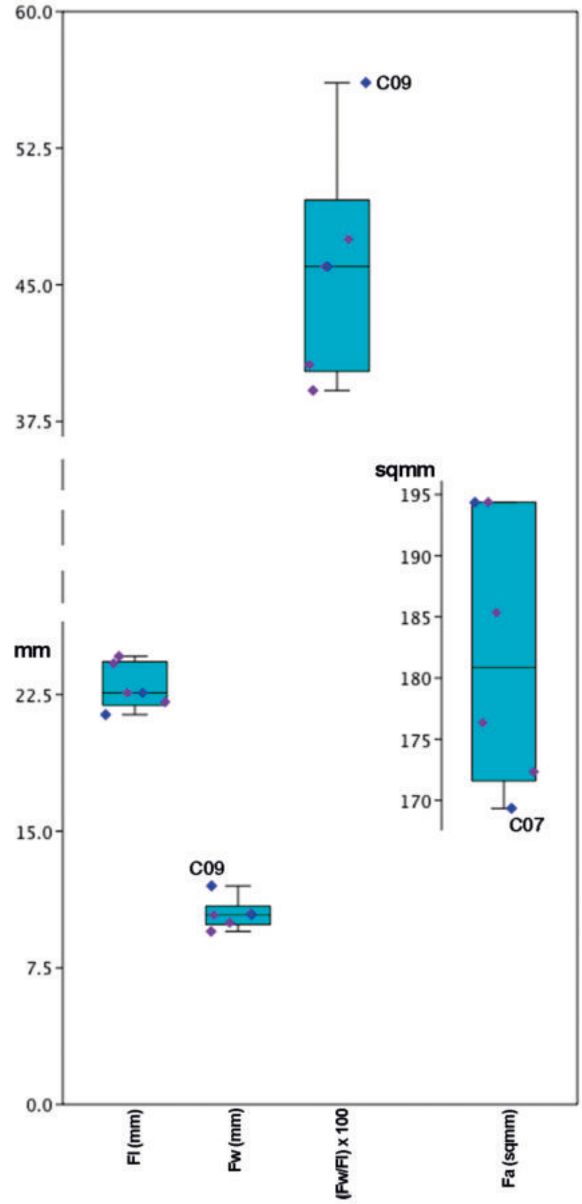

Fig. 13 - Box plot illustrating the variation range of all the measured footprints (Sample A) impressed in the Trackway C on the surface of the slope of the ignimbrite deposit at the Foresta/"Devil's Trails" palaeoichnosite. Abbreviations and symbols as in figure 10a.

velocity, changing direction time by time as they moved down the slope.

4.1.2.4. Similarity analysis

Results obtained by the clustering analysis on the one hand highlight the difficulty of defining groups of footprints sharing similar size and proportions and, in turn, of separating the footprints of each trackway from the others. On the other hand, the results confirm some slight differences in the footprint proportion belonging to the same trackway. These differences likely mainly depend on the ways in which trackmakers place the foot on the different points of the slope and on the load exerted on the uneven ground, and its variable granulometry. Footprints E02 and E03, the only measurable of the short E sequences, however, generally form a cluster clearly separated from the others. The single F02 footprint sometimes clusters together or close to E02 and E03, whereas the single D01 footprints rarely fall in large clusters.

Unravelling the different trackways is easier when only the footprint of Sample B, whose preservation status permitted measurements more compelling than those of footprints showing less clear anatomical details, is analysed. When only the basic dimensions Fl and Fw are considered and the data derived from them (Fa e Fw/Fl) are excluded, the separation into two clusters, trackways A and B, is rather well-defined. In this case, the value of the cophenetic correlation coefficient (CCC) is significantly higher than the lower value of the CCC in other dendrograms, whereas the distance among groups is reduced.

In the analysis of the whole measured footprints (Sample A) obtained by using all the variables (Fl, Fw, Fa, and Fw/Fl) (Fig. 14a), the footprints setting is mainly unrelated to their belonging to one or another trackway. The value of CCC is quite lower (0.788) as well as the similarity among the main clusters, whereas it is significantly higher among the minor groups. The groups that are the furthest apart are those of E03 and E02 footprints in cluster B, which are separated in an outgroup-like fashion.

In the dendrogram resulting from the analysis of the Sample B footprints (Fig. 14b), most of footprints of the A and B trackways gather in separate groups, though the CCC value is still low (0.7636). A1.1 only includes Trackway A footprints, whereas A1.2 primarily includes the Trackway B footprints. Some Trackway B footprints fall in the A2 cluster together with A24 and F02, setting separately from the others. The isolated position of E03 is confirmed.

The results obtained for the Sample A footprints by removing Fw and Fl from the analysis (Fig. 15a), are roughly similar to the previous one, but CCC is moderately higher (0.793), and in the main cluster A, a few Trackway A footprints fall in the group A2 that is clearly separated from the large group A1, which encompasses all the other footprints. Once again, E02 and E03 form a distinct cluster, B, to which also F02 joins. The main difference between the dendrograms resulting from the analysis of Sample B footprints using all four variables (Fig. 15b) and using only three variables (Fl, Fw, and Fa) (Fig. 14b) is the setting of A244 and F02 that gather together in sister group relation, A2.2 of the group, A.21, which includes some Trackway B footprints as well as C05, the only of Trackway C selected for the analysis.

The footprints in the dendrogram obtained for the Sample A footprints using the variables Fl, Fw, and Fw/Fl (Fig. 16a) are mostly randomly distributed in the various groups of the largest cluster A, whereas E03 and E02 are grouped together in cluster B. Contrary to the previous dendrograms, F02 falls in group A.1.1 of cluster A. The results obtained seem to suggest a limited correlation between Fl and Fw variations in some less preserved

Tab. 3 - Summary of the univariate analysis statistics' data obtained for the samples A (all the measured footprints) and B (best-preserved footprints) impressed of the Foresta/"Devil's Trails" slope of the ignimbrite deposit and in each main trackway (trackways A, B, and C).

UNIVARIATE STATISTICS

Sample A (all the measured footprints)					Sample B (best-preserved footprints)				
All Footprints	Footprint Length	Footprint width	Footprint area	Lengh against Width ratio	All Footprints	Footprint Length	Footprint width	Footprint area	Lengh against Width ratio
N	50	50	50	50	N	21	21	21	21
Min	19.3	9	135	38.9	Min	22.6	10	162	38.9
Max	27	12	246	59.6	Max	27	11.8	244	47.8
Sum	1171.3	535.3	9618.5	2292.5	Sum	504.5	225.9	4186.5	941
Mean	23.426	10.706	192.37	45.85	Mean	24.02381	10.75714	199.3571	44.80952
Std. error	0.2157627	0.08677487	3.360661	0.5201432	Std. error	0.2465867	0.1227796	4.211823	0.4736839
Variance	2.327678	0.3764939	5.647021	1.352745	Variance	1.276905	0.3165714	3.725286	4.711905
Stand. dev	1.525673	0.613591	23.76346	3.677968	Stand. dev	1.130002	0.5626468	19.301	2.170692
Median	23.1	10.5	194	45.5	Median	24.5	10.5	199	45.2
25 prcntil	22.5	10375	178.5	43.675	25 prcntil	23.05	10.4	184	43.6
75 prcntil	24.5	11.2	205.25	47.125	75 prcntil	24.6	11.3	212	46.25
Skewness	0.0719521	-0.08107937	0.08404799	1.246	Skewness	0.9267267	0.5611684	0.2476553	-1194277
Kurtosis	0.5649397	0.171182	0.462491	3.846	Kurtosis	0.7872371	-0.7797774	0.2594083	1898636
Geom. mean	23.37716	10.68864	190.9094	45.7124	Geom. mean	2399909	1074335	1984709	4475748
Coeff. var	6.512	5.731	12.353	8.021	Coeff. var	4.703676	5.230448	9.681619	4.844265
Trackway A	Footprint Length	Footprint width	Footprint area	Lengh against Width ratio	Trackway A	Footprint Length	Footprint width	Footprint area	Lengh against Width ratio
N	23	23	23	23	N	9	9	9	9
Min	20.9	9	135	42.3	Min	24.5	10.7	199	43.7
Max	25.7	11.8	244	51.1	Max	24.8	11.8	244	47.8
Sum	550.9	251.8	4616	1051.7	Sum	221.3	101.6	1944	413.2
Mean	23.95217	10.94783	20.06957	45.72609	Mean	24.58889	11.28889	216	45.91111
Std. error	0.2388932	0.1342332	5240627	0.4507884	Std. error	0.04547418	0.1358558	4409586	0.5210685
Variance	1312609	0.4144269	6316759	4673834	Variance	0.01861111	0.1661111	175	2443611
Stand. dev	1145691	0.64376	2513316	2161905	Stand. dev	0.1364225	0.4075673	1322876	1563205
Median	24.5	11.1	200	45.4	Median	24.5	11.4	212	46.5
25 prcntil	23.1	10.5	182	44.1	25 prcntil	24.5	10.85	207.5	44.3
75 prcntil	24.7	11.4	218	46.9	75 prcntil	24.75	11.65	222.5	47.3
Skewness	-0.7968577	-1207619	-0.4667217	0.6987684	Skewness	1.011219	-0.3244872	1.138383	-0.23488
Kurtosis	0.8235094	2365487	0.6873681	0.4566072	Kurtosis	-1.133091	-1.091812	1.854589	-1.720532
Geom. mean	23.92527	10.9288	199.098	45.67806	Geom. mean	24.58855	11.28231	.	45.88735
Coeff. var	4.783246	5.880254	12.52302	4.727947	Coeff. var	0.5548138	3.61034	6.124424	3.404852
Trackway B	Footprint Length	Footprint width	Footprint area	Lengh against Width ratio	Trackway B	Footprint Length	Footprint width	Foot print area	Lengh against Width ratio
N	17	17	17	17	N	9	9	9	9
Min	21	10	152	43.1	Min	23	10	162	43.1
Max	23.2	11	206	50	Max	23.2	10.6	205	45.9
Sum	383.7	177.2	3156	785.7	Sum	207.7	92.9	1685	402.4
Mean	22.57059	10.42353	185.6471	46.21765	Mean	23.07778	10.32222	1872222	44.71111
Std. error	0.1765196	0.08511645	3.926663	0.5598211	Std. error	0.02777778	0.08296214	4803869	0.3489844
Variance	0.5297059	0.1231618	262.1176	5.327794	Variance	0.006944444	0.06194444	2076944	10.96111
Stand. dev	0.727809	0.3509441	16.19005	2.308201	Stand. dev	0.08333333	0.2488864	1441161	1.046953

Tab. 3 -... Continued

Sample A (all the measured footprints)					Sample B (best-preserved footprints)				
All Footprints	Footprint Length	Footprint width	Footprint area	Lengh against Width ratio	All Footprints	Footprint Length	Footprint width	Footprint area	Lengh against Width ratio
Trackway B	Footprint Length	Footprint width	Footprint area	Lengh against Width ratio	Trackway B	Footprint Length	Footprint width	Foot print area	Lengh against Width ratio
Median	23	10.5	194	45.6	Median	23.1	10.4	195	45.2
25 prcntil	22	10	173	44.7	25 prcntil	23	10	176	43.5
75 prcntil	23.1	10.55	198	48.25	75 prcntil	23.15	10.5	198	45.5
Skewness	-1.280016	0.3288698	-0.5911545	0.5936057	Skewness	0.5005714	-0.6373	-0.5745038	-0.6676454
Kurtosis	0.6295855	-0.69387	-0.7047984	-0.8045287	Kurtosis	-1.68395	-1.68395	-0.8915777	-1.4482
Geom. mean	22.55926	10.418	184.9581	46.16425	Geom. mean	23.07764	10.31953	1867159	44.70012
Coeff. var	3.22459	3.366845	8.720875	4.994199	Coeff. var	0.3610977	2.411171	7697595	2.341595
Trackway C	Footprint Length	Footprint width	Footprint area	Lengh against Width ratio					
N	6	6	6	6					
Min	21.4	9.5	169	39.2					
Max	24.6	12	194	56.1					
Sum	137.5	62.8	1090	275.4					
Mean	22.91667	10.46667	181.6667	45.9					
Std. error	0.5049202	0.342215	4.477102	2.446767					
Variance	1.529667	0.7026667	120.2667	35.92					
Stand. dev	1.236797	0.8382521	10.96662	5.99333					
Median	22.6	10.4	180.5	46					
25 prcntil	21.925	9.875	171.25	40.25					
75 prcntil	24.3	10.875	194	49.65					
Skewness	0.4418692	1.324025	0.1527514	0.8579499					
Kurtosis	-1.314453	2.892181	-2.286171	1.147444					
Geom. mean	22.88911	10.43983	181.3916	45.58592					
Coeff. var	5.396932	8.008779	6.036669	13.05736					
E	Footprint Length	Footprint width	Footprint area	Lengh against Width ratio					
N	2	2	2	2					
Min	27	10.5	183	38.9					
Max	27	11	246	40.7					
Sum	54	21.5	429	79.6					
Mean	27	10.75	214.5	39.8					
Std. error	0	0.25	31.5	0.9					
Variance	0	0.125	1984.5	1.62					
Stand. dev	0	0.3535534	44.54773	1.272792					
Median	27	10.75	214.5	39.8					
25 prcntil	27	10.5	183	38.9					
75 prcntil	27	11	246	40.7					
Skewness	0	0	0	0					
Kurtosis	0	-2.75	-2.75	-2.75					
Geom. mean	27	10.74709	212.1745	39.78982					
Coeff. var	0	3.288869	20.76817	3.19797					

footprints. The hypothesis is at least partially supported by the clustering of Sample B footprints (Fig. 16b). In the dendrogram, indeed, the footprints of Trackway A gather together, falling into the two separate groups A2 and A.1.1.1. The latter is the sister group of A.1.1.2, which included most of the Trackway-B footprints as well as C05. The other footprints of Trackway B are moderately similar to the previous ones and form the small A.1.2 group inside A1.1, whereas E03 and F02 are set separately in cluster B. Moreover, the CCC value (0.9063) is rather high.

In a last attempt to explore if, and to what extent, the footprint cluster may depend on the trackmaker's autopodiun anatomy or be randomly distributed because their position on the slope diversely affected their shape and dimensions, we performed the analysis using only the two basic footprint dimensions Fl and Fa as variables. In the dendrogram obtained for the Sample A footprints (Fig. 17a), the similarity among groups is high, and the footprint distribution is reasonably coherent with their belonging to Trackway A and B, though some departures are present, such as the presence of two groups, including respectively B04 plus B01, and A10, A02, and A01, in the sub-cluster A2. The large A1 sub-cluster is divided into two groups: A.1.1, mainly including Trackway A footprints together with C10 and C12, and the larger group A.1.2, including the majority of Trackway B footprints as well as a few footprints of Trackway A and the other footprints of Trackway C, except for C09, which falls in the group B2 of the cluster B together with E03 and E02, as well as F02 and D01, forming the group B1. When the cases analysed are limited to the Sample B footprints (Fig. 17b), the split of the footprints of Trackway A and B into two sub-clusters, A1 and A2, respectively, is clear, the similarity among groups increases, and CCC reaches its maximum value (0.9063). The footprint C09 falls in the cluster of Trackway B footprints, but in a separate ramus within the group A1.1, whereas E03 and F02 fall together, forming cluster B, sharply distinct from the main cluster A that includes all other footprints.

Tab. 4 - Normality Test data resulting from the analysis of the samples A (all the measured footprints) and B (best-preserved footprints) impressed on all the Foresta/"Devil's Trails" slope of the ignimbrite deposit and in each main trackway (trackways A, B, and C).

TESTS FOR NORMAL DISTRIBUTION

Sample A (all the measured footprints)					Sample B (best-preserved footprints)				
Trackway A	Footprint Length	Footprint width	Footprint area	Lengh against Width ratio	Trackway A	Footprint Length	Footprint width	Footprint area	Lengh against Width ratio
N	23	23	23	23	N	9	9	9	9
Shapiro-Wilk W	0.9373	0.912	0.9654	0.9542	Shapiro-Wilk W	0.6602	0.9215	0.916	0.9061
p(normal)	0.1569	0.04492	0.5814	0.3561	p(normal)	0.0004856	0.4052	0.3604	0.2895
Anderson-Darling A	0.5764	0.4837	0.2536	0.3564	Anderson-Darling A	1.486	0.3158	0.3961	0.3738
p(normal)	0.1185	0.2069	0.7016	0.4265	p(normal)	0.0003085	0.4706	0.2915	0.3336
p(Monte Carlo)	0.1341	0.2092	0.7284	0.4345	p(Monte Carlo)	0.0001	0.5018	0.3199	0.3568
Lilliefors L	0.2055	0.1306	0.09388	0.1039	Lilliefors L	0.4093	0.1633	0.2177	0.2024
p(normal)	0.013	0.3816	0.8635	0.7426	p(normal)	0.0001	0.6931	0.2482	0.3525
p(Monte Carlo)	0.012	0.3778	0.8657	0.7416	p(Monte Carlo)	0.0001	0.6977	0.262	0.3502
Jarque-Bera JB	2.279	7.424	0.8122	1.644	Jarque-Bera JB	1.56	0.8712	1.375	0.9038
p(normal)	0.32	0.02443	0.6663	0.4396	p(normal)	0.4584	0.6469	0.5028	0.6364
p(Monte Carlo)	0.1114	0.0189	0.5399	0.2035	p(Monte Carlo)	0.0921	0.3174	0.1156	0.2857
Trackway B	Footprint Length	Footprint width	Foot print area	Lengh against Width ratio	Trackway B	Footprint Length	Footprint width	Foot print area	Lengh against Width ratio
N	17	17	17	17	N	9	9	9	9
Shapiro-Wilk W	0.7798	0.866	0.9194	0.8942	Shapiro-Wilk W	0.8084	0.7856	0.912	0.8467
p(normal)	0.001085	0.01897	0.1441	0.05434	p(normal)	0.02543	0.01395	0.3303	0.06849
Anderson-Darling A	1.517	0.8401	0.583	0.6915	Anderson-Darling A	0.7416	0.9115	0.4391	0.6925
p(normal)	0.000422	0.02383	0.1107	0.0579	p(normal)	0.03345	0.01146	0.2235	0.0456
p(Monte Carlo)	0.0003	0.0229	0.1093	0.0556	p(Monte Carlo)	0.0342	0.0117	0.2324	0.0462
Lilliefors L	0.3106	0.1804	0.2265	0.2018	Lilliefors L	0.2691	0.2893	0.2608	0.2754
p(normal)	0.0001	0.1439	0.02059	0.0616	p(normal)	0.05697	0.02892	0.07414	0.04643
p(Monte Carlo)	0.0001	0.1447	0.0212	0.0654	p(Monte Carlo)	0.0584	0.031	0.0718	0.0482
Jarque-Bera JB	3.851	0.7524	1.328	1.425	Jarque-Bera JB	0.8602	1.241	0.7647	1.149
p(normal)	0.1458	0.6865	0.5149	0.4903	p(normal)	0.6504	0.5378	0.6822	0.563
p(Monte Carlo)	0.0408	0.5365	0.2382	0.2026	p(Monte Carlo)	0.3218	0.1494	0.4116	0.1582
Trackway C	Footprint Length	Footprint width	Foot print area	Lengh against Width ratio					
N	6	6	6	6					
Shapiro-Wilk W	0.9161	0.8695	0.8831	0.9127					
p(normal)	0.4777	0.2241	0.2836	0.4544					
Anderson-Darling A	0.3289	0.4873	0.3421	0.3379					
p(normal)	0.3813	0.1326	0.3505	0.36					
p(Monte Carlo)	0.4201	0.1402	0.3925	0.3937					
Lilliefors L	0.2677	0.3175	0.203	0.2281					
p(normal)	0.1964	0.05647	0.6121	0.4234					
p(Monte Carlo)	0.2035	0.059	0.6093	0.4361					
Jarque-Bera JB	0.5317	0.9395	0.6856	0.4463					
p(normal)	0.7665	0.6252	0.7098	0.8					
p(Monte Carlo)	0.5626	0.139	0.3429	0.6711					

All results considered, the similarity analysis points out on the one hand a significant similarity in the dimension pattern of the footprints of the trackways A, B, and C and, on the other hand, the peculiarity of the measurable footprints of the short Trackway E, as well as of the footprints F01 and F02, though to a much lesser degree.

4.1.2.5 Principal Component Analysis

We ran the PCA first on the total footprint dataset (Sample A) and then on the dataset of the most compelling footprint measurements (Sample B). For each dataset, the PCA was computed first using all the variables (Fl, Fw, Fa, Fin) (Figs. 18, 21), then excluding Fin (Figs. 19, 22), and afterward using the Fl, Fw, and Fin variables (Figs. 20, 23).

The PCA results obtained from the total dataset (Sample A) by using the three different groups of variables (Figs.

Tab. 5 - Summary of intraspecific bivariate allometry of the samples A (all the measured footprints) and B (best-preserved footprints) impressed on all the Foresta/"Devil's Trails" slope of the ignimbrite deposit and in each main trackway (trackways A, B, and C). AE = allometric exponent; CIl = lower value in the 95% bootstrapped confidence interval (N=1999); CIu = upper value in the 95% bootstrapped confidence interval (N=1999); r^2 = determination coefficient; p = predictive value (testing the null hypothesis of no correlation and no association between the independent changes and dependent variables shifts).

Reduced Major Axis (RMA)

SAMPLE A	Independent Variable	Slope (AE)	Std. Error	95% Cil	95% Ciu	Intercept (AC)	Std. error	95% Cil	95% Ciu	r2	p	Allometry
All footprints	Footprint width	1.1528	0.16454	0.82285	3.7878	0.41185	0.39032	-5.8424	1.201	0.022097	0.2979	P
	Footprint area	0.5049	0.043471	0.43069	0.57754	0.49624	0.22814	0.10762	0.88456	0.64418	0.0001	N
	Footprint Length against Footprint Width ratio	-0.81611	0.0827	-0.93723	-0.61631	6.2715	0.3169	5.5039	6.7422	0.50711	0.0001	N
Trackway A	Footprint width	0.79878	0.13131	0.46864	0.95594	1.2647	0.31412	0.88857	2.0525	0.43253	0.0017	N
	Footprint area	0.36937	0.03841	0.2622	0.43975	1.2195	0.20306	0.84373	1.794	0.78373	0.0001	N
	Footprint Length against Footprint Width ratio	-1.0263	0.22809	-3.6635	-0.78603	7.0963	0.87237	0.84373	1.794	0.78373	0.0001	N
Trackway B	Footprint width	-0.98022	0.25178	-3.482	-0.56122	5.4133	0.59015	4.4386	11.275	0.010348	0.7017	N
	Footprint area	0.3662	0.085221	0.24868	1.084	1.2045	0.44495	-2.5524	1.8163	0.18763	0.0781	N
	Footprint Length against Footprint Width ratio	-0.66568	0.11613	-0.95881	-0.34158	5.6672	0.44507	4.432	6.7823	0.5435	0.001	N
Trackway C	Footprint width	-0.68983	0.17859	-1.0233	0.81454	4.7487	0.41907	1.2421	5.5551	0.7319	0.0126	N
	Footprint area	0.88969	0.4437	-0.0057296	3.1876	-1.4963	2.3077	-1.3493	3.2083	0.0051294	0.871	N (I)
	Footprint Length against Footprint Width ratio	-0.42099	0.066743	-0.58058	-0.15959	4.7387	0.25503	3.7471	5.3623	0.89946	0.0054	N
SAMPLE B	Independent Variable	Slope (AE)	Std. Error	95% Cil	95% Ciu	Intercept (AC)	Std. error	95% Cil	95% Ciu	r2	p	Allometry
All footprints	Footprint width	0.89389	0.17957	0.37559	1.209	0.45847	0.18522	-0.13813	0.98482	0.23323	0.0233	N (I)
	Footprint area	0.47767	0.10242	0.23347	1.5749	0.65082	0.54196	-5.1896	1.9337	0.12658	0.1077	N
	Footprint Length against Footprint Width ratio	-0.92637	0.19258	-3.0914	-0.7512	6,.6994	0.73214	6.0425	14.971	0.17885	0.0535	N
Trackway A	Footprint width	0.15254	0.053289	0.059607	0.53379	2.8326	0.12915	1.9074	3.0562	0.14573	0.3099	N
	Footprint area	0.092524	0.029991	-0.018946	0.34601	2.7051	0.16117	1.348	3.2996	0.26452	0.1618	N
	Footprint Length against Footprint Width ratio	0.162	0.059183	0.068054	0.58691	2.5824	0.22646	0.95372	2.9452	0.065719	0.4905	N
Trackway B	Footprint width	0.14873	0.055602	0.02532	0.5006	2.7917	0.12979	1.9683	3.0832	0.021636	0.7248	N
	Footprint area	-0.045899	0.017192	-0.17122	-0.019714	3.3789	0.08992	3.2404	4.0387	0.017941	0.7298	N
	Footprint Length against Footprint Width ratio	-0.15313	0.057873	-0.53912	-0.080895	3.7207	0.21992	3.4461	5.1882	0.00013839	0.9767	N

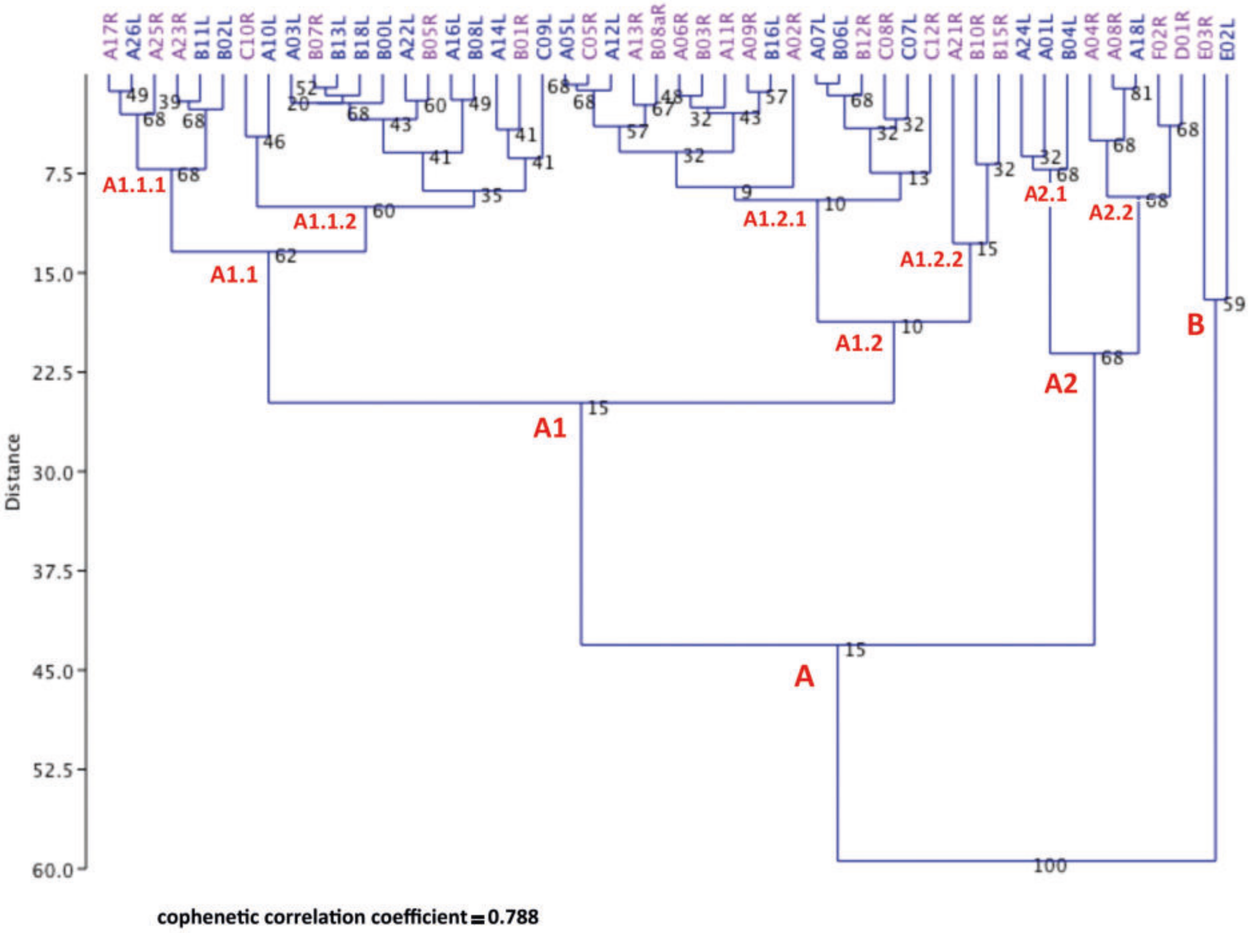

Fig. 14a - Q-mode dendrogram showing how all footprints (Sample A) impressed on the F Foresta/"Devil's Trails" slope of the ignimbrite deposit cluster using the dimensional Fl, Fw, Fa, and Fw/Fl variables.
Fl = Footprint length; Fw = Footprint width; Fa = Footprint Area; Fw/Fl = (Footprint length against footprinf width) x 100.

18, 19, and 20; Tables SI3, and SI4 in Supplementary Information), highlight an overlapping of scores of the trackways A, B, and C, with those of trackway A and B showing the main similarity in score dispersion, though the dispersion area of the Trackway B footprints indicates they are on average slightly smaller than those of Trackway A. Moreover, scores of some footprints (e.g., A01, A10, A14, A24, B04, B10, C09, C10, and C12) fall quite far from the other of the same sample. The single D01 footprint score and those of the short E and F sequences generally fall outside the variation ranges of trackway footprints. The eigenvalue and the variance percentage captured by the first component (PC1) are definitely greater than those of the second component (PC2), and in turn, the variance of axis 1 is greater than it is on axis 2 in the PCA obtained by using the first two groups of variables, whereas those of PC2 are greater than those of PCI considering the Fl, Fw, and Fin variables (Table SI4). The eigenvalue and percentage of variance captured by the other components are always negligible.

More in detail, in the PCA biplot obtained for Sample A using all variables (Fl, Fw, Fa, and Fin) (Fig. 18), the variance accumulated by PC1 (which accounts for as much as possible of the variability in the data) and PC2, reaches 95.512% and 2.3986%, respectively. As a result, the sum of the variances of the two components nearly equals the total variance, and PC1 is sufficient to describe the essence of the data. In PC1, Fa is the variable that contributes the most to PC1, as evidenced by its large and positive loading (Tab. SI4). Fin is the variable that has the major effect on PC2, followed by Fl. Fin and Fl correlate with PC2 positively and negatively, respectively. Therefore, the variable loading could suggest that the proportion of footprints has some influence in determining the position of scores in the PCA biplot. The orientation and length of the vectors, corresponding to the loading of each variable, show that an increase in the Fa variable influences where scores plot in the space, with smaller footprints distributed on the left of axis 2. Fin, with a vector is significantly away from the axis origin, and, subordinately, Fw variables influence their position in the quadrants above axis 1, where the scores of the proportionally narrower footprints plot, whereas Fl influences the position where the longer and wider

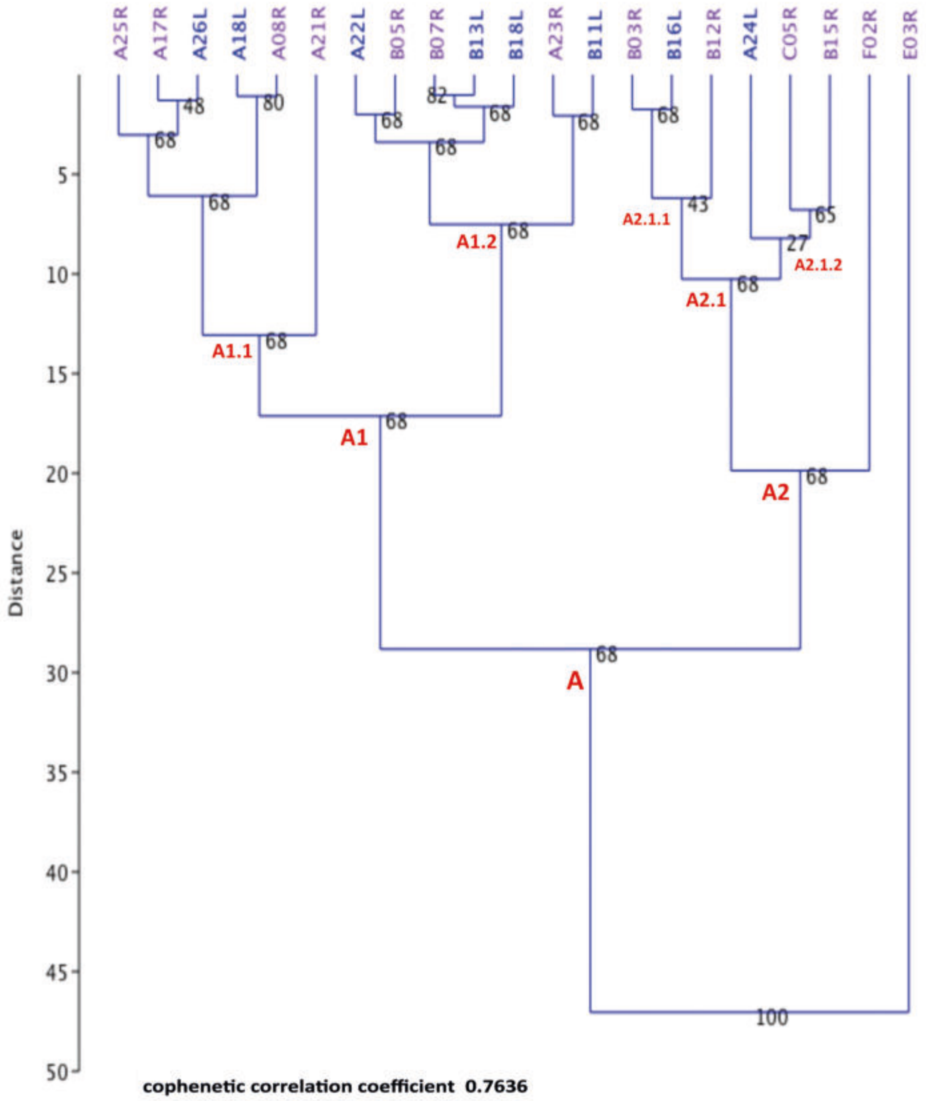

Fig. 14b - Q-mode dendrogram showing how the best-preserved footprints (Sample B) impressed on the Foresta/"Devil's Trails" slope of the ignimbrite deposit cluster using the dimensional Fl, Fw, Fa, and Fw/Fl variables. Abbreviations as in figure 14a.

footprint scores plot in the quadrants below axis 1. Fin and Fw vectors strongly correlate with each other and negatively correlate with Fl, whereas Fa slightly positively and negatively correlates with Fin and Fw, and Fl, respectively. The scores' position in the PCA biplot (Fig. 18) suggests that the D01 footprint is the shortest, but the proportionally largest despite its small area, and E03 footprint is the longest and narrowest. In the Trackway A footprint sample, the position of the A10 score, which plots far from the others, likely depends on the anomalous proportions of the footprint (oval, with the sole medio-laterally inclined towards the slope bottom) that are opposite to that of the A24, which is deep and well-defined. The scores of Trackway B footprints plot closer to axis 2 than Trackway A scores, mainly falling in the quadrants on the left of the axis, as it happens for the scores of Trackway C footprints, except for the shortest and widest C09 score and C10 and C12 that are the lengthiest and narrowest of the sample.

In the PCA biplot resulting from the analysis of the variables Fl, Fw, and Fa (Fig. 19), PC1 largely describes the essence of the data, almost corresponding to the total variance (99.75%), whereas the variance accumulated by PC2 and PC3 is insignificant. The variable loadings in PC1 are all positive, but Fa is the variable that contributes the most to this component, as evidenced by its large loading (Tab. SI4). Its loading is, on the other hand, extremely low and negative in PC2, where the variable with the greatest effect on the total variance is Fl, followed by the relatively low loading of Fw. Therefore, the variable loading could suggest that the footprint length, partially affecting their area value, has a rather significant effect in determining the position of scores in this PCA biplot. This hypothesis is supported by the length and orientation of the notable length of the Fl vector, which negatively correlates with Fw, which rests in

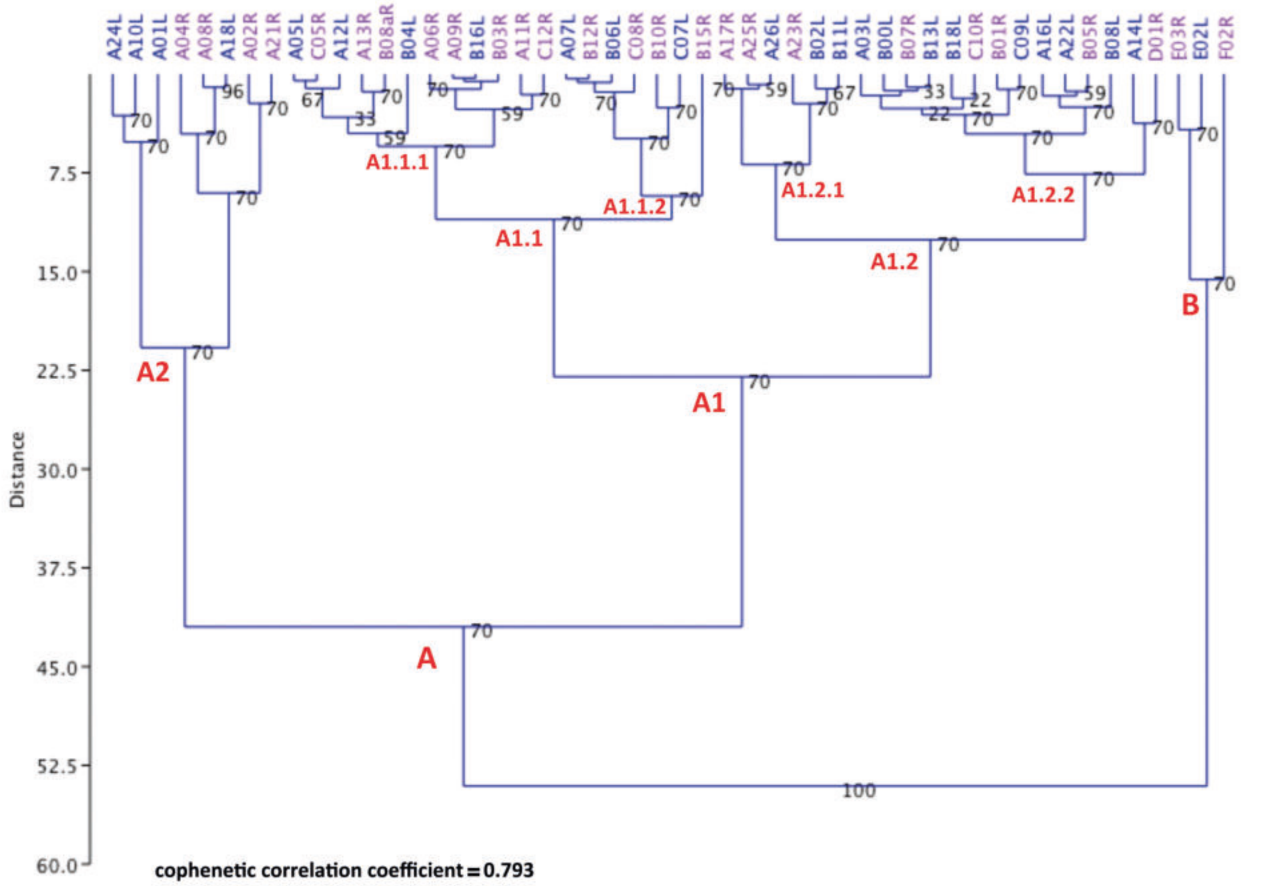

Fig. 15a - Q-mode dendrogram showing how all footprints (Sample A) impressed on the Foresta/"Devil's Trails" slope of the ignimbrite deposit cluster using the dimensional Fl, Fw, and Fa, variables. Abbreviations as in figure 14a.

the opposite position on axis 2 and is definitely shorter, as it is Fa that slightly negatively correlates with Fl and Fw, respectively (Fig. 19). The position of the scores roughly confirms most of the evidence provided by the previous PCA results. In addition, the position of the F02 score accounts for the quite significant length of this footprint. In the PCA obtained for Sample A, using the variables Fl, Fw, and Fin (Fig. 20), the variance accumulated by the first principal component (which still largely describes the essence of the data), and the second components reaches 96.364% and 3,4487%, respectively. In PC1, the variable loadings are all positive, and Fin is the variable that most contributes to this component, followed by Fl. In PC2, the same variables have a negative and positive loading, respectively, with Fl being the most influential (Table SI6). The vectors corresponding to the loading of the three variables are positively correlated. Fl is the longest, followed by Fw, which is the most correlated with PC2, and Fin, which is slightly shorter and has a lower correlation degree. The scores of the trackway A, B, and C footprints changed their positions (Fig. 20). The majority of scores of Trackway A plot in the quadrants above axis 1, which gathers the scores of footprints with the major dimensions and are roughly equally scattered on the left end the right of axis 2. The scores of Trackway B footprints plot in the two quadrants below axis 1 and are closer to each other on the left of axis 2 than on its right. The scores of Trackway C footprints also plot in the quadrants below axis 1, except for the C09 score that plots far from the others in the quadrant above axis 1, on the right of axis 2, where the scores with the highest Fw/Fl index plot. The position of the D01, E02 and E03, and F02 scores support the indications given by the previous PCA, confirming the small dimension of the D01 footprint as well as the major length of the quite narrow E03 footprint.

The PCA biplots obtained, reducing the case to the most compelling footprint measurements (Sample B) (Figs. 21, 22, and 23; Tables SI3, and SI4 in Supplementary Information) give more convincing results. The footprints of trackways A and B are always clearly separated and fall in distinct quadrants, suggesting that two different individuals ran across the F/DT slope of the ignimbrite deposit, as indicated by the footprints of trackways A and B. The presence of a third trackmaker, who impressed the Trackway C footprints, cannot be confidently confirmed because only in one footprint, C05, the preservation status allowed for perfect measurements. This footprint, however, falls in all box plots in a separate position, not far from the position of the scores of the Trackway B footprints.

In the PCA run by using all variables (Fig. 21), PC1 and

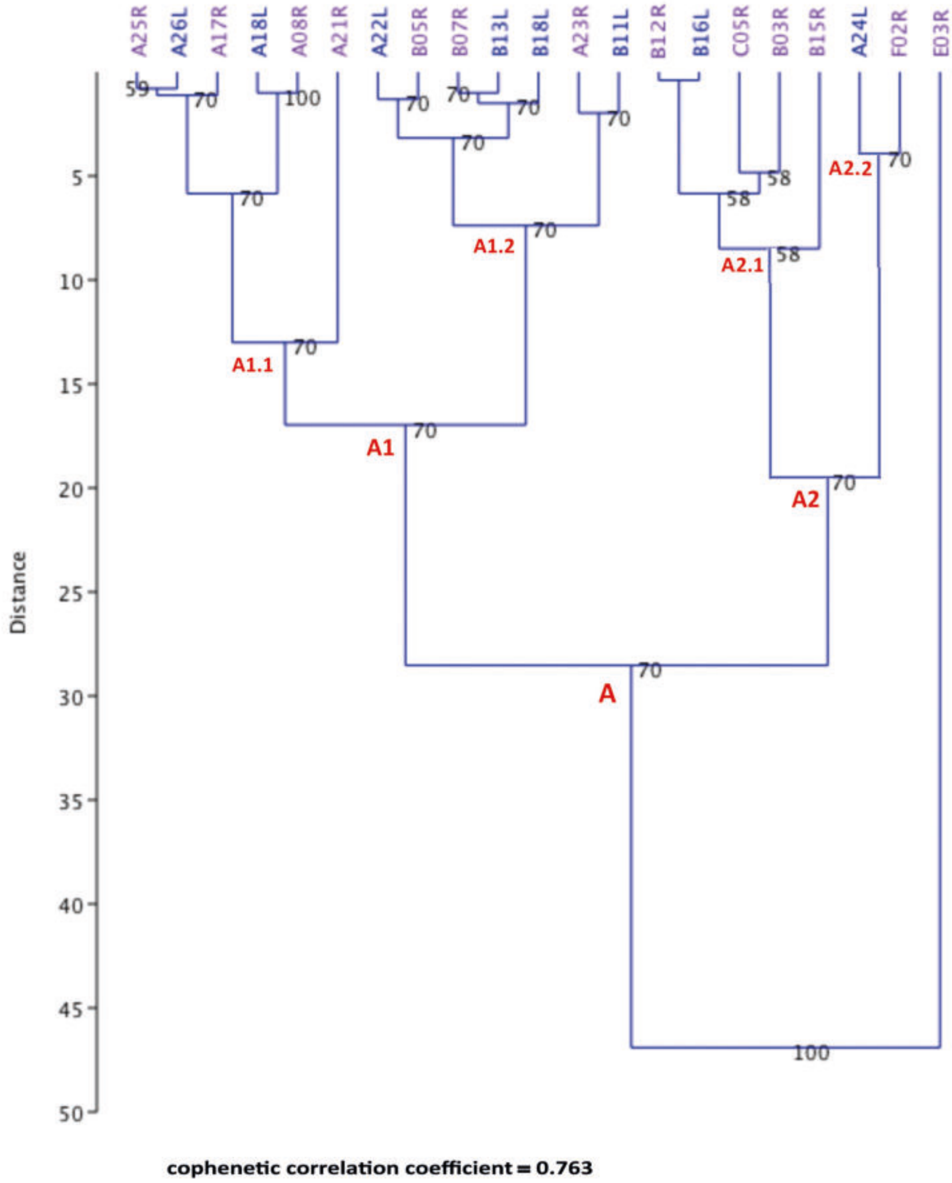

Fig. 15b - Q-mode dendrogram showing how the best-preserved footprints (Sample B) impressed on the Foresta/"Devil's Trails" slope of the ignimbrite deposit cluster using the dimensional Fl, Fw, and Fa, variables. Abbreviations as in figure 14a.

PC2 account for 98.78% and 1.0643% of the variance, respectively, whereas PC3 and PC4 have too low a loading to exert any significant influence. Fa is the variable that most influences PC1, where all variables have a positive loading. The most influential variable for PC2 is Fin, which shows a positive loading, followed by Fl, which shows a negative loading (Tab. SI4). Indeed, the vectors corresponding to the two variables, which are very long for Fin, are uncorrelated with each other. The Fa vector correlates positively with Fl and negatively with Fin and the very short Fw vector. The scores of the Trackway A and B footprints plot clearly separately on the right and left of axis 2, suggesting some difference in the proportions between the footprints of the two trackways, with the footprints of Trackway B being on average slightly narrower, shorter, and smaller than those of Trackway A.

The position of the F02 footprint and especially the E03 one indicates they are the longest in the sample B.

In the PCA boxplot obtained by using the Fl, Fw, and Fa variables (Fig. 22), the first component accounts for almost all the total variance (99.667%) and nearly fully describes the essence of the data. The loading of the variables is positive in PC1, whereas in PC2, Fa has a slightly negative loading. Fa and Fl are the most influential variables for PC1 and PC2, respectively (Tab. SI4). The corresponding vectors are negatively correlated, whereas the Fw vector correlates positively with Fl and slightly negatively with Fa. Most of the footprint scores of the two trackways A and B plot in opposite quadrants, except for A24 and B11, as well as A22 and B05 that plot on axis 2 above and below axis 1, respectively. As a result, the two groups are clearly separated. The score position of

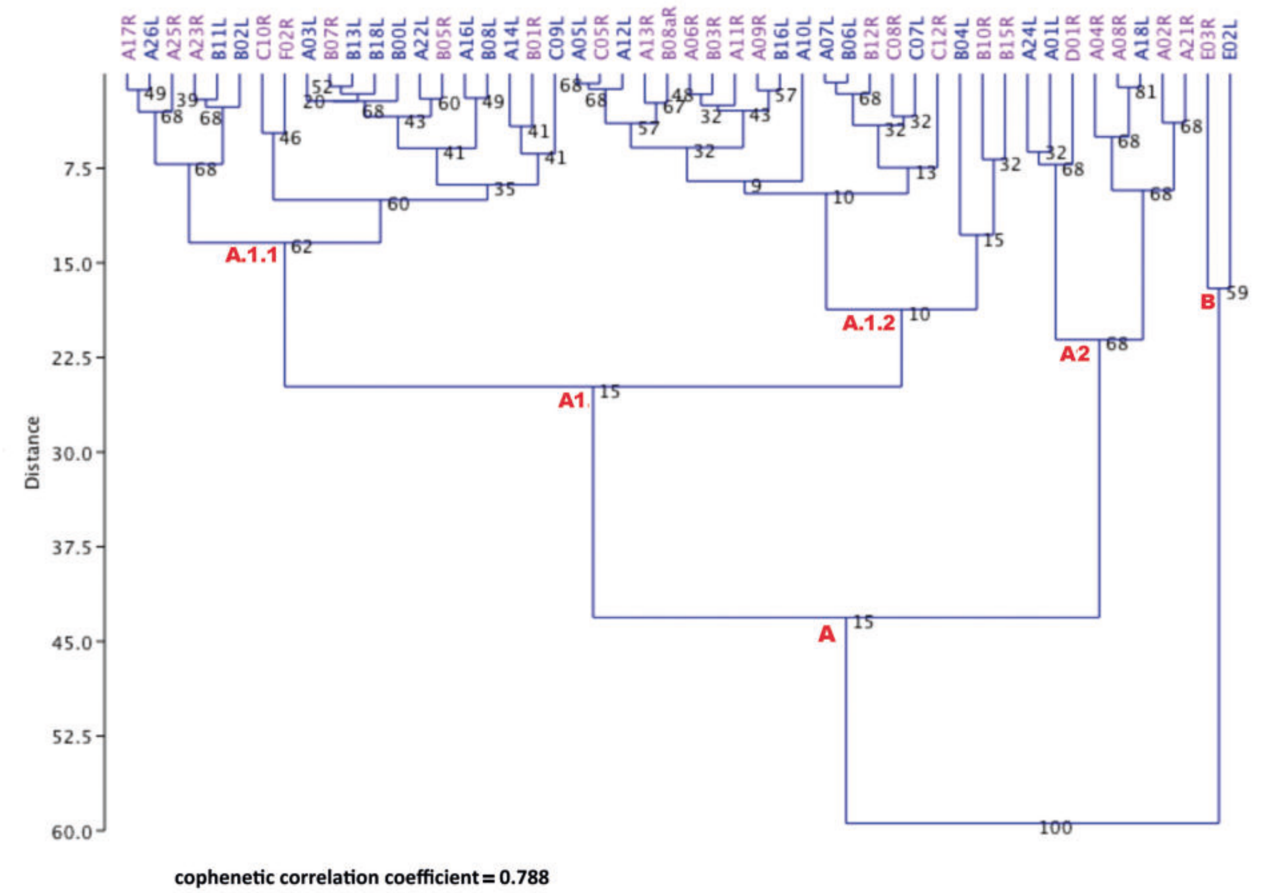

Fig. 16a - Q-mode dendrogram showing how all footprints (Sample A) impressed on the Foresta/"Devil's Trails" slope of the ignimbrite deposit cluster using the dimensional Fl, Fw, and Fw/Fl variables. Abbreviations as in figure 14a.

Trackway B footprints again indicates that they result on average shorter and narrower than those of the Trackway A, whereas E03 and F02 footprints once again clearly appear to be the lengthiest in the sample B.

In the PCA obtained after excluding from the analysis the variable that most influenced PC1, Fa, in the PCA discussed above and using the variables Fl, Fw, and Fin (Fig. 23), PC1 and PC2 accumulate 79.814% and 20.181% of the variance, respectively. Fin is the variable that most influences PC1, followed by Fl, whose negative loading is lower than the positive one of Fin (Tab. SI4). The loading of the variables is positive in PC2, which is more influenced by Fl than by Fw and Fin. The corresponding vectors are positively correlated, with Fl being the longest. The footprint scores of the two trackways A and B plot in opposite quadrants above and below axis 1, respectively, where the scores of the relatively larger and smaller footprints fall.

All things considered, the PCA results, on the one hand, indicate that the first component always accounts for nearly the total of the variance (from 96.36% to 99.75%,) with a single exception (79.8% in the PCA obtained for the Sample B, using Fl, Fw, and Fw/Flx100 variables), substantially describes the relationships among the footprint dimensions, whose values are generally positively correlated with such a variable. On the other hand, it underlines the wide variability of the footprint measurements included in Sample A that hampers a clear separation among the footprints belonging to the main trackways. This is not surprising because most of the footprints are not perfectly preserved, and, in turn, the measurements cannot be regarded as totally compelling. Indeed, the separation between the footprints of trackways BA and B becomes clearer, as do the differences in proportions of the footprints E03 and F02 with respect to those of all the other footprints. Unfortunately, in the Trackway C only one footprint, C05, is best preserved. As a result, the statistical analysis cannot confirm or reject the hypothesis about whether the footprints of this trackway were impressed or not by a further trackmaker.

5. DISCUSSION

The correct identification of the minimum number of human trackmakers who left their footprints frequenting or visiting a site, as well as inferring their main characteristics (e.g., physical parameters, age, and sex), is frequently a difficult task. Identification is generally possible by comparing the dimensional and directional differences of well-preserved footprints, aligned in well-readable distinct trackways impressed on the sub-planar

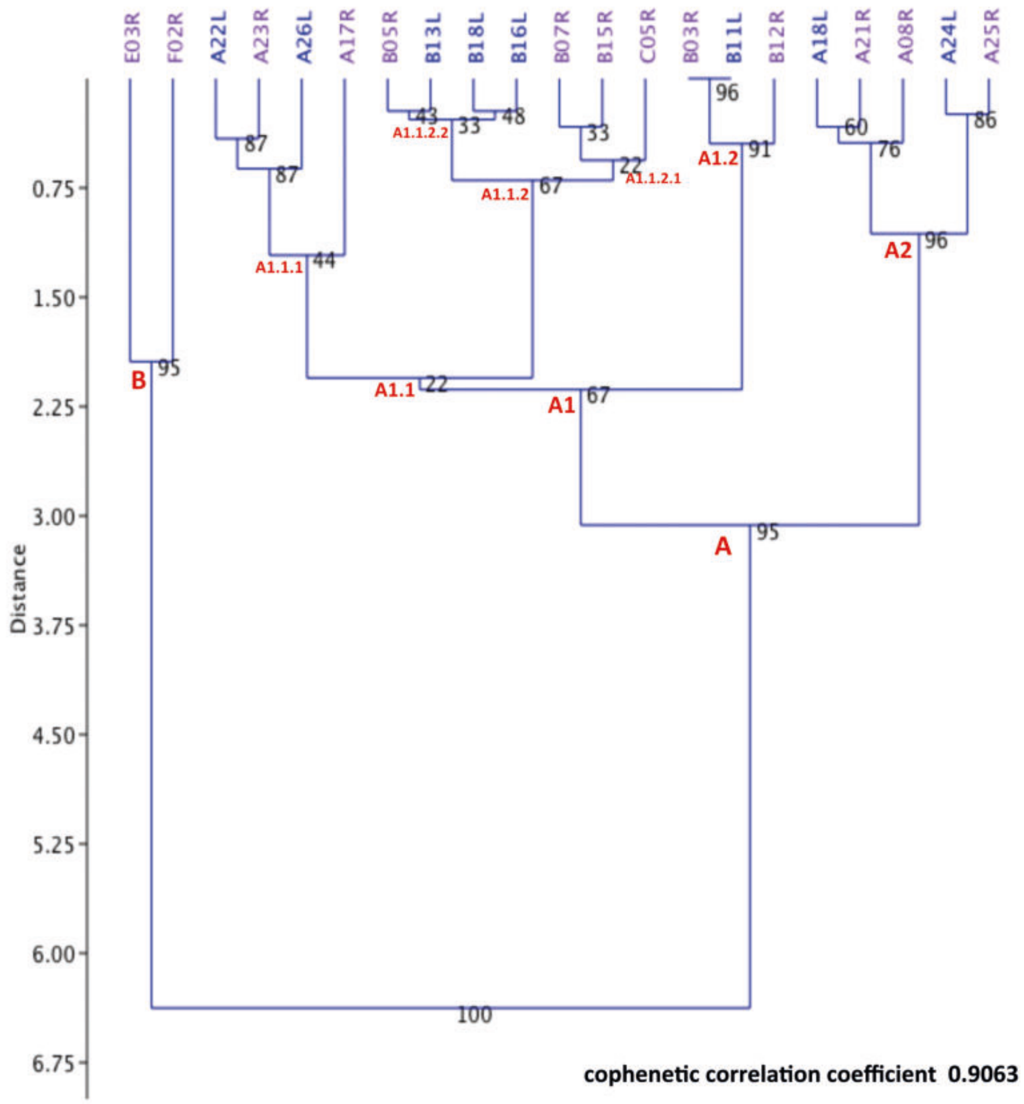

Fig. 16b - Q-mode dendrogram showing how the best-preserved footprints (Sample B) impressed on the Foresta/"Devil's Trails" slope of the ignimbrite deposit cluster using the dimensional Fl, Fw, and Fw/Fl variables. Abbreviations as in figure 14a.

surfaces of substrates with uniform, thin granulometry, or footprints impressed by individuals of different age and stature, as occurs, for example, in the famous Latest Glacial Willandra Lakes region (southeastern Australia) (Webb et al., 2006 a,b, 2007), and the slightly more recent Engare Sero ichnosites (East African Rift, Tanzania) (Hewitt et al., 2010; Zimmer et al., 2012, 2018; Liutkus-Pierce et al., 2016; Hatala et al., 2020 and references therein). The distinction between one trackmaker and another is made even easier if the footprints show foot anomalies or post-traumatic details that are repeated along a specific trackway, as can be seen in some recent *Homo sapiens* trackways (see, for example, Kennedy et al., 2003; Panarello, 2016 and references therein). In the most fortunate cases, the very receptive substrate permits the identification of different footprint morphotypes due to the presence of very sharp anatomical details, for instance at the latest Pleistocene site of Grotta della Basura (Liguria, Italy) (Citton et al., 2017; Avanzini et al., 2020 and references therein; Romano et al., 2019), and at the Holocene Acahualinca site (Manague Lake, Nicaragua), where the peculiar morphology of the footprints suggested the formalization of a new ichnotaxon, "*Hominipes modernus*" (Schmicke et al., 2009, 2010; Lockley et al., 2009; Romano et al., 2019).

The identification of the trackmaker number becomes more difficult when the footprints are not well-preserved or impressed on coarse substrates, or when the footprints are partially or completely over-imposed and altered by the almost simultaneous passage of various trackmakers in the same trackway direction, as occurred, for example, for the footprints left by G2 and G3 hominins at the Pliocene Laetoli G site (Olduvai Gorge, East Africa) (Masao et al., 2016 and references therein). In such cases, as at the F/DT ichnosite, some hypotheses could be advanced statistically by analysing data based on anatomical landmarks. The

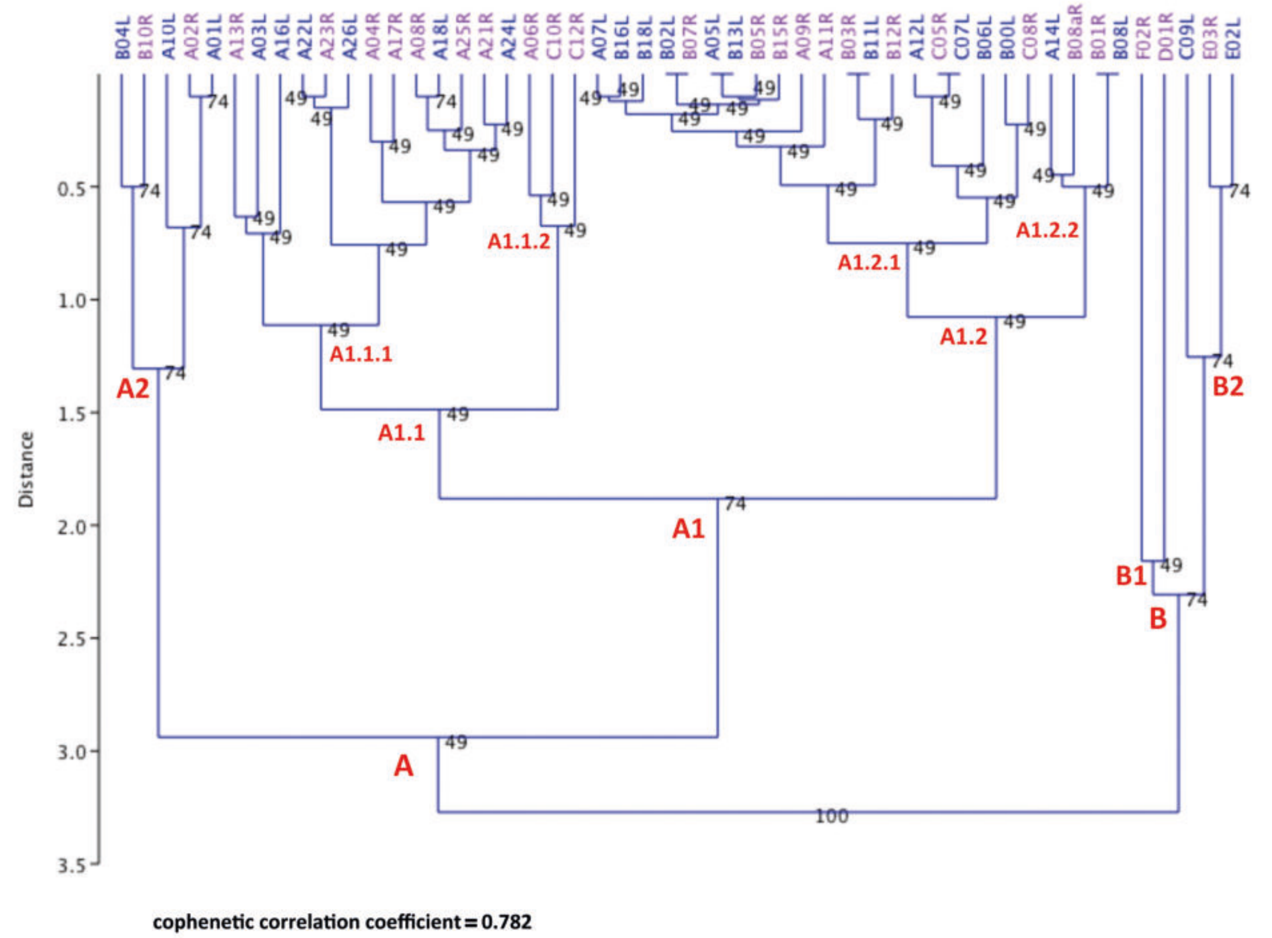

Fig. 17a - Q-mode dendrogram showing how all footprints (Sample A) impressed on the Foresta/"Devil's Trails" slope of the ignimbrite deposit cluster using the dimensional Fl, and Fw variables. Abbreviations as in figure 14a.

Early Pleistocene ichnosites of Ileret and Koobi Fora Formation (Kenya) (Behrensmeyer and Laporte, 1981; Bennett et al., 2009; Bobe and Carvalho, 2018; Dingwall et al., 2013; Hatala et al, 2016, 2017; Roach et al., 2016, 2018), Happisburgh (Norfolk, UK) (Ashton et al., 2014; Ashton, 2021; Wiseman et al., 2020), and Gombore II (Melka Kunture, Ethiopia) (Altamura, 2019; Altamura et al., 2017, 2018, 2020) are a few examples.

Identification is also problematic when the footprints are few, isolated, chaotically arranged, or altered by bioturbation, even if they were impressed during the same time slice by one or more trackmakers. In these cases, only unusual morphometric features and inferences based on archaeological rather than palaeontological or biomechanical data may allow some inferences [e.g., among the oldest, some footprints from Koobi Fora "ichnosite" (Behrensmeyer and Laporte, 1980; Bennett et al., 2009; Hatala et al., 2017; Roach et al., 2016, 2018 and references therein; Bobe and Carvalho, 2018 and references therein), and those from the early Late Pleistocene Langebaan Lagoon site (Roberts and Berger, 1997; Roberts, 2008)].

Furthermore, at some ichnosites, a single trackmaker may have visited the same site several times and left different footprints or may be walking with a different gait. As a result, footprints left by the same individual could differ in preservation, morpho-structural characteristics, dimensions, and proportions in the same trackway, making it problematic to determine the trackmaker minimum number even if the trackways are clearly identifiable. This is most likely the case with the F/DT footprints, where the trackmaker's gait is further influenced by the coarse, uneven ground surface, and slope acclivity may vary from one point to another, forcing the trackmaker to change pace and direction.

Indeed, the nature of the substrate represents the most influential factor affecting the morphology of animal and human footprints and the quality and quantity of the preserved anatomical details of the trackmakers' feet. Bennett and Morse (2014), for instance, demonstrated that substrate properties (grain-size, sorting, grain shape, porosity, packing, consolidation, and water content) significantly influence the presence, structure, and topology of fossil footprints (Marty et al., 2009; Bennett and Morse, 2014 and references therein). Furthermore, granulometry, water content, and other substrate

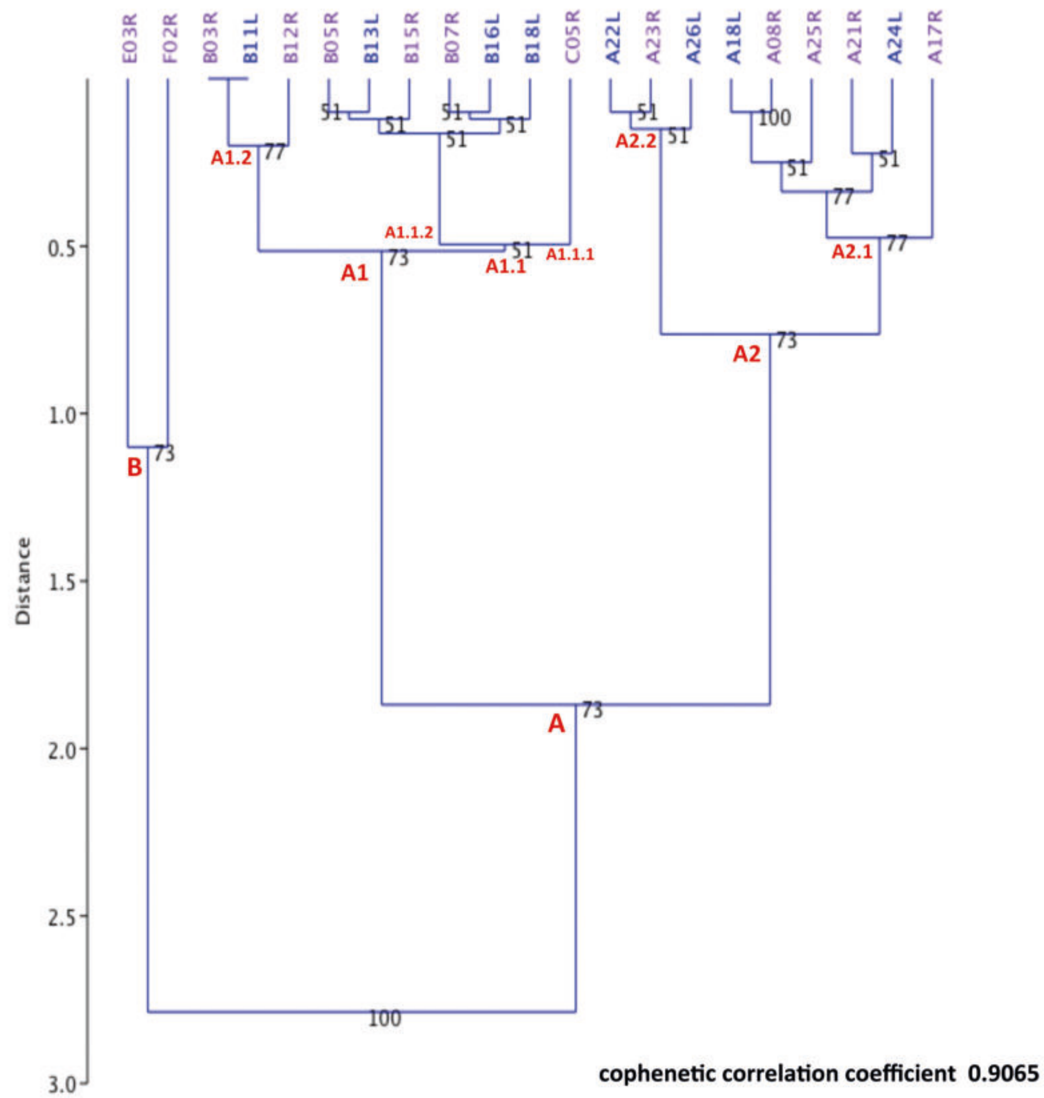

Fig. 17b - Q-mode dendrogram showing how the best-preserved footprints (ample B) impressed on the Foresta/"Devil's Trails" slope of the ignimbrite deposit cluster using the dimensional Fl, and Fw variables. Abbreviations as in figure 14a.

characteristics can change along a single trackway, as can the acclivity of the substrate, the consolidation degree, and the footprint preservation status.

At the F/DT ichnosite, all such conditions occur simultaneously. Moreover, the length of F/DT footprints suggests that most of them were left by some individuals (if not by a single trackmaker) of roughly the same size and age.

Accordingly, the hypothesis that at the F/DT ichnosite the same trackmaker may have left different footprints walking through substrate zones with different characteristics and, in turn, that a single trackmaker might descend the slope more than once could be rejected based on the statistical analysis conducted in the present contribution. Moreover, the results obtained coupled with the deduction resulting from the analysis of the characteristics and the distribution of the footprints on the slope suggest that most likely at least four different individuals walked on the slope (the trackmakers of A, B, C, and E trackways), though some inconsistencies have been observed that find some explanation considering the position of the footprints along the trackway and on the slope. The shape of the footprints, indeed, was almost certainly conditioned not only by the characteristics and the slope of the substrate but also by the conscious or unconscious movements of the trackmakers, as well as by the repeated translations, sliding, and oriented sinking caused by the need to maintain balance and, hypothetically, by the trackmakers' attempts to descend the irregular slope with the minimum possible effort. For instance, when the walking direction veers toward the bottom of the slope, the footprint may be proportionally longer. In the footprint diagonally oriented to the slope, the footprint of the foot downslope is deformed on its lateral margin, whereas the deformation affects the medial margin in the footprint of the other foot. When

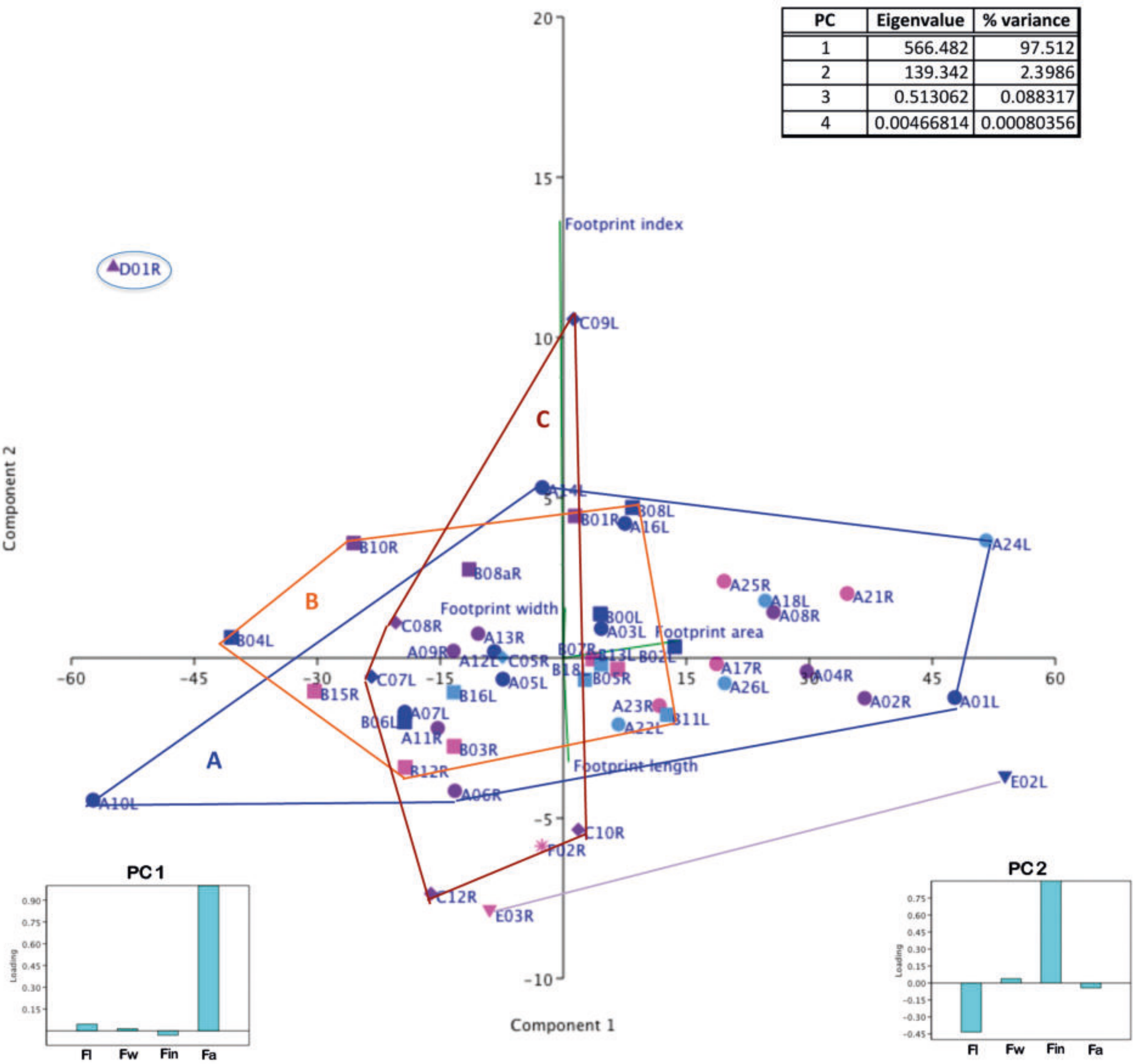

Fig. 18 - Biplot diagram produced by the principal components analysis (PCA) using all variables (Fl, Fw, Fa, and Fw/Fl) and all footprints (Sample A) impressed on the Foresta/"Devil's Trails" slope of the ignimbrite deposit. The component loadings (below) show the degree to which the different original variables enter into components 1 and 2. Abbreviation as in figure 14a.

the footprint orientation is consciously varied in search of greater stability, footprints left by the same foot can appear smaller or more evanescent than most of the others.

In the Trackway A, for example, the anomalous proportions of the A10 left footprint, which stand out in the PCA analysis diagrams (Figs. 18, 19, and 20), results from the significant gravity slide of the entire foot outwards while this foot is consciously straightened by the trackmaker, who turns it clockwise and orients it towards the walking progression line. As a result, the foot placement angle is -30° negative. This forces the trackmaker to insert the second foot right away, shortening the stance time of the forefoot and, as a result, fine-tuning the footprint. Indeed, the general shape is altered by a strong sliding towards the lateral side and then by the sudden rotation of the foot to the antero-medial direction caused by the higher slope-break and the lower stage of consolidation of the substrate. The distal region of the A10L footprint appears truncated in comparison to the A11R footprint due to the rapid support of the right heel of the foot, which shortens it even further. The footprint A01 (left), located in a fairly sub-planar part of the slope at a very short distance from the prehistoric pathway, has an uncertain outline and an almost flat midfoot area, but clearly visible posterior and anterior margins. Some anatomical details are evident, but the heel area (which is shallower than the ball one) and the distal limit of the forefoot are well-defined, permitting a compelling measure of the length. A01, moderately larger

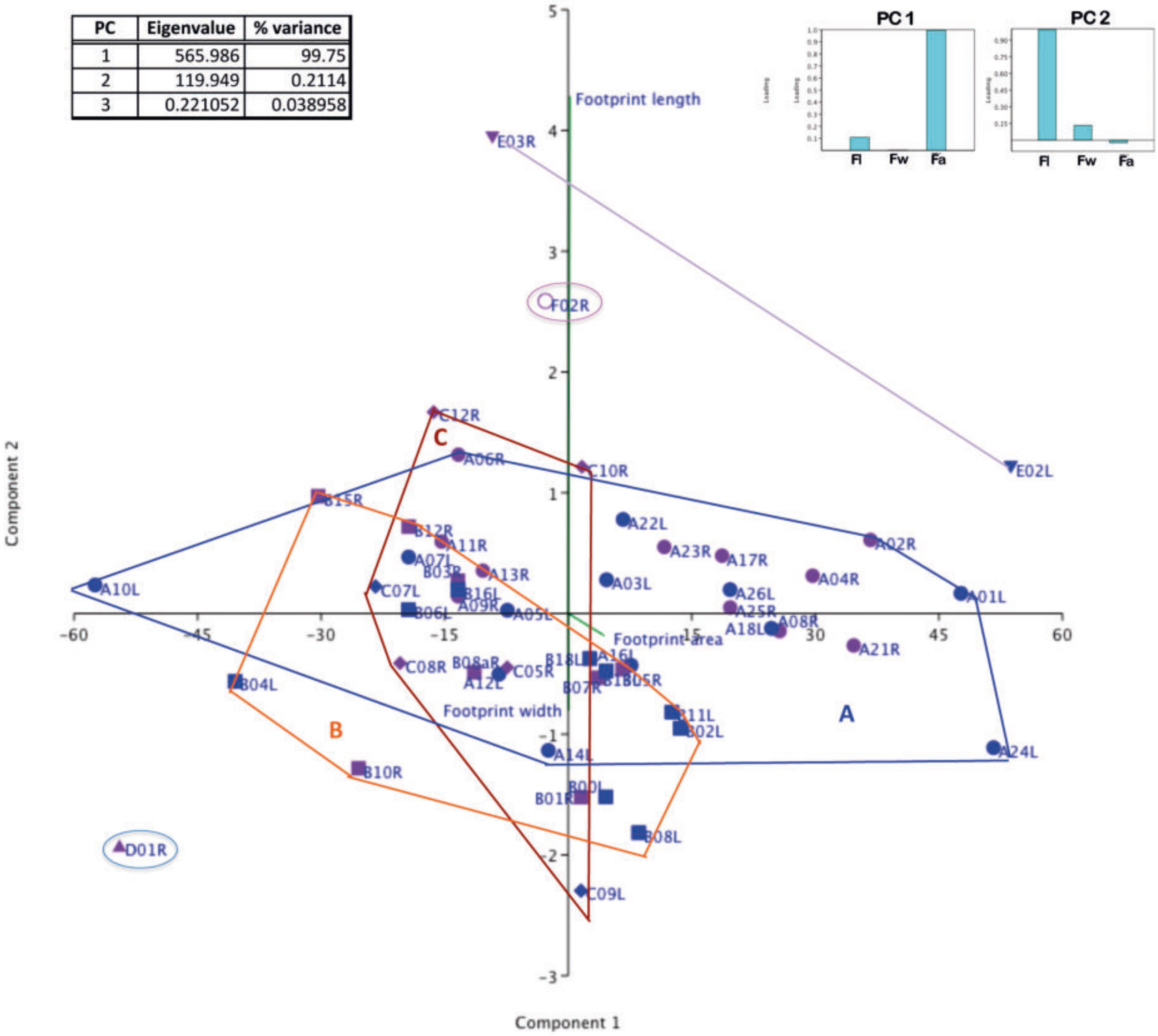

Fig. 19 - Biplot diagram produced by the principal components analysis (PCA) using all variables (Fl, Fw, and Fa) and all the footprints (Sample A) impressed on the Foresta/"Devil's Trails" slope of the ignimbrite deposit. The component loadings (below) show the degree to which the different original variables enter into the components 1 and 2. Abbreviation as in figure 14a.

than the Trackway A better preserved set of footprints was most likely left on slick ground, causing a small sliding motion in an anteromedial direction, which widened the forefoot (Panarello et al., 2022 a,b,d, table 1). Two support phases and a loading movement phase can be detected in A24 (left), which is well-impressed and sub-elliptical in shape. The first causes a moderate sinking, whereas in the second, the heel sinks much more in the soft substrate. The foot shifted towards the inside due to the body weight shifting perpendicularly to the direction of advancement, as the preserved structural marks document. The latter show the successive stages from the impact area of the foot on the plastic substrate to the final standing area, with forward slides and rotations of the foot. Although the footprint dimensions were measured at the moment of the maximum balance of the trackmaker (i.e., just before the push-off of the foot), the proportion of the A24 differs from the majority of the Trackway A footprints (Panarello et al., 2022 a,b,d, table 1).

In Trackway B, B04 and B10 footprints show the most significant differences from the others (see, for example, Figs. 18, 19, and 20). This may depend on the fact that footprint B04 is positioned in a south-easterly direction at the innermost position with respect to the edge of the slope, perhaps because this was the safest area in which to find stability while walking on the unevenly consolidated ground. This resulted in a slight torsion of the foot towards the south and a slight translation of the entire foot towards the steepest slope. The footprint B10, slightly shorter than the others, being truncated at its distal part, represents the first point where the trackmaker regained his body balance after a long slide of the whole leg. The footprint was likely impressed when the body was leaning forward to support the full weight of the body before

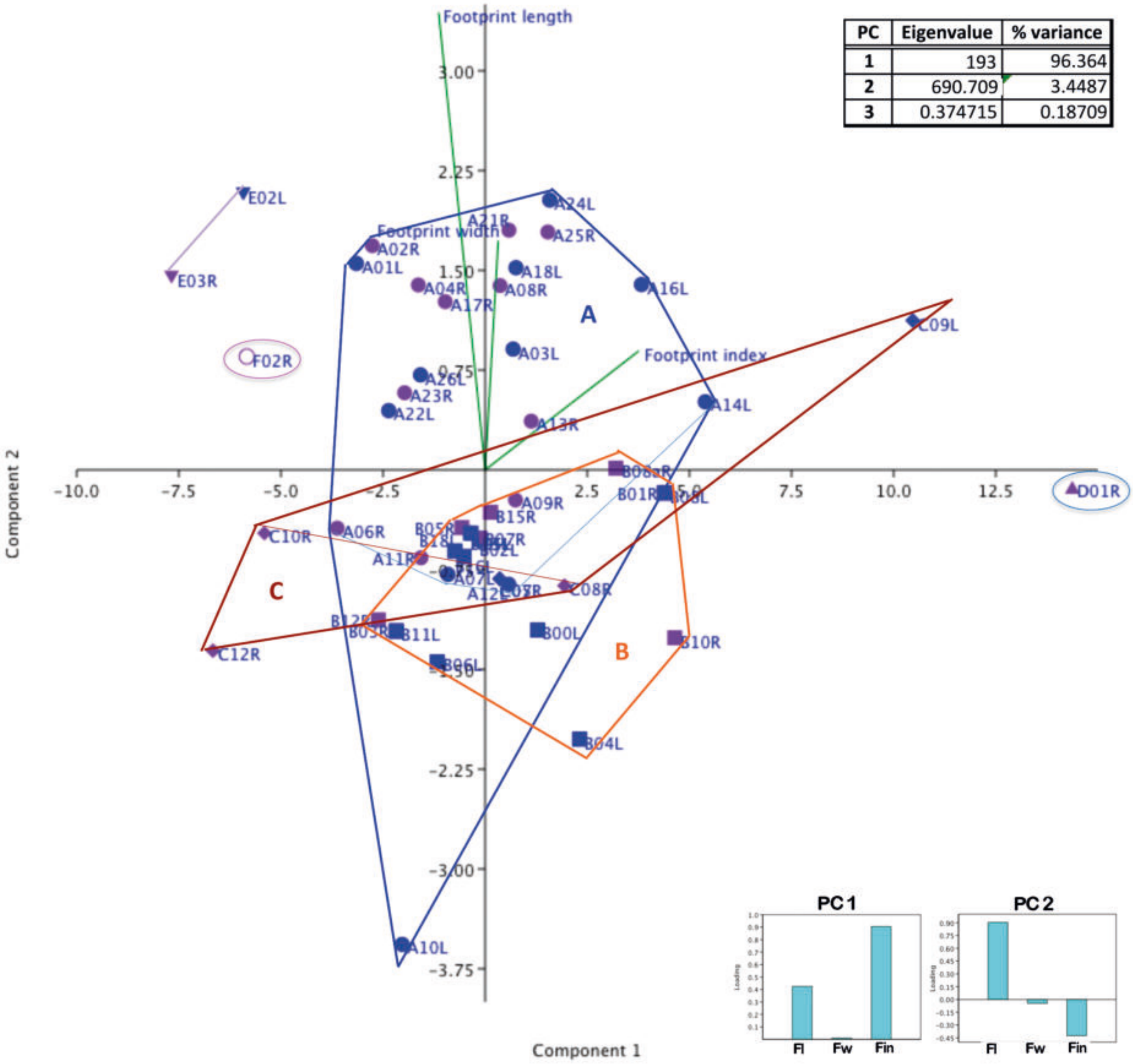

Fig. 20 - Biplot diagram produced by the principal components analysis (PCA) using all variables (Fl, Fw, Fa, and Fw/Fl) and the best-preserved footprints (Sample B) impressed on the Foresta/"Devil's Trails" right slope of the ignimbrite deposit. The component loadings (below) show the degree to which the different original variables enter into the components 1 and 2. Abbreviation as in figure 14a.

performing the step-crossing hop, which ends with the footprint B11 (Mietto et al., 2003; Avanzini et al., 2008; Panarello, 2020; Panarello et al., 2022 a,b,d).

As regards the other footprints, the E03 right footprint, despite being the longest (27 cm), appears narrow because it represents the first antero-medial downhill subsidence of a track up to sub-planar in a non-homogeneously plastic area, which forces the foot to an unnatural lateral displacement that produces a measurable concavity at the bottom of the cavity outer wall. The footprint F02 also appears disproportionally longer because it is located along a ledge narrower than the maximum width of the foot. As a result, the trackmaker was forced to put the big toe on the upstream wall to avoid falling (Panarello et al., 2020).

These examples show how much the peculiarity of the F/DT floor and the difficulty of descending a slipping slope may have affected the shape of the footprints.

On the one hand, the obtained results provide quite solid clues for confirming the different identities of Trackways A and B, as well as the not entirely preserved sequence E; on the other hand, the hypothesis of a fourth trackmaker, who impressed the Trackway C footprints, is clearly less solid. Actually, the trackway is poorly defined and has some peculiarities that raise some uncertainties. Therefore, it is quite difficult to understand the causal factors behind the anomalous proportion of poorly preserved footprints, as with most of the Trackway C footprints (Panarello et al., 2020; Panarello et al., 2022 a,b). For instance, the C09 footprint can be recognised

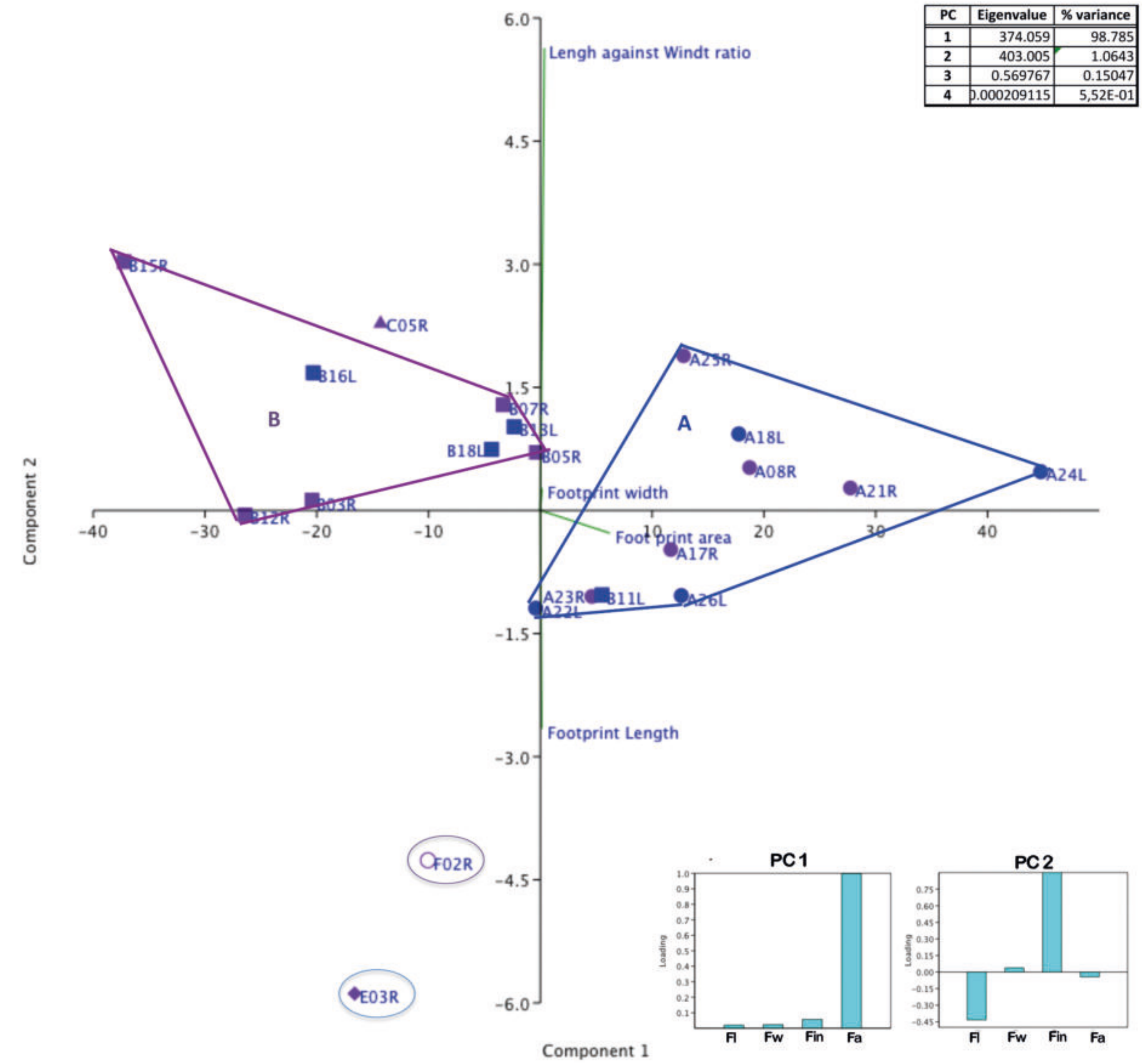

Fig. 21 - Biplot diagram produced by the principal components analysis (PCA) using all variables (Fl, Fw, Fa, and Fw/Fl) and all footprints (Sample B) impressed on the Foresta/"Devil's Trails" slope of the ignimbrite deposit. The component loadings (below) show the degree to which the different original variables enter into components 1 and 2. Abbreviation as in figure 14a.

only for its surface, flattened with respect to the uneven one of the surrounding substrate areas, and for being in line with the other, better-preserved footprints because no anatomical details are detectable (Panarello et al., 2022 a,b,d). The C12 footprint is stretched in an anteromedial direction, so the length (24.2 cm) is disproportioned with respect to the width (9.5 cm), as confirmed by the dimensions and proportions of the only well-preserved C05 footprint (22.6x10.4 cm) (Tab. 1, Fig. 18).

The arrangement of the Trackway C footprints on the ignimbrite slope deposit could account for these dimensional inconsistencies. Indeed, more accurate studies demonstrate that Trackway C, initially described as two successions of 10 footprints separated by an extended gap (Mietto et al., 2003; Avanzini et al., 2008), consists of two segments (1C and 2C), belonging to the same trackway but differently oriented and inclined due to the geomorphological constraints of the slope. As a result, the footprints of the more inclined segment 1C show signs of sliding towards an antero-medial direction, whereas the footprints of segment 2C, which runs southeast in a quite sub-planar direction, are more regular and less deep. However, despite the dimensional variation of the poorly preserved Trackway C footprints, to date, no unquestionable evidence has been found indicating that the 1C and 2C segments are part of two different trackways. As a result, the hypothesis that Trackway C may be imprinted by a single trackmaker, not the same as Trackways A, B, and E, appears to be the most appropriate.

Unfortunately, the peculiarity of the F/DT ichnosite

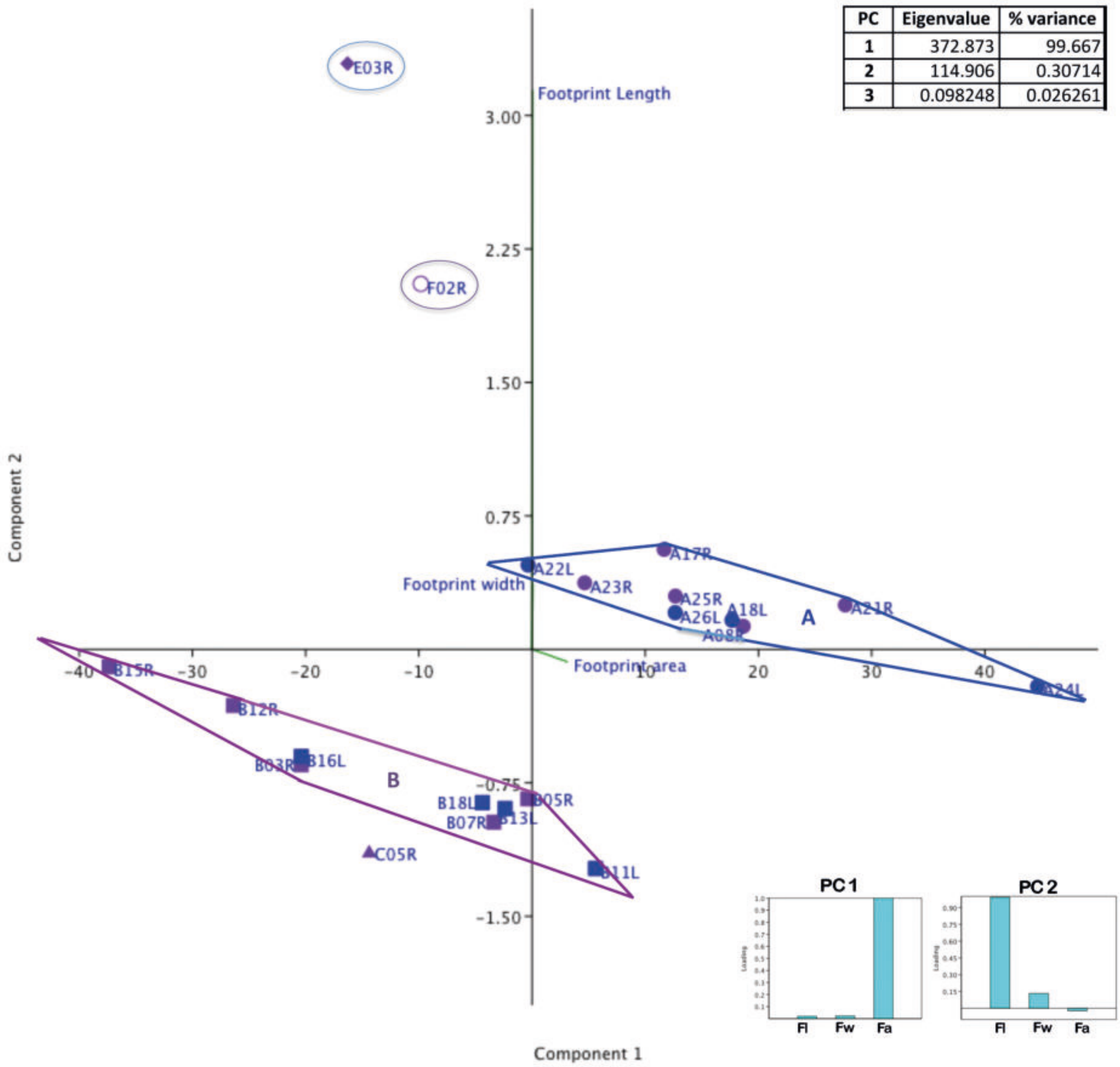

Fig. 22 - Biplot diagram produced by the principal components analysis (PCA) using all variables (Fl, Fw, and Fa) and the best-preserved footprints (Sample B) impressed on the Foresta/"Devil's Trails" slope of the ignimbrite deposit. The component loadings (below) show the degree to which the different original variables enter into the components 1 and 2. Abbreviation as in figure 14a.

prevents the comparison of their pattern with human footprints from other ichnosites. Some of the South African coastal ichnosites, which include a large and best-preserved record of Late Pleistocene hominin tracks mainly dated to MIS 5e, are the only known thus far where the footprints were impressed on the slope substrate of aeolian dune systems (Roberts and Berger, 1997; Roberts, 2008; Helm et al., 2018 a,b, 2019 a,b, 2020 a,b, 2021). However, a compelling comparison aimed at determining how much the characteristics of the substrate, particularly its acclivity, could have affected human gaits, and footprint morphometry is problematic due to a variety of factors. For instance, some imprinted aeolian dune blocks are not in the primary position. This reduces the possibility of determining both the slope acclivity in the track where humans were walking and the actual position of the footprint on it. Furthermore, some footprints were likely impressed by individuals of different ages; some are preserved as concave epirelief, others as convex hyporelief, and some are visible only in section. As a result, morphometric data may be inhomogeneous (Tab. SI5).

For instance, among the tracksites recording the largest human footprint samples, at Brenton 1 (Brenton-on-Sea), the footprint length values show a mesocurtic distribution even if the footprints range from rather short (12 cm) to large (23 cm), suggesting the presence of both young and adult individuals. Conversely, the width variation range is much larger, perhaps suggesting some influence of the substratum acclivity (Figs. 21 and 6, Tab.

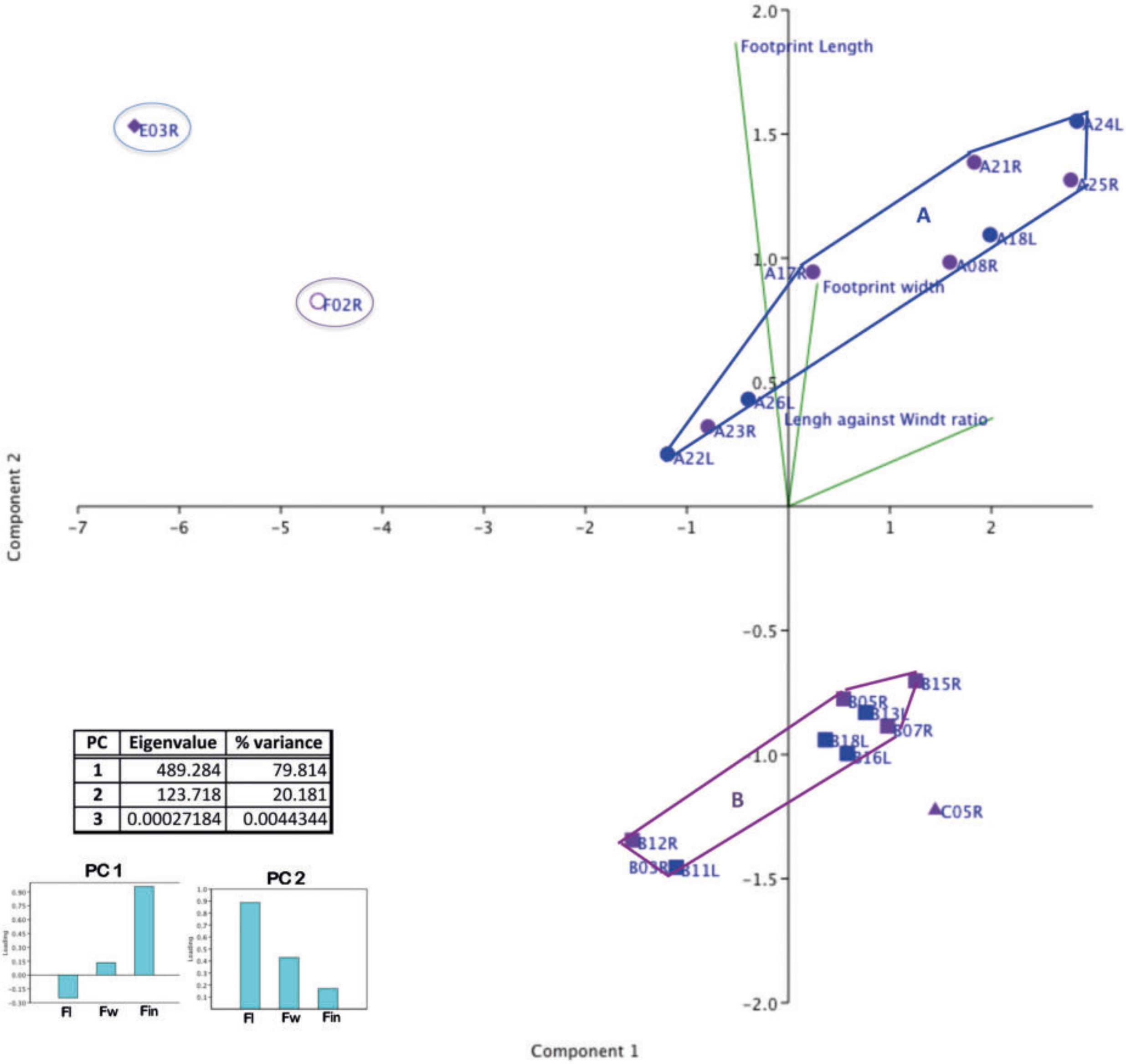

Fig. 23 - Biplot diagram produced by the principal components analysis (PCA) using all variables (Fl, Fw, and Fw/Fl) and all the footprints (Sample B) impressed on the Foresta/"Devil's Trails" slope of the ignimbrite deposit. The component loadings (below) show the degree to which the different original variables enter into the components 1 and 2. Abbreviation as in figure 14a.

6). The length of footprints at the Goukamma 2 tracksite (Goukamma Nature Reserve), which are less numerous, have a moderate range of variation, and the small-sized footprints prevail. The width variation range is larger than at Brenton 1, so Goukamma 2's scores are less dispersed in the PCA graph (Figs. 24 and 25, Tab. 6). However, it is challenging to hypothesise whether some differences in the substrate characteristics might have determined the different patterns characterised by the footprints of these two sites.

As a result, any inference about the causal factors affecting the proportions of these South African footprints cannot be regarded as compelling for a sound comparison of their pattern with that of the F/DT sample.

7. CONCLUSION

At the F/DT ichnosite, the two long trackways, A and B, of human footprints that run along the the ignimbric flow on the very steep slope surface of the deposit are so well-delineated and visible that they have been noticed by the local population since the 19th century, with the folkloric name "Ciampate del Diavolo." The team led by P. Mietto (Mietto et al., 2002; Panarello et al., 2023) conducted field and laboratory research for approximately twenty years (2001-2018), resulting in the discovery of several other humans' footprints arranged in short trackways (the two detached sectors of Trackway C and the four footprints of Trackway E), or in very short sequences, as well as the poorly preserved footprints of the pathway,

Tab. 6 - Summary of the univariate analysis statistics' data obtained for the footprint samples from the Cape South Coast (South African) ichnosites of Brenton 1 (Brenton-on-Sea) and Goukamma site 2 (Goukamma Nature Reserve). Data from Helm et al. (2018 a,b, 2019 a,b, 2020 a,b).

UNIVARIATE STATISTICS

	Brenton 1 (Brenton-on-Sea)				Goukamma site 2 (Goukamma Nature Reserve)		
	Footprint Length (mm)	Footprint width (mm)	Lengh against Width ratio		Footprint Length (mm)	Footprint width (mm)	Lengh against Width ratio
N	27	27	27	N	13	13	13
Min	12	1.5	9.38	Min	12	5.5	44.44
Max	23	10	58.33	Max	20	10	62.5
Sum	478.5	189	1073.04	Sum	195	100	668.95
Mean	17.72222	7	39.74222	Mean	15	7.692308	51.45769
Std. error	0.5197888	0.4401502	2.284571	Std. error	0.6201737	0.342214	1.63917
Variance	7.294872	.	14.09201	Variance	5	1.522436	3.492944
Stand. dev	2.700902	2.287087	11.87098	Stand. dev	2.236068	1.23387	5.910113
Median	17.5	7	41.67	Median	15	8	50
25 prcntil	16	6	37.5	25 prcntil	13	7	46.41
75 prcntil	20	9	47.06	75 prcntil	16	8	55.495
Skewness	-1.723306	-0.7447823	-1.378286	Skewness	0.8984928	0.1044676	0.8208693
Kurtosis	0.09753222	0.3067398	1.531307	Kurtosis	0.7054545	0.3012234	-0.390666
Geom. mean	17.51482	6.48349	37.01799	Geom. mean	14.85439	7.59932	51.15796
Coeff. var	15.2402	32.67268	29.86994	Coeff. var	14.90712	16.04031	11.48538

NORMALITY TESTS

	Brenton 1 (Brenton-on-Sea)				Goukamma site 2 (Goukamma Nature Reserve)		
	Footprint Length	Footprint width	Lengh against Width ratio		Footprint Length	Footprint width	Lengh against Width ratio
N	27	27	27	N	13	13	13
Shapiro-Wilk W	0.9722	0.919	0.8394	Shapiro-Wilk W	0.9273	0.9189	0.8996
p(normal)	0.6616	0.03732	0.000715	p(normal)	0.3143	0.2424	0.1321
Anderson-Darling A	0.2732	0.7543	1737	Anderson-Darling A	0.3971	0.6224	0.5138
p(normal)	0.6391	0.04352	0.0001406	p(normal)	0.3161	0.0818	0.1565
p(Monte Carlo)	0.671	0.044	0.0002	p(Monte Carlo)	0.3308	0.0797	0.1633
Lilliefors L	0.1137	0.1667	0.2182	Lilliefors L	0.1735	0.2477	0.2128
p(normal)	0.4843	0.05054	0.0001	p(normal)	0.3444	0.02813	0.105
p(Monte Carlo)	0.4818	0.0518	0.0015	p(Monte Carlo)	0.3452	0.0299	0.1077
Jarque-Bera JB	0.1392	2224	8846	Jarque-Bera JB	1357	0.04733	1386
p(normal)	0.9328	0.3289	0.012	p(normal)	0.5073	0.9766	0.5
p(Monte Carlo)	0.9343	0.1251	0.0176	p(Monte Carlo)	0.1771	0.9836	0.1779

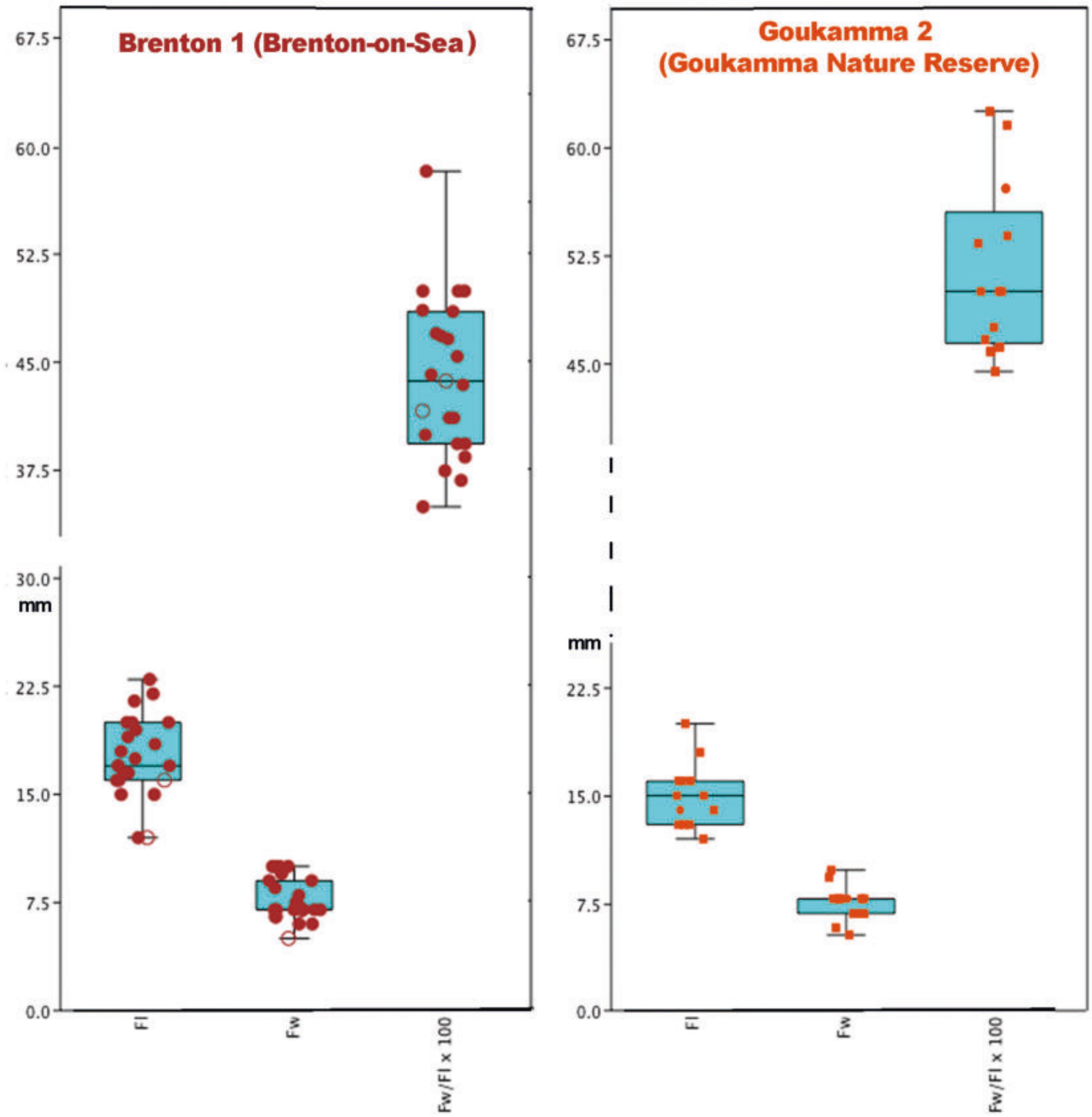

Fig. 24 - Box plot illustrating the variation range of footprints impressed on the aeolian deposits surface at Brenton 1 and Goukamma 2 (Goukamma Nature Reserve) ichnosites (Cape South Coast, South Africa). Footprint length (Fl and width (Fw) (data from Helm et al., 2018 a,b, 2019 a,b, 2019 a,b, 2020 a,b).

running at the top of the slope. In this contribution, we have attempted to objectively ascertain the minimum number of individuals who descended the slope using the soundest available data (state of preservation of the footprints, morphometric features, quantity and quality of anatomical details, position on the slope with respect to the other footprints of the same track, and precision of the recorded measurements) for the latter, for which the precise number of trackmakers is difficult to hypothesize.

The obtained results and the direct inspections of the footprint arrangement at the ichnosite allow us to state that most likely at least four trackmakers (A, B, C, and E) walked on the ignimbrite slope deposit. In more detail, assuming that foot size and stature are actually positively related, the footprints of trackways A, and B, were likely left by two individuals of similar stature, whereas the individual who made the Trackway E footprints was likely taller. Furthermore, it is highly probable that an individual of comparable stature to that of trackmakers A and B left the Trackway C footprints, as suggested by field observations. On the other hand, more solid evidence is needed to support the hypothesis that a fifth, smaller individual left the footprints of short sequence D, which is based solely on a single imperfectly preserved footprint.

Furthermore, the results underline how much substrate conditions (coarse granulometry, plasticity, and slipperiness) along with slope acclivity influenced the trackmaker gait (velocity, and stride length), the walking direction and its changing, the pace stability, and the way in which the foot rests against the substrate slope. The combined action of these factors conditioned the footprint shape and size proportions, resulting in variation of the footprint proportions along the same path.

All things considered, the set of data confirms the

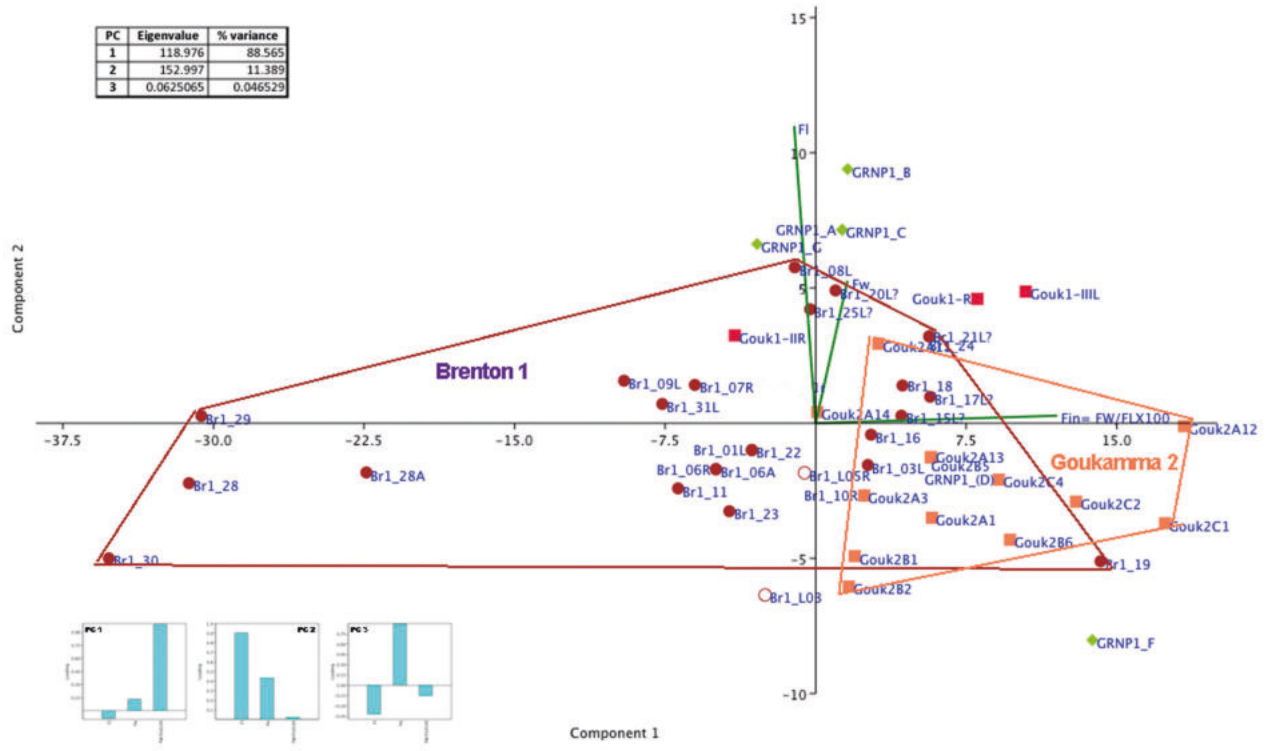

Fig. 25 - Biplot diagram produced by the principal components analysis (PCA) computed for the human footprint samples from some Cape South Coast (South African) ichnosites [Brenton-on-sea (Br), Garden Route National Park-Site 1 (GRNP), Goukamma Tracksite 1 (Gouk1), Goukamma Nature Reserve, Tracksite 2 (Gouk2). The component loadings (below) show the degree to which the different original variables enter into components 1, 2, and 3. Abbreviation as in figure 11a.

peculiar characteristics of the footprints of the site and the difficulty of being able to compare their pattern with those of other sites with human footprints from Pleistocene ichnosites.

ACKNOWLEDGEMENTS - We thank the reviewers J. Duveau and M. Romano for critically reading the earlier version of this manuscript and for their constructive suggestions.

REFERENCES

Altamura F., 2019. Ichnology and archaeology in the African record: a complementary approach. In: Di Lernia S., Gallinaro M. (Eds.), Papers from the 1st Workshop Archaeology in Africa. Potential and Perspectives on Laboratory & Fieldwork Research. Arid Zone Archaeology, Monographs 8. Sesto Fiorentino: All'Insegna del Giglio, 127-140.

Altamura F., Melis R.T., Mussi M., 2017. A Middle Pleistocene hippo tracksite at Gombore II-2 (Melka Kunture, Upper Awash, Ethiopia). Palaeogeography, Palaeoclimatology, Palaeoecology 470, 122-131.

Altamura F., Bennett M.R., D'Août K., Gaudzinski-Windheuser S., Melis R.T., Reynolds S.C., Mussi M., 2018. Archaeology and ichnology at Gombore II-2, Melka Kunture,Ethiopia: everyday life of a mixedage hominin group 700,000 years ago. Scientific Reports 8, 2815.

Altamura F., Bennett M.R., Marchetti L. Melis R.T., Reynolds S.C., Mussi M., 2020. Ichnological and archaeological evidence from Gombore II OAM, Melka Kunture, Ethiopia: An integrated approach to reconstruct local environments and biological presences between 1.2 and 0.85 Ma. Quaternary Science Reviews 244, 106506.

Antonelli M., Romano M., De Sario F., Pignatti J., Sacco E., Petti F.M., 2023. Inferred oviraptorosaur footprints in the Apenninic Carbonate Platform: New tools for the identification of trackmakers from the Sezze ichnosite (lower-middle Cenomanian; central Italy). Cretaceous Research 141, 105362.

Aronhime S., Calcagno C., Jajamovich G. H., Dyvorne H.A., Robson P., Dieterich D., Fiel M.I., Martel-Laferriere V., Chatterji M., Rusinek H., Taouli B., 2014. DCE-MRI of the liver: effect of linear and nonlinear conversions on hepatic perfusion quantification and reproducibility. Journal of Magnetic Resonance Imaging 40, 90-98.

Ashton N., 2021. Steps from History. In: Pastoors A., Lenssen-Erz T. (Eds.), Reading Prehistoric Human Tracks. Springer, Cham, 153-168.

Ashton N., Lewis S.G., De Groote I., Duffy S.M., Bates M., Bates R., Hoare P., Lewis M., Parfitt S.A., Peglar S., Williams C., Stringer C., 2014. Hominin Footprints from Early Pleistocene Deposits at Happisburgh, UK. PlosOne, 9, e88329.

Avanzini M., Citton P., Mietto P., Panarello A., Raia P., Romano M., Salvador I., 2020. Human footprints from Italy: the state of the art. In: Romano M., Citton P. (Eds.), Tetrapod ichnology in Italy: the state of the art. Journal of Mediterranean Earth Sciences 12 (Special Issue), 213-232.

Avanzini M., Mietto P., Panarello A., De Angelis M., Rolandi G., 2008. The Devil's Trails: Middle Pleistocene human footprints preserved in a volcanoclastic deposit of southern Italy. Ichnos 15, 179-189.

Ballini A., Barberi F., Laurenzi M.A., Mezzetti F., Oddone M., Villa I.M., 1990. Chrono-Stratigraphy of Roccamonfina volcanic complex. In: Civetta L., Capaldi G., Orsi G., Peccerillo A. (Eds.), Genesi e differenziazione del magmatismo potassico del Bordo Tirrenico. Atti del convegno autunnale della Società Italiana di Mineralogia e Petrologia (Ischia 15-18 ottobre 1990). Plinius, 4, Supplement to European Journal of Mineralogy.

Behrensmeyer A.K., Laporte L.F., 1981. Footprints of a Pleistocene hominid in northern Kenya. Nature 289, 167-169.

Belvedere M., Jalil N.E., Breda A., Gattolin G., Bourget H., Khaldoune F., Dyke G.J., 2013. Vertebrate footprints from the Kem Kem beds (Morocco): A novel ichnological approach to faunal reconstruction. Palaeogeography, Palaeoclimatology, Palaeoecology 383-384, 52-58.

Bennett M.R., Bustos D., Odess D., Urban T.M., Lallensack J.N., Budka M., Santucci V.L., Martinez P., Wiseman A.L.A., Reynolds S.C., 2020. Walking in mud: remarkable Pleistocene human trackways from white sands national park (New Mexico). Quaternary Science Reviews 249, 106610.

Bennett M.R., Harris J.W.K., Richmond B.G., Braun D.R., Mbua E., Kiura P., Olago D., Kibunjia M., Omuombo C., Behrensmeyer A.K., Huddart D., Gonzalez S., 2009. Early hominin foot morphology based on 1,5-million-year-old footprints from Ileret, Kenya. Science 323, 1197-1201.

Bennett M.R., Morse S.A., 2014. Human Footprints: Fossilised Locomotion? Springer, Cham-Heidelberg-New York-Dordrecht-London.

Bobe R., Carvalho S., 2018. Hominin diversity and high environmental variability in the Okote Member, Koobi Fora Formation, Kenya. Journal of Human Evolution 126, 91-105.

Cheng, H., Edwards, R. L., Broecker, W. S., Denton, G. H., Kong, X., Wang, Y., Rhan, R., Wang, X., 2009. Ice age terminations. Science 326, 248-252.

Citton P., Romano M., Salvador I., Avanzini M., 2017. Reviewing the upper Pleistocene human footprints from the 'Sala dei Misteri' in the Grotta della Bàsura (Toirano, northern Italy) cave: An integrated morphometric and morpho-classificatory approach. Quaternary Science Reviews 169, 50-64.

Cole P.D., Guest J.E., Duncan A.M., Chester D.K., Bianchi R., 1992. Post-collapse volcanic history of calderas on a composite volcano: an example from Roccamonfina, southern Italy. Bulletin of Volcanology 54, 253-266.

Cole P.D., Guest J.E., Duncan A.M., 1993. The emplacement of intermediate volume ignimbrites: A case study from Roccamonfina volcano, Southern Italy. Bulletin of Volcanology 55, 467-480.

De Rita D., Giordano G., 1996. Volcanological and structural evolution of Roccamonfina volcano (Italy): origin of the summit caldera. In: McGuire W.J., Jones A.P., Neuberg J. (Eds.), Volcano Instability on the Earth and Other Planets. Geological Society, London, Special Publications, 110, 209-224.

Di Vito M.A., 2022. Il geosito delle "Ciampate del diavolo". In: Mietto P., Panarello A., Di Vito M. (Eds.), 2001-2021: Vent'anni di ricerche sulle "Ciampate del diavolo". Dalla leggenda alla realtà scientifica. Miscellanea Istituto Nazionale di Geofisica e Vuclanologia 64, 49-56.

Dingwall H.L., Hatala K.G., Wunderlich R.E., Richmond B.G., 2013. Hominin stature, body mass, and walking speed estimates based on 1.5 million-year-old fossil footprints at Ileret, Kenya. Journal of Human Evolution 64, 556-568.

Duveau J., Berillon G., Laisné G., Verna C., Cliquet D., 2018. From footprints to locomotor anatomy? The contribution of geometric morphometrics to the study of the hominin footprints from the Upper Pleistocene site of Rozel (Normandie, France). In: International Union of the Prehistoric and Protohistoric Sciences Congress.

Duveau J., Berillon G., Verna C., Laisné G., Cliquet D., 2019. The composition of a Neandertal social group revealed by the hominin footprints at Le Rozel (Normandy, France). Proceedings of the National Academy of Sciences 116, 19409-19414.

Falkingham P.L., Bates K.T., Avanzini M., Bennett M., Bordys E.M., Breithaup B.H., Castanera D., Citton P., Díaz-Martínez I., Farlow J.O., Fiorillo A.R., Gates S.M., Getty P., Hatala K.G., Hornung J.J., Hyatt J.A., Klein H., Lallensack J.N., Martin A.J., Mary D., Matthews N.A., Meyer C.A., Milàn J., Minter N.J., Razzolini N.L., Romilio A., Salisbur S.W, Sciscio L., Tanaka I., Wiseman A.L.A., Xing L.D., Belvedere M., 2018. A standard protocol for documenting modern and fossil ichnological data. Palaeontology 61, 469-480.

Hammer Ø., Harper, D.A.T., 2005. Introduction to multivariate data analysis. In: Hammer Ø., Harper D.A.T. (Eds.), Paleontological Data Analysis. Wiley Online Library, 61-77.

Hammer Ø., Harper D.A.T., 2006. Paleontological Data Analysis. Oxford, Blackwell Publishing.

Hammer Ø., Harper D.A.T., Ryan P.D., 2001. PAST: Paleontological Statistics Software Package for Education and Data Analysis. Palaeontologia Electronica 4, art. 4, pp. 9, http://palaeo-electronica.org/2001_1/past/issue1_01.htm

Hatala K.G., 2014. Fossil Hominin Footprints and the Dynamics of Footprint Formation (Doctoral dissertation, The George Washington University).

Hatala K.G., Roach N.T., Ostrofsky K.R., Wunderlich R.E., Dingwall H.L., Villmoare B.A., Green D.J., Harris J.W.K, Braun D.R., Richmond B.G. 2016. Footprints reveal direct evidence of group behavior and locomotion in Homo erectus. Scientific Reports 6, 28766.

Hatala K.G., Roach N.T., Ostrofsky K.R., Wunderlich R.E., Dingwall H.L., Villmoare B.A., Green D.J., Braun D.R., Harris J.W.K., Behrensmeyer A.K., Richmond B.G., 2017. Hominin track assemblages from Okote Member deposits near Ileret, Kenya, and their implications for understanding fossil hominin paleobiology at 1.5 Ma. Journal of Human Evolution 112, 93-104.

Hatala K.G., Harcourt-Smith W.E.H., Gordon A.D., Zimmer B.W., Richmond B.G., Pobiner B.L., Green D.J., Metallo A., Rossi V., Liutkus-Pierce C.M., 2020. Snapshots of human anatomy, locomotion, and behaviour from Late Pleistocene footprints at Engare Sero, Tanzania. Scientific Reports 10, 7740.

Helm C.W., McCrea R.T., Cawthra H.C., Lockley M.G., Cowling R.M., Marean C.W., Thesen G.H.H., Pigeon T.S., Hattingh S., 2018a. A New Pleistocene Hominin Tracksite from the Cape South Coast, South Africa. Scientific Reports 8, 3772.

Helm C.W., McCrea R.T., Lockley M.G., Cawthra H.C., Thesen G.H.H., Mwankunda J.M., 2018b. Late Pleistocene vertebrate trace fossils in the Goukamma Nature Reserve, Cape south coast, South Africa. Palaeontologia Africana 52, 89-101.

Helm C.W., Lockley M.G., Cole K., Noakes T.D., McCrea R.T., 2019a. Hominin tracks in southern Africa: A review and an approach to identification. Paleontologia Africana 53, 81-96.

Helm C.W., Cawthra H.C., Hattingh R., Hattingh S., McCrea R.T., Thesen G.H.G., 2019b. Pleistocene vertebrate trace fossils of Robberg Nature Reserve. Palaeontologia Africana 54, 36-47.

Helm C.W., Lockley M.G., Cawthra H.C., De Vynck J.C., Dixon M.G., Helm C.J.Z., Thesen G.H.H., 2020a. Newly identified hominin trackways from the Cape south coast of South Africa. South African Journal of Science 116, 8156.

Helm C.W., Cawthra H.C., Cowling R.M., De Vynck J.C., Lockley M.G., Marean C.W., Thesen G.H.H., Venter J.A., 2020b. Pleistocene vertebrate tracksites on the Cape south coast of South Africa and their potential palaeoecological implications. Quaternary Science Reviews 235, 105857.

Helm C.M., Cawthra H.C., De Vynck J.C., Dixon M., Stear W., 2021. ElephantTracks: A Biogenic Cause of Potholes in Pleistocene South African Coastal Rocks. Journal of Coastal Research 37, 59-74.

Hewitt S.M., Zimmer B., Liutkus C., Carmichael S.K., McGinnis K., 2010. Field-mapping and petrographic analysis of volcanoes surrounding the Lake Natron Homo sapiens footprint site, northern Tanzania. American Geophysical Union, Fall Meeting 2010.

Huxley J.S., Teissier G., 1936. Terminology of relative growth. Nature 137, 780-781.

Jolliffe I.T., 2002. Principal Component Analysis. 2nd Ed. Springer, New York.

Jolliffe I.T., Cadima J., 2016. Principal component analysis: a review and recent development. Philosophical Transactions of the Royal Society A, Mathematical, Physical and Engineering Sciences 374. doi: 10.1098/rsta. 2015.0202.

Kennedy R.B., Pressman I.S., Chen S., Petersen P.H., Pressman A.E., 2003. Statistical analysis of barefoot impressions. Journal of Forensic Sciences 48, 55-63.

LaBarbera M., 1989. Analyzing body size as a factor in ecology and evolution. Annual Review of Ecology and Systematics 20, 97-117.

Liutkus-Pierce C.M., Zimmer B.W., Carmichael S.K., McIntosh W., Deino A., Hewitt S.M., McGinnis K.J., Hartney T., Brett J., Mana S., Deocampo D., Richmond B.G., Hatala K., Harcourt-Smith W., Pobiner B., Metallo A., Rossi V., 2016. Radioisotopic age, formation, and preservation of Late Pleistocene human footprints at Engare Sero, Tanzania. Palaeogeography, Palaeoclimatology, Palaeoecology 463, 68-82.

Lockley M.G., Vasquez R.G., Espinoza E. and Lucas S.G., 2009. America's most famous human footprints: history, context and first description of Mid-Holocene tracks from the shores of Lake Managua, Nicaragua. Ichnos 16, 55-69.

Luhr J.F., Giannetti B., 1987. The Brown Leucitic Tuff of Roccamonfina Volcano (Roman region, Italy). Contributions to Mineralogy and Petrology 95, 420-436.

Mahmoudvand R., Hassani H., 2009. Two new confidence intervals for the coefficient of variation in a normal distribution. Journal of Applied Statistics 36, 429-442.

Mallison H., Wings O., 2014. Photogrammetry in paleontology-a practical guide. Journal of Paleontological Technique 12, 1-31.

Marty D., Strasser A., Meyer C.A., 2009. Formation and taphonomy of human footprints in microbial mats of present-day tidal-flat environments: implications for the study of fossil footprints. Ichnos 16, 127-142.

Masao F.T., Ichumbaki E.B., Cherin M., Barili A., Boschian G., Iurino D.A., Menconero S., Moggi-Cecchi J., Manzi G., 2016. New footprints from Laetoli (Tanzania) provide evidence for marked body size variation in early hominins. eLife 5, e19568.

Mietto P., Avanzini M., Rolandi G., 2003. Human footprints in Pleistocene volcanic ash. Nature 422, 133.

Panarello A., 2016. Elementi di Paleoicnologia degli Ominidi. Armando Caramanica Editore, Marina di Minturno.

Panarello A., 2020. A snapshot on some everyday actions of a Middle Pleistocene hominin: the Trackway B at the Devil's Trails palaeontological site (Tora e Piccilli, Caserta, Central Italy). Journal of Anthropological Sciences 98, 27-47.

Panarello A., 2022. Rilevare, analizzare e interpretare le orme umane fossili. In: Mietto P., Panarello A., Di Vito M. (Eds.), 2001-2021: Vent'anni di ricerche sulle "Ciampate del diavolo". Dalla leggenda alla realtà scientifica. Miscellanea Istituto Nazionale di Geofisica e Vulcanologia 64, 107-122.

Panarello A., Mietto P., 2022a. Il sentiero più antico del mondo. In: Mietto P., Panarello A., Di Vito M. (Eds.), 2001-2021: Vent'anni di ricerche sulle "Ciampate del diavolo". Dalla leggenda alla realtà scientifica. Miscellanea Istituto Nazionale di Geofisica e Vulcanologia 64, 177-194.

Panarello A., Mietto P., 2022b. Atlante visuale del sentiero preistorico P1 di Tora e Piccilli. SUPPLEMENTO 4 to: Mietto P., Panarello A., Di Vito M.A. (Eds.), 2001-2021: Vent'anni di ricerche sulle "Ciampate del diavolo". Dalla leggenda alla realtà scientifica. Miscellanea Istituto Nazionale di Geofisica e Vulcanologia 64S3, pp. 232.

Panarello A., Santello L., Farinaro G., Bennett M.R., Mietto P., 2017a. Walking along the oldest human fossil pathway (Roccamonfina volcano, Central Italy)? Journal of Archaeological Science: Reports 13, 476-490.

Panarello A., Palombo M.R., Biddittu I., Mietto P., 2017b. Fifteen years along the "Devil's Trails": achievements and perspectives. Alpine and Mediterranean Quaternary 30, 137-154.

Panarello A., Palombo M.R., Biddittu I., Di Vito M.A., Farinaro G., Mietto P., 2020. On the devil's tracks: unexpected news from the Foresta ichnosite (Roccamonfina volcano, central Italy). Journal of Quaternary Science 35, 444-456.

Panarello A., Farinaro G., Mietto P., 2022a. L'icnosito della località Foresta di Tora e Piccilli e le impronte umane fossili. In: Mietto P., Panarello A., Di Vito M. (Eds.), 2001-2021: Vent'anni di ricerche sulle "Ciampate del diavolo". Dalla leggenda alla realtà scientifica. Miscellanea Istituto Nazionale di Geofisica e Vulcanologia 64, 123-164.

Panarello A., Farinaro G., Mietto P., 2022b. Il dataset dimensionale completo delle "Ciampate del diavolo". SUPPLEMENTO 1 to: Mietto P., Panarello A., Di Vito M.A. (Eds.), 2001-2021: Vent'anni di ricerche sulle "Ciampate del diavolo". Dalla leggenda alla realtà scientifica. Miscellanea Istituto Nazionale di Geofisica e Vulcanologia 64S1, pp. 38.

Panarello A., Farinaro G., Mietto P., 2022c. Costruzioni geometriche per la creazione del dataset dimensionale completo delle "Ciampate del diavolo". SUPPLEMENTO 2 to: Mietto P., Panarello A., Di Vito M.A. (Eds.), 2001-2021: Vent'anni di ricerche sulle "Ciampate del diavolo". Dalla leggenda alla realtà scientifica. Miscellanea Istituto Nazionale di Geofisica e Vulcanologia 64S2, pp. 46.

Panarello A., Farinaro G., Mietto P., 2022d. Atlante visuale delle "Ciampate del diavolo". SUPPLEMENTO 3 to: Mietto P., Panarello A., Di Vito M.A. (Eds.), 2001-2021: Vent'anni di ricerche sulle "Ciampate del diavolo". Dalla leggenda alla realtà scientifica. Miscellanea Istituto Nazionale di Geofisica e Vulcanologia 64S3, pp. 232.

Panarello A., Palombo, M.R., Mietto P., 2023. The Middle Pleistocene footprints of Foresta (Southern-Central Italy): research activities, achievements, and perspectives. Journal of Mediterranean Earth Sciences, 15, 1-22.

Pélabon C., Hilde C.H., Einum S., Gamelon M., 2020. On the use of the coefficient of variation to quantify and compare trait variation. Evolution Letters 4, 180-188.

Radicati di Brozolo F., Di Girolamo P., Turi B., Oddone M., 1988. ^{40}Ar-^{39}Ar and K-Ar dating of K-rich rocks from Roccamonfina volcano, Roman Comagmatic Region, Italy. Geochimica et Cosmochimica Acta 52, 1435-1441.

Raichlen D.A., Pontzer H., Sockol M.D., 2008. The Laetoli footprints and early hominin locomotor kinematics. Journal of Human Evolution 54, 112-117.

Roach N.T., Hatala K.G., Ostrofsky K.R., Villmoare B., Reeves J.S., Du A., Braun D.R., Harris J.W.K., Behrensmeyer A.K., Richmond B.G., 2016. Pleistocene footprints show intensive use of lake margin habitats by Homo erectus groups. Scientific Reports 6, 26374.

Roach N.T., Du A. Kevin, Hatala G., Ostrofsky K.R., Reeves J.S., Braun D.R., Harris J.W.K., Behrensmeyer A.K., Richmond B.G., 2018. Pleistocene animal communities of a 1.5 million-year-old lake margin grassland and their relationship to Homo erectus paleoecology. Journal of Human Evolution 122, 70-83.

Roberts D.L., 2008. Last Interglacial Hominid and Associated Vertebrate Fossil Trackways in Coastal Eolianites, South Africa. Ichnos 15, 190-207.

Roberts D., Berger L.R., 1997. Last Interglacial (c. 117 kyr) human footprints from South Africa. South African Journal of Science 93, 349-350.

Romano M., Citton P., 2017. Crouching theropod at the seaside. Matching footprints with metatarsal impressions and theropod authopods: a morphometric approach. Geological Magazine 154, 946-962.

Romano M., Citton P., Salvador I., Arobba D., Rellini I., Firpo M., Negrino F., Zunino M., Starnini E., Avanzini M., 2019. A multidisciplinary approach to a unique Palaeolithic human ichnological record from Italy (Bàsura Cave). Elife 8, e45204.

Rouchon V., Gillot P.Y., Quidelleur X., Chiesa S., Floris B., 2008. Temporal evolution of the Roccamonfina volcanic complex (Pleistocene), Central Italy. Journal of Volcanology and Geothermal Research 177, 500-514.

Santello L., 2010. Analysis of a trampled formation: the Brown Leucitic Tuff (Roccamonfina volcano, Southern Italy). PhD Dissertation in Earth Sciences - Department of Geosciences, Padua University, Padova (Italy), pp.134.

Scaillet S., Vita-Scaillet G., Guillou H., 2008. Oldest human footprints dated by Ar/Ar. Earth and Planetary Science Letters 275, 320-325.

Schmincke H.-U., Kutterolf S., Perez W., Rausch J., Freundt A., Strauch W., 2009. Walking through volcanic mud: the 2,100-year-old Acahualinca footprints (Nicaragua). I: Stratigraphy, lithology, volcanology and age of the Acahualinca section. Bulletin of Volcanology 71, 479-493.

Schmincke H.-U., Rausch J., Kutterolf S., Freundt A., 2010. Walking through volcanic mud: the 2,100 year-old Acahualinca footprints (Nicaragua) II: the Acahualinca people, environmental conditions and motivation. International Journal of Earth Sciences 99, 279-292.

Schmidt-Nielsen K., 1984. Scaling: Why is Animal Size So Important? Cambridge University Press.

Shechtman O., 2013. The coefficient of variation as an index of measurement reliability. In: Doi S., Williams G. (Eds.), Methods of Clinical Epidemiology. Springer Series on Epidemiology and Public Health. Springer, Berlin, Heidelberg, 39-49.

Sheret M., 1984. The coefficient of variation: weighting considerations. Social Indicators Research 15, 289-295.

Sokal R.R., Rohlf F.J., 1995. Biometry. W.H. Freeman and Company, New York.

Smith R.J., 2009. Use and misuse of the reduced major axis for line-fitting. American Journal of Physical Anthropology 140, 476-486.

Warton D.I., Wright I.J., Falster D.S., Westoby M., 2006. Bivariate line-fitting methods for allometry. Biological Review 81, 259-291.

Webb S., Cupper M.L., Robins R., 2006a. Pleistocene human footprints from the Willandra Lakes, southeastern Australia. Paper posted at ePublication@Bond University. http://epublications.bond.edu.au/hss_pubs/40.

Webb S., Cupper M.L., Robins R., 2006b. Pleistocene human footprints from the Willandra Lakes, southeastern Australia. Journal of Human Evolution 50, 405-413.

Webb S., 2007. Further research of the Willandra Lakes fossil footprint site, southeastern Australia. Journal of Human Evolution 52, 711-715.

Wiseman A.L.A., Stringer C.B., Ashton N., Bennett M.R., Hatala K.G., Duffy S., O'Brien T., De Groote I., 2020. The morphological affinity of the Early Pleistocene footprints from Happisburgh, England, with other footprints of Pliocene, Pleistocene, and Holocene age. Journal of Human Evolution 144, 102776.

Zimmer B., Liutkus C., Carmichael S., Richmond B., Hewitt S., Hatala K., Harcourt-Smith W.E.H., Gordon A., Mana S., Brett J., 2012. A snapshot in time: determining the age, environment, and social structures of early Homo Sapiens using trace fossils in volcaniclastic rocks at the Engare Sero footprint site, Lake Natron, Tanzania. Paper No. 8-4, Session No. 8-Booth #35 Volcanology (Posters), Cordilleran Section - 108th Annual Meeting (29-31 March 2012), Geological Society of America Abstracts with Programs 44, 13.

Zimmer B., Liutkus-Pierce C., Marshall S.T., Hatala K.G., Metallo A., Rossi V., 2018. Using differential structure-from-motion photogrammetry to quantify erosion at the Engare Sero footprint site, Tanzania. Quaternary Science Reviews 198, 226-241.

SAMPLE A (all footprints) - Reduced Major Axis (RMA) regression - Statistics

All Footprints

RMA Regression: Footprint width (Fw)-Footprint length (Fl)			
Slope AE	1.1528	Std. error a:	0.16454
t:	7.006	p (slope):	7.198E-9
Intercept AC	0.41185	Std. error b:	0.39032
95% bootstrapped confidence intervals (N=1999):			
Slope AE	(0.82285. 3.7878)		
Intercept AC	(-5.8424. 1.201)		
Correlation:			
r:	0.14865		
r2:	0.022097		
t:	1.0414		
p (uncorr.):	0.30289		
Permutation p:	0.2979		
RMA Regression: Footprint area (Fa)-Footprint length (Fl)			
Slope AE	0.5049	Std. error a:	0.043471
t:	11.615	p (slope):	1.5093E-15
Intercept AC	0.49624	Std. error b:	0.22814
95% bootstrapped confidence intervals (N=1999):			
Slope AE	(0.43069. 0.57754)		
Intercept AC	(0.10762. 0.88456)		
Correlation:			
r:	0.80261		
r2:	0.64418		
t:	9.322		
p (uncorr.):	2.3954E-12		
Permutation p:	0.0001		
RMA Regression: Fw/Fl x 100 (Fin)-Footprint length (Fl)			
Slope AE	-0.81611	Std. error a:	0.0827
t:	9.8683	p (slope):	3.9018E-13
Intercept AC	6.2715	Std. error b:	0.3169
95% bootstrapped confidence intervals (N=1999):			
Slope AE	(-0.93723. -0.61631)		
Intercept AC	(5.5039. 6.7422)		
Correlation:			
r:	-0.71211		
r2:	0.50711		
t:	-70274		
p (uncorr.):	6.6758E-9		
Permutation p:	0.0001		

Trackway A

RMA Regression: Footprint width (Fw)-Footprint length (Fl)			
Slope AE	0.79878	Std. error a:	0.13131
t:	6.0833	p (slope):	0.048969
Intercept AC	1.2647	Std. error b:	0.31412
95% bootstrapped confidence intervals (N=1999):			
Slope AE	(0.46864. 0.95594)		
Intercept AC	(0.88857. 2.0525)		
Correlation:			
r:	0.65767		
r2:	0.43253		
t:	4.0008		
p (uncorr.):	0.00064853		
Permutation p:	0.0017		
RMA Regression: Foot print area (Fa)-Footprint length (Fl)			
Slope AE	0.36937	Std. error a:	0.03841
	t:	96165	p (slope):
Intercept AC	1.2195	Std. error b:	0.20306
95% bootstrapped confidence intervals (N=1999):			
Slope AE	(0.26221. 0.43975)		
Intercept AC	(0.84373. 1.794)		
Correlation:			
r:	0.88529		
r2:	0.78373		
t:	8.5134		
p (uncorr.):	0.00044012		
Permutation p:	0.0001		
RMA Regression: Fw/Fl x 100 (Fin)-Footprint length (Fl)			
Slope AE	-1.0263	Std. error a:	0.22809
t:	4.4994	p (slope):	0.00021908
Intercept AC	7.0963	Std. error b:	0.87237
95% bootstrapped confidence intervals (N=1999):			
Slope AE	(-3.6635. -0.78603)		
Intercept AC	(6.1987. 17.171)		
Correlation:			
r:	-0.10992		
r2:	0.012082		
t:	-0.49457		
p (uncorr.):	0.62629		
Permutation p:	0.6274		

Trackway B

RMA Regression: Footprint width (Fw)-Footprint length (Fl)			
Slope AE	-0.98022	Std. error a:	0.25178
t:	3.8932	p (slope):	0.0014411
Intercept AC	5.4133	Std. error b:	0.59015
95% bootstrapped confidence intervals (N=1999):			
Slope AE		(-3.482. -0.56122)	
Intercept AC		(4.4386. 11.275)	
Correlation:			
r:	-0.10173		
r2:	0.010348		
t:	-0.39604		
p (uncorr.):	0.69765		
Permutation p:	0.7017		
RMA Regression: Footprint area (Fa)-Footprint length (Fl)			
Slope AE	0.3662	Std. error a:	0.085221
t:	4.297	p (slope):	0.00063558
Intercept AC	1.2045	Std. error b:	0.44495
95% bootstrapped confidence intervals (N=1999):			
Slope AE	(0.24868. 1.084)		
Intercept AC	(-2.5524. 1.8163)		
Correlation:			
r:	0.43316		
r2:	0.18763		
t:	1.8613		
p (uncorr.):	0.082412		
Permutation p:	0.0781		
RMA Regression: Fw/Fl x 100 (Fin)-Footprint length (Fl)			
Slope AE	-0.66568	Std. error a:	0.11613
t:	5.7323	p (slope):	0.03965
Intercept AC	5.6672	Std. error b:	0.44507
95% bootstrapped confidence intervals (N=1999):			
Slope AE	(-0.95881. -0.34158)		
Intercept AC	(4.432. 6.7823)		
Correlation:			
r:	-0.73723		
r2:	0.5435		
t:	-4.226		
p (uncorr.):	0.00073343		
Permutation p:	0.001		

Trackway C

RMA Regression: Footprint width (Fw)-Footprint length (Fl)			
Slope AE	-0.68983	Std. error a:	0.17859
t:	3.8626	p (slope):	0.018107
Intercept AC	4.7487	Std. error b:	0.41907
95% bootstrapped confidence intervals (N=1999):			
Slope AE	1.0233. 0.81454)		
Intercept AC	(1.2421. 5.5551)		
Correlation:			
r:	-0.85551		
r2:	0.7319		
t:	-3.73045		
p (uncorr.):	0.029807		
Permutation p:	0.0126		
RMA Regression: Footprint area (Fa)-Footprint length (Fl)			
Slope AE	0.88969	Std. error a:	0.4437
t:	2.0051	p (slope):	0.11544
Intercept AC	-1.4963	Std. error b:	2.3077
95% bootstrapped confidence intervals (N=1999):			
Slope AE	057296. 3.1876)		
Intercept AC	-1.3493. 3.2083)		
Correlation:			
r:	0.07162		
r2:	0.0051294		
t:	0.14361		
p (uncorr.):	0.89275		
Permutation p:	0.871		
RMA Regression: Fw/Fl x 100 (Fin)-Footprint length (Fl)			
Slope AE	-0.42099	Std. error a:	0.066743
t:	6.3076	p (slope):	0.0032302
Intercept AC	4.7387	Std. error b:	0.25503
95% bootstrapped confidence intervals (N=1999):			
Slope AE	58058. -0.15959)		
Intercept AC	(3.7471. 5.3623)		
Correlation:			
r:	-0.9484		
r2:	0.89946		
t:	-59821		
p (uncorr.):	0.0039253		
Permutation p:	0.0054		

SAMPLE B (selected footprints) - Reduced Major Axis (RMA) regression - Statistics

All Footprints

RMA Regression: Footprint width (Fw)-Footprint length (Fl)			
Slope AE	0.89389	Std. error a:	0.17957
t:	49.779	p (slope):	0.83526
Intercept b:	0.45847	Std. error b:	0.18522
95% bootstrapped confidence intervals (N=1999):			
Slope a:	(0.37559. 1.209)		
Intercept b:	(-0.13813. 0.98482)		
Correlation:			
r:	0.48294		
r2:	0.23323		
t:	2.404		
p (uncorr.):	0.026582		
Permutation p:	0.0233		
RMA Regression: Footprint area (Fa)-Footprint length (Fl)			
Slope AE	0.47767	Std. error a:	0.10242
t:	46.641	p (slope):	0.0001691
Intercept AC	0.65082	Std. error b:	0.54196
95% bootstrapped confidence intervals (N=1999):			
Slope AE	(0.23347. 1.5749)		
Intercept AC	(-5.1896. 1.9337)		
Correlation:			
r:	0.35578		
r2:	0.12658		
t:	16.594		
p (uncorr.):	0.11345		
Permutation p:	0.1077		
RMA Regression: Fw/Fl x 100 (Fin)-Footprint length (Fl)			
Slope AE	-0.92637	Std. error a:	0.19258
t:	48.102	p (slope):	0.00012163
Intercept AC	66.994	Std. error b:	0.73214
95% bootstrapped confidence intervals (N=1999):			
Slope AE	(-3.0914. -0.7512)		
Intercept AC	(6.0425. 14.971)		
Correlation:			
r:	-0.42291		
r2:	0.17885		
t:	-20.343		
p (uncorr.):	0.056122		
Permutation p:	0.0535		

Trackway A

RMA Regression: Footprint width (Fw)-Footprint length (Fl)			
Slope AE	0.15254	Std. error a:	0.053289
t:	28.625	p (slope):	0.024249
Intercept AC	28.326	Std. error b:	0.12915
95% bootstrapped confidence intervals (N=1999):			
Slope AE	(0.059607. 0.53379)		
Intercept AC	(1.9074. 3.0562)		
Correlation:			
r:	0.38175		
r2:	0.14573		
t:	10.928		
p (uncorr.):	0.31067		
Permutation p:	0.3099		
RMA Regression: Foot print area (Fa)-Footprint length (Fl)			
Slope AE	0.092524	Std. error a:	0.029991
	30.851	p (slope):	0.017689
Intercept AC	27.051	Std. error b:	0.16117
95% bootstrapped confidence intervals (N=1999):			
Slope AE	(-0.018946. 0.34601)		
Intercept AC	(1.348. 3.2996)		
Correlation:			
r:	0.51431		
r2:	0.26452		
t:	15.867		
p (uncorr.):	0.15661		
Permutation p:	0.1618		
RMA Regression: Fw/Fl x 100 (Fin)-Footprint length (Fl)			
Slope AE	0.162	Std. error a:	0.059183
t:	27.372	p (slope):	0.029034
Intercept AC	25.824	Std. error b:	0.22646
95% bootstrapped confidence intervals (N=1999):			
Slope AE	(0.068054. 0.58691)		
Intercept AC	(0.95372. 2.9452)		
Correlation:			
r:	0.25636		
r2:	0.065719		
t:	0.70171		
p (uncorr.):	0.50551		
Permutation p:	0.4905		

Trackway B

RMA Regression: Footprint width (Fw)-Footprint length (Fl)			
Slope AE	0.14873	Std. error a:	0.055602
t:	26.748	p (slope):	0.031776
Intercept AC	27.917	Std. error b:	0.12979
95% bootstrapped confidence intervals (N=1999):			
Slope AE	(0.02532. 0.5006)		
Intercept AC	(1.9683. 3.0832)		
Correlation:			
r:	0.14709	0.14709	
r2:	0.021636	0.021636	
t:	0.39345	0.39345	
p (uncorr.):	0.7057	0.7057	
Permutation p:	0.7248	0.7248	
RMA Regression: Footprint area (Fa)-Footprint length (Fl)			
Slope AE	-0.045899	Std. error a:	0.017192
t:	26.698	p (slope):	0.032009
Intercept AC	33.789	Std. error b:	0.08992
95% bootstrapped confidence intervals (N=1999):			
Slope AE	(-0.17122. -0.01971)		
Intercept AC	(3.2404. 4.0387)		
Correlation:			
r:	-0.13394		
r2:	0.017941		
t:	-0.35761		
p (uncorr.):	0.73118		
Permutation p:	0.7298		
RMA Regression: Fw/Fl x 100 (Fin)-Footprint length (Fl)			
Slope AE	-0.15313	Std. error a:	0.057873
t:	26.459	p (slope):	0.033137
Intercept AC	37.207	Std. error b:	0.21992
95% bootstrapped confidence intervals (N=1999):			
Slope AE	(-0.53912. -0.080895)		
Intercept AC	(3.4461. 5.1882)		
Correlation:			
r:	-0.011764		
r2:	0.00013839		
t:	-0.031127		
p (uncorr.):	0.97604		
Permutation p:	0.9767		

TABLE SI2 – The residuals' table reports the distances from each data point to the regression line. in the x and y directions (first and third columns). The results of the Durbin-Watson and Breusch-Pagan tests for normal distribution and independence between independent variable and residual variance (homoskedasticity) are reported in the second and fourth columns.

SAMPLE A (all the measured footprints) - RMA Regression - Residuals

All footprints / **TESTS**

RMA Regression: Footprint width (Fw)-F length (Fl)

Fw (Fw)	Fl (Fl)	Regress.	Residual	Std. Error of estimates	0.087174
24.069	32.465	31.865	0.060012		
24.159	32.465	31.968	0.049673	**Durbin-Watson statistic**	14815
24.159	31.781	31.968	-0.018764	*p* (no pos. autocoorelation)	0.03242
24.159	32.229	31.968	0.02605		
23.514	31.398	31.224	0.017412	**Breusch- Pagan statistic**	2366
23.224	31.822	3.089	0.093207	*p* (homoskedastic)	0.12882
23.321	31.355	31.003	0.035242		
24.336	31.987	32.172	-0.018548		
23.702	31.355	31.442	-0.0086774		
21.972	30.397	29.447	0.095027		
23.321	31.485	31.003	0.048202		
23.418	31.135	31.114	0.0021257		
23.979	31.527	3.176	-0.023311		
24.336	31.046	32.172	-0.11263		
24.596	3.157	32.472	-0.090164		
24.159	32.108	31.968	0.014026		
24.423	31.987	32.273	-0.028616		
2.451	32.108	32.373	-0.026426		
23.702	31.987	31.442	0.054502		
23.795	31.987	31.549	0.043778		
24.681	32.068	3.257	-0.050172		
24.596	31.987	32.472	-0.048492		
23.888	31.987	31.655	0.033154		
23.321	3.091	31.003	-0.0092093		
23.979	3.091	3.176	-0.085005		
23.514	31.355	31.224	0.013073		
23.026	31.355	30.662	0.069317		
23.026	30.445	30.662	-0.021655		
23.514	31.442	31.224	0.021731		
23.026	31.135	30.662	0.047338		
23.514	31.355	31.224	0.013073		
23.979	3.091	3.176	-0.085005		
23.979	31.135	3.176	-0.062532		
23.514	30.445	31.224	-0.077898		
23.026	31.355	30.662	0.069317		
23.026	31.442	30.662	0.077975		
23.514	31.398	31.224	0.017412		
23.609	31.398	31.333	0.0064851		
23.418	31.355	31.114	0.024105		
23.418	31.398	31.114	0.028443		
23.514	30.956	31.224	-0.026843		
24.849	30.634	32.764	-0.21296		
23.026	32.027	30.662	0.13657		
22.513	31.864	3.007	0.1793		
23.418	31.179	31.114	0.0065603		
23.418	31.179	31.114	0.0065603		
24.423	29.601	32.273	-0.26718		
24.423	29.601	32.273	-0.26718		
23.979	32.958	3.176	0.11979		
23.514	32.542	31.224	0.13182		

RMA Regression: Foot print area (Fa)-F length (Fl)

Fa	Fl (Fl)	Regress.	Residual	Std. Error of estimates	0.041975
54.806	32.465	32.634	-0.016946		
54.337	32.465	32.397	0.0067426	**Durbin-Watson statistic**	1.6432
52.832	31.781	31.638	0.014303	*p* (no pos. autocoorelation)	0.13376
54.027	32.229	32.241	-0.001206		
52.204	31.398	3.132	0.0078135	**Breusch- Pagan statistic**	0.41464
51.874	31.822	31.154	0.066839	*p* (homoskedastic)	0.51962
51.533	31.355	30.982	0.037336		
53.845	31.987	32.149	-0.01622		
51.874	31.355	31.154	0.020122		
49.053	30.397	29.729	0.066816		
51.761	31.485	31.097	0.038754		
52.149	31.135	31.293	-0.015767		
5.204	31.527	31.238	0.028972		
5.247	31.046	31.455	-0.040897		
52.983	3.157	31.714	-0.014382		
53.519	32.108	31.984	0.012429		
53.799	31.987	32.126	-0.013899		
5.425	32.108	32.353	-0.024476		
52.933	31.987	31.689	0.029822		
53.181	31.987	31.814	0.017293		
54.972	32.068	32.718	-0.064979		
53.566	31.987	32.008	-0.0021292		
53.566	31.987	32.008	-0.0021292		
52.832	3.091	31.638	-0.072709		
52.679	3.091	3.156	-0.064961		
53.279	31.355	31.863	-0.050812		
51.874	31.355	31.154	0.020122		
50.239	30.445	30.328	0.011704		
52.933	31.442	31.689	-0.024699		
51.533	31.135	30.982	0.015357		
52.781	31.355	31.612	-0.025688		
53.033	3.091	31.739	-0.082858		
51.985	31.135	3.121	-0.0074672		
5.118	30.445	30.803	-0.035814		
5.323	31.355	31.838	-0.048355		
51.533	31.442	30.982	0.045994		
52.832	31.398	31.638	-0.023919		
50.876	31.398	3.065	0.074844		
51.874	31.355	31.154	0.020122		
5.273	31.398	31.586	-0.018766		
51.475	30.956	30.952	0.00034644		
52.679	30.634	3.156	-0.092612		
52.679	32.027	3.156	0.046743		
51.705	31.864	31.068	0.079514		
52.204	31.179	3.132	-0.014069		
51.299	31.179	30.863	0.031603		
49.273	29.601	2.984	-0.023926		
49.273	29.601	2.984	-0.023926		

SAMPLE B (best-preserved footprints) - RMA Regression - Residuals

All footprints / **TESTS**

RMA Regression: Footprint width (Fw)-F length (Fl)

Fw (Fw)	Fl (Fl)	Regress.	Residual	Std. Error of estimates	0.045879
24.336	31.987	3231,0000	-0.032374		
24.159	32.108	32152,0000	-0.0043824	**Durbin-Watson statistic**	1.1698
24.423	31.987	32389,0000	-0.040181	*p* (no pos. autocoorelation)	0.020223
2.451	32.108	32466,0000	-0.03575		
23.702	31.987	31744,0000	0.024271	**Breusch- Pagan statistic**	0.0014155
23.795	31.987	31827,0000	0.015956	*p* (homoskedastic)	0.96999
24.681	32.068	32619,0000	-0.055071		
24.596	31.987	32543,0000	-0.055594		
23.888	31.987	3191,0000	0.0077171		
23.026	31.355	31139,0000	0.021572		
23.514	31.442	31575,0000	-0.013383		
23.514	31.355	31575,0000	-0.022041		
23.026	31.355	31139,0000	0.021572		
23.026	31.442	31139,0000	0.03023		
23.514	31.398	31575,0000	-0.017703		
23.609	31.398	3166,0000	-0.026176		
23.418	31.355	3149,0000	-0.013487		
23.418	31.398	3149,0000	-0.009149		
23.418	31.179	3149,0000	-0.031032		
23.514	32.958	31575,0000	0.1383		
23.514	32.542	31575,0000	0.096707		

RMA Regression: Foot print area (Fa)-F length (Fl)

Fa	Fl (Fl)	Regress.	Residual	Std. Error of estimates	0.051211
53.845	31.987	32.228	-0.024174		
53.519	32.108	32.073	0.0035864	**Durbin-Watson statistic**	1.4232
53.799	31.987	32.207	-0.021978	*p* (no pos. autocoorelation)	0.87766
5.425	32.108	32.422	-0.031328		
52.933	31.987	31.793	0.019385	**Breusch- Pagan statistic**	0.7465
53.181	31.987	31.911	0.0075317	*p* (homoskedastic)	0.38759
54.972	32.068	32.767	-0.069865		
53.566	31.987	32.095	-0.010843		
53.566	31.987	32.095	-0.010843		
51.874	31.355	31.287	0.006801		
52.933	31.442	31.793	-0.035136		
52.781	31.355	3.172	-0.036538		
5.323	31.355	31.935	-0.057983		
51.533	31.442	31.124	0.031745		
52.832	31.398	31.745	-0.03463		
50.876	31.398	3.081	0.058806		
51.874	31.355	31.287	0.006801		
5.273	31.398	31.696	-0.029756		
52.204	31.179	31.444	-0.026492		
52.095	32.958	31.392	0.15659		
52.444	32.542	31.559	0.098321		

RMA Regression: Fl/Fw-Fl (Fl)-F length (Fl)

Fl/Fw	Fl (Fl)	Regress.	Residual	Std. Error of estimates	0.048469
38.395	31.987	31.426	0.056039		
38.111	32.108	31.689	0.041942	**Durbin-Watson statistic**	0.63906
3.848	31.987	31.347	0.063973	*p* (no pos. autocoorelation)	0.0000798
38.459	32.108	31.367	0.074166		
37.773	31.987	32.002	-0.0014928	**Breusch- Pagan statistic**	4.1132
37.865	31.987	31.917	0.0069479	*p* (homoskedastic)	0.04255
3.867	32.068	31.171	0.089712		
38.649	31.987	3.119	0.079642		
37.955	31.987	31.834	0.015313		
37.728	31.355	32.044	-0.068921		
38.111	31.442	31.689	-0.02475		
38.199	31.355	31.607	-0.025246		
37.728	31.355	32.044	-0.068921		
37.635	31.442	3.213	-0.068821		
38.155	31.398	31.648	-0.024979		
38.265	31.398	31.547	-0.014833		
38.111	31.355	31.689	-0.033408		
38.067	31.398	3.173	-0.033177		
38.286	31.179	31.526	-0.0347		
3.661	32.958	3.308	-0.012116		
37.013	32.542	32.706	-0.01637		

Track A / **TESTS**

RMA Regression: Footprint width (Fw)-F length (Fl)

Fw (Fw)	Fl (Fl)	Regress.	Residual	Std. Error of estimates	0.00584
24.336	31.987	32.039	-0.0051909		
24.159	32.108	32.012	0.0096795	**Durbin-Watson statistic**	2.6246
24.423	31.987	32.052	-0.0065232	*p* (no pos. autocoorelation)	0.89606
2.451	32.108	32.065	0.0043266		
23.702	31.987	31.942	0.0044755	**Breusch- Pagan statistic**	0.66703
23.795	31.987	31.956	0.0030565	*p* (homoskedastic)	0.41409
24.681	32.068	32.091	-0.0023214		
24.596	31.987	32.078	-0.0091533		
23.888	31.987	3.197	0.0016506		

RMA Regression: Foot print area (Fa)-F length (Fl)

Fa	Fl (Fl)	Regress.	Residual	Std. Error of estimates	0.0051443
53.845	31.987	32.033	-0.0046101		
53.519	32.108	32.003	0.01058	**Durbin-Watson statistic**	2.5738
53.799	31.987	32.029	-0.0041847	*p* (no pos. autocoorelation)	0.9091
5.425	32.108	3.207	0.0038173		
52.933	31.987	31.948	0.0038272	**Breusch- Pagan statistic**	0.30789
53.181	31.987	31.971	0.0015312	*p* (homoskedastic)	0.57898
54.972	32.068	32.137	-0.006905		
53.566	31.987	32.007	-0.0020279		
53.566	31.987	32.007	-0.0020279		

RMA Regression: Fl/Fw-Fl (Fl)-F length (Fl)

Fl/Fw	Fl (Fl)	Regress.	Residual	Std. Error of estimates	0.006654
38.395	31.987	32.044	-0.0057565		
38.111	32.108	31.998	0.011008	**Durbin-Watson statistic**	2.6968
3.848	31.987	32.058	-0.007144	*p* (no pos. autocoorelation)	0.91081
38.459	32.108	32.055	0.0053723		
37.773	31.987	31.944	0.0043043	**Breusch- Pagan statistic**	0.5923
37.865	31.987	31.958	0.0028282	*p* (homoskedastic)	0.44153
3.867	32.068	32.089	-0.0020932		

55.053	32.958	32.759	0.019933		
52.444	32.542	31.442	0.11009		
RMA Regression: Fl/Fw-Fl (Fl)-F length (Fl)					
Fl/Fw	Fl (Fl)	Regress.	Residual	**Std. Error of estimates**	0.050692
37.658	32.465	31.981	0.048348		
37.751	32.465	31.906	0.05587	**Durbin-Watson statistic**	1.0831
38.437	31.781	31.346	0.043489	*p* (no pos. autocoorelation)	0.00033995
37.977	32.229	31.721	0.050754		
38.155	31.398	31.576	-0.017773	**Breusch- Pagan statistic**	0.63867
37.448	31.822	32.153	-0.033113	*p* (homoskedastic)	0.42419
38.022	31.355	31.685	-0.032969		
38.395	31.987	31.381	0.060606		
38.395	31.355	31.381	-0.0025733		
37.635	30.397	3.2	-0.16028		
37.887	31.485	31.795	-0.031013		
3.833	31.135	31.433	-0.029835		
38.501	31.527	31.293	0.023397		
39.338	31.046	30.611	0.043504		
3.908	3.157	30.821	0.074887		
38.111	32.108	31.612	0.049635		
3.848	31.987	31.311	0.067596		
38.459	32.108	31.328	0.078024		
37.773	31.987	31.888	0.0099218		
37.865	31.987	31.813	0.017358		
3.867	32.068	31.156	0.091239		
38.649	31.987	31.173	0.081399		
37.955	31.987	31.739	0.024727		
38.459	3.091	31.328	-0.041777		
3.912	3.091	30.788	0.0122		
38.199	31.355	3.154	-0.018524		
37.728	31.355	31.925	-0.057001		
38.628	30.445	3.119	-0.074464		
38.111	31.442	31.612	-0.017056		
37.932	31.135	31.758	-0.062267		
38.199	31.355	3.154	-0.018524		
3.912	3.091	30.788	0.0122		
38.898	31.135	3.097	0.016518		
3.912	30.445	30.788	-0.03432		
37.728	31.355	31.925	-0.057001		
37.635	31.442	3.2	-0.055882		
38.155	31.398	31.576	-0.017773		
38.265	31.398	31.487	-0.0088339		
38.111	31.355	31.612	-0.025714		
38.067	31.398	31.648	-0.024995		
38.607	30.956	31.207	-0.025125		
40.271	30.634	29.849	0.078493		
37.038	32.027	32.488	-0.046054		
36.687	31.864	32.774	-0.091086		
38.286	31.179	31.469	-0.028941		
38.286	31.179	31.469	-0.028941		
40.877	29.601	29.355	0.024598		
40.877	29.601	29.355	0.024598		
37.062	32.958	32.468	0.049044		
37.013	32.542	32.508	0.0034298		

Track A				TESTS	
RMA Regression: Footprint width (Fw)-F length (Fl)					
Fw (Fw)	Fl (Fl)	Regress.	Residual	**Std. Error of estimates**	0.039507
24.069	32.465	31.874	0.05914		
24.159	32.465	31.945	0.051976	**Durbin-Watson statistic**	1219
24.159	31.781	31.945	-0.016461	*p* (no pos. autocoorelation)	0.0305637
24.159	32.229	31.945	0.028353		
23.514	31.398	3.143	-0.0031306	**Breusch- Pagan statistic**	0.95606
23.224	31.822	31.198	0.062403	*p* (homoskedastic)	0.32818
23.321	31.355	31.276	0.0078926		
24.336	31.987	32.087	-0.00998		
23.702	31.355	3.158	-0.022541		
21.972	30.397	30.198	0.019918		
23.321	31.485	31.276	0.020852		
23.418	31.135	31.353	-0.021804		
23.979	31.527	31.801	-0.027386		
24.336	31.046	32.087	-0.10407		
24.596	3.157	32.294	-0.072401		
24.159	32.108	31.945	0.016329		
24.423	31.987	32.156	-0.016956		
2.451	32.108	32.225	-0.011702		
23.702	31.987	3.158	0.040638		
23.795	31.987	31.655	0.033208		
24.681	32.068	32.362	-0.029397		
24.596	31.987	32.294	-0.030729		
23.888	31.987	31.728	0.025846		
RMA Regression: Foot print area (Fa)-F length (Fl)					
Fa	Fl (Fl)	Regress.	Residual	**Std. Error of estimates**	0.02158
54.337	32.465	32.265	0.019988		
52.832	31.781	31.709	0.0071472	**Durbin-Watson statistic**	21468
54.027	32.229	3.215	0.0078315	*p* (no pos. autocoorelation)	0.65847
52.204	31.398	31.477	-0.00786		
51.874	31.822	31.355	0.046697	**Breusch- Pagan statistic**	0.0083332
51.533	31.355	31.229	0.012573	*p* (homoskedastic)	0.92727
53.845	31.987	32.083	-0.0096472		
51.874	31.355	31.355	-0.20352		
49.053	30.397	30.313	0.0084373		
51.761	31.485	31.314	0.017089		
52.149	31.135	31.457	-0.032175		
5.204	31.527	31.417	0.011082		
5.247	31.046	31.575	-0.052956		
52.983	3.157	31.765	-0.019489		
53.519	32.108	31.963	0.014578		
53.799	31.987	32.066	-0.007949		
5.425	32.108	32.233	-0.012419		
52.933	31.987	31.746	0.024035		
53.181	31.987	31.838	0.01487		
54.972	32.068	32.499	-0.043135		
53.566	31.987	3.198	0.00066136		
53.566	31.987	3.198	0.00066136		
RMA Regression: Fl/Fw-Fl (Fl)-F length (Fl)					
Fl/Fw	Fl (Fl)	Regress.	Residual	**Std. Error of estimates**	0.061721
37.751	32.465	32.221	0.024422		

38.649	31.987	32.086	-0.009884		
37.955	31.987	31.973	0.0013654		

Track B				TESTS	
RMA Regression: Footprint width (Fw)-F length (Fl)					
Fw (Fw)	Fl (Fl)	Regress.	Residual	**Std. Error of estimates**	0.44434
23.026	31.355	31.342	0.0013078		
23.514	31.442	31.414	0.0027095	**Durbin-Watson statistic**	2.0351
23.514	31.355	31.414	-0.0059486	*p* (no pos. autocoorelation)	0.62746
23.026	31.355	31.342	0.0013078		
23.026	31.442	31.342	0.0099658	**Breusch- Pagan statistic**	0.97445
23.514	31.398	31.414	-0.0016102	*p* (homoskedastic)	0.32357
23.609	31.398	31.429	-0.0030199		
23.418	31.355	3.14	-0.0045253		
23.418	31.398	3.14	-0.00018694		
RMA Regression: Foot print area (Fa)-F length (Fl)					
Fa	Fl (Fl)	Regress.	Residual	**Std. Error of estimates**	0.44775
51.874	31.355	31.408	-0.0053072		
52.933	31.442	31.359	0.0082124	**Durbin-Watson statistic**	2.3667
52.781	31.355	31.366	-0.0011428	*p* (no pos. autocoorelation)	0.86381
5.323	31.355	31.346	0.0009178		
51.533	31.442	31.424	0.001786	**Breusch- Pagan statistic**	0.11722
52.832	31.398	31.364	0.0034291	*p* (homoskedastic)	0.73207
50.876	31.398	31.454	-0.005549		
51.874	31.355	31.408	-0.0053072		
5.273	31.398	31.369	0.0029608		
RMA Regression: Fl/Fw-Fl (Fl)-F length (Fl)					
Fl/Fw	Fl (Fl)	Regress.	Residual	**Std. Error of estimates**	0.0047829
37.728	31.355	3.143	-0.0075376		
38.111	31.442	31.372	0.0069908	**Durbin-Watson statistic**	2.1533
38.199	31.355	31.358	-0.0003181	*p* (no pos. autocoorelation)	0.68719
37.728	31.355	3.143	-0.0075376		
37.635	31.442	31.444	-0.00029408	**Breusch- Pagan statistic**	1.1207
38.155	31.398	31.365	0.0033472	*p* (homoskedastic)	0.29876
38.265	31.398	31.348	0.0050244		
38.111	31.355	31.372	-0.0016672		
38.067	31.398	31.378	0.0019921		

38.437	31.781	31.516	0.026477	**Durbin-Watson statistic**	11505
37.977	32.229	31.988	0.024071	*p* (no pos. autocoorelation)	0.0119306
38.155	31.398	31.806	-0.040718		
37.448	31.822	32.531	-0.070923	**Breusch- Pagan statistic**	10462
38.022	31.355	31.942	-0.05871	*p* (homoskedastic)	0.30639
38.395	31.987	3.156	0.042692		
38.395	31.355	3.156	-0.020487		
37.635	30.397	32.339	-0.19416		
37.887	31.485	3.208	-0.059589		
3.833	31.135	31.626	-0.049109		
38.501	31.527	3.145	0.0077309		
39.338	31.046	30.592	0.045417		
3.908	3.157	30.856	0.071383		
38.111	32.108	31.851	0.025762		
3.848	31.987	31.472	0.051482		
38.459	32.108	31.494	0.061462		
37.773	31.987	32.197	-0.021045		
37.865	31.987	32.104	-0.011694		
3.867	32.068	31.277	0.07912		
38.649	31.987	31.298	0.06884		
37.955	31.987	32.011	-0.0024269		

Track B				**TESTS**	
RMA Regression: Footprint width (Fw)-F length (Fl)					
Fw (Fw)	**Fl (Fl)**	**Regress.**	**Residual**	**Std. Error of estimates**	0.042743
23.321	3.091	31.273	-0.036269		
23.979	3.091	30.629	0.028182	**Durbin-Watson statistic**	21119
23.514	31.355	31.085	0.027034	*p* (no pos. autocoorelation)	0.62992
23.026	31.355	31.563	-0.020792		
23.026	30.445	31.563	-0.11176	**Breusch- Pagan statistic**	0.74963
23.514	31.442	31.085	0.035692	*p* (homoskedastic)	0.38659
23.026	31.135	31.563	-0.04277		
23.514	31.355	31.085	0.027034		
23.979	3.091	30.629	0.028182		
23.979	31.135	30.629	0.050655		
23.514	30.445	31.085	-0.063938		
23.026	31.355	31.563	-0.020792		
23.026	31.442	31.563	-0.012133		
23.514	31.398	31.085	0.031372		
23.609	31.398	30.992	0.040663		
23.418	31.355	31.178	0.017653		
23.418	31.398	31.178	0.021992		
RMA Regression: Foot print area (Fa)-F length (Fl)					
Fa	**Fl (Fl)**	**Regress.**	**Residual**	**Std. Error of estimates**	0.33954
52.832	3.091	31.392	-0.048201		
52.679	3.091	31.336	-0.042581	**Durbin-Watson statistic**	14683
53.279	31.355	31.556	-0.020108	*p* (no pos. autocoorelation)	0.19246
51.874	31.355	31.042	0.031339		
50.239	30.445	30.443	0.00024298	**Breusch- Pagan statistic**	10521
52.933	31.442	31.429	0.0012098	*p* (homoskedastic)	0.0502
51.533	31.135	30.917	0.021846		
52.781	31.355	31.374	-0.0018857		
53.033	3.091	31.466	-0.055562		
51.985	31.135	31.082	0.0052914		
5.118	30.445	30.787	-0.034221		
5.323	31.355	31.538	-0.018326		
51.533	31.442	30.917	0.052483		
52.832	31.398	31.392	0.00058913		
50.876	31.398	30.676	0.07222		
51.874	31.355	31.042	0.031339		
5.273	31.398	31.355	0.0043259		
RMA Regression: Fl/Fw-Fl (Fl)-F length (Fl)					
Fl/Fw	**Fl (Fl)**	**Regress.**	**Residual**	**Std. Error of estimates**	0.23118
38.459	3.091	3.107	-0.015998		
3.912	3.091	3.063	0.02803	**Durbin-Watson statistic**	17918
38.199	31.355	31.243	0.011162	*p* (no pos. autocoorelation)	0.37193
37.728	31.355	31.557	-0.020223		
38.628	30.445	30.958	-0.051235	**Breusch- Pagan statistic**	25561
38.111	31.442	31.302	0.013955	*p* (homoskedastic)	0.10987
37.932	31.135	31.421	-0.02857		
38.199	31.355	31.243	0.011162		
3.912	3.091	3.063	0.02803		
38.898	31.135	30.778	0.035694		
3.912	30.445	3.063	-0.01849		
37.728	31.355	31.557	-0.020223		
37.635	31.442	31.619	-0.017714		
38.155	31.398	31.273	0.012574		
38.265	31.398	3.12	0.019866		
38.111	31.355	31.302	0.0052969		
38.067	31.398	31.331	0.0066833		

Track C				**TESTS**	
RMA Regression: Footprint width (Fw)-F length (Fl)					
Fw (Fw)	**Fl (Fl)**	**Regress.**	**Residual**	**Std. Error of estimates**	0.026314
23.514	30.956	31.267	-0.031119		
24.849	30.634	30.346	0.028808	**Durbin-Watson statistic**	15626
23.026	32.027	31.604	0.042393	*p* (no pos. autocoorelation)	0.57673
22.513	31.864	31.957	-0.0093846		
23.418	31.179	31.333	-0.015348	**Breusch- Pagan statistic**	0.1074
23.418	31.179	31.333	-0.015348	*p* (homoskedastic)	0.74312
RMA Regression: Foot print area (Fa)-F length (Fl)					
Fa	**Fl (Fl)**	**Regress.**	**Residual**	**Std. Error of estimates**	0.066702
51.475	30.956	30.834	0.012215		
52.679	30.634	31.904	-0.12706	**Durbin-Watson statistic**	23579
52.679	32.027	31.904	0.012298	*p* (no pos. autocoorelation)	0.8162
51.705	31.864	31.038	0.082537		
52.204	31.179	31.482	-0.030236	**Breusch- Pagan statistic**	0.87812
51.299	31.179	30.677	0.050242	*p* (homoskedastic)	0.34872
RMA Regression: Fl/Fw-Fl (Fl)-F length (Fl)					
Fl/Fw	**Fl (Fl)**	**Regress.**	**Residual**	**Std. Error of estimates**	0.015726
38.607	30.956	31.133	-0.017768		
40.271	30.634	30.433	0.0201	**Durbin-Watson statistic**	16289
37.038	32.027	31.794	0.023322	*p* (no pos. autocoorelation)	0.57154
36.687	31.864	31.942	-0.0078449		
38.286	31.179	31.269	-0.0089045	**Breusch- Pagan statistic**	0.23976
38.286	31.179	31.269	-0.0089045	*p* (homoskedastic)	0.62438

TABLE SI3 - PCA analysis: Scores of the Foresta "Devil Trails" footprints included in the samples A (all the measured footprints) and B (best-preserved footprints), obtained by using different sets of their measurements. The PCA scores were computed using vector products with the original data.

Sample A - PCA Scores

Variables: Footprint length, windth, area, windth/length ratio x 100					Variables: Footprint length, windth, area				Variables: Footprint length, windth, windth/lengthratio x 100			
Cases	PC 1	PC 2	PC 3	PC 4	Cases	PC 1	PC 2	PC 3	Cases	PC 1	PC 2	PC 3
A01L	47.743	-12.379	-0.23417	-0.080925	A01L	47.685	0.16647	-0.28107	A01L	-31.528	15.516	-0.030937
A02R	36.75	-12.564	0.33261	-0.036947	A02R	36.699	0.60855	0.067861	A02R	-27.631	16.859	-0.019958
A03L	46.305	0.9192	0.66449	0.069183	A03L	4.658	0.27882	0.48526	A03L	0.68509	0.90798	0.04716
A04R	29.704	-0.41706	0.25444	0.0071297	A04R	29.679	0.31241	0.11733	A04R	-16.359	1.39	0.022232
A05L	-73.626	-0.6614	-0.1447	0.035053	A05L	-73.794	0.026362	-0.0943	A05L	-0.35181	-0.47572	0.033594
A06R	-13.219	-41.465	0.35942	0.0082141	A06R	-13.332	13.148	-0.069006	A06R	-36.222	-0.43826	-0.023791
A07L	-19.333	-16.941	0.084441	0.034908	A07L	-19.373	0.46738	-0.03575	A07L	-0.9115	-0.78602	0.012116
A08R	25.629	14.275	0.2838	0.053949	A08R	25.66	-0.14618	0.29499	A08R	0.3661	13.853	0.066722
A09R	-13.388	0.21961	0.28237	0.059491	A09R	-13.374	0.1425	0.22064	A09R	0.74262	-0.22629	0.036373
A10L	-57.336	-44.352	-10.271	0.031342	A10L	-57.444	0.23554	-0.8326	A10L	-2.032	-35.671	0.017059
A11R	-15.308	-21.915	0.085531	0.030646	A11R	-15.364	0.59452	-0.071878	A11R	-15.705	-0.66074	0.010679
A12L	-84.138	0.20051	-0.54677	0.010178	A12L	-8.407	-0.50255	-0.27983	A12L	0.57654	-0.86056	0.02549
A13R	-10.385	0.75748	0.72169	0.085543	A13R	-10.355	0.35444	0.52047	A13R	11.284	0.36622	0.047735
A14L	-25.645	53.184	0.25444	0.04348	A14L	-24.082	-11.344	0.52954	A14L	53.897	0.51189	0.037947
A16L	75.175	41.981	0.8154	0.10606	A16L	76.393	-0.42988	0.81658	A16L	38.273	13.932	0.084792
A17R	18.69	-0.18443	0.54544	0.029904	A17R	18.678	0.47832	0.31296	A17R	-0.97689	12.647	0.023669
A18L	24.62	17.872	0.43332	0.071481	A18L	24.662	-0.12274	0.41605	A18L	0.75578	15.196	0.077701
A21R	34.622	20.109	0.30897	0.04714	A21R	34.666	-0.2652	0.34148	A21R	0.58184	18.018	0.067584
A22L	67.326	-2.074	0.32209	-0.16052	A22L	66.711	0.7782	0.040001	A22L	-23.617	0.44545	-0.010129
A23R	11.714	-14.873	0.22124	0.0016485	A23R	11.667	0.55046	0.024343	A23R	-1.972	0.57972	0.00084954
A24L	51.563	36.652	-0.24081	0.029852	A24L	51.645	-11.119	0.13231	A24L	15.809	20.286	0.090021
A25R	19.607	23.932	0.85754	0.11448	A25R	19.671	0.049739	0.72654	A25R	15.351	17.881	0.099658
A26L	19.691	-0.78723	-0.0047863	-0.0046207	A26L	19.659	0.19712	-0.059676	A26L	-15.823	0.71398	0.011828
B00L	45.234	13.757	-1.477	-0.049617	B00L	45.541	-15.194	-0.76604	B00L	12.852	-12.036	0.016907
B01R	14.426	44.315	-0.52877	-0.013866	B01R	15.678	-15.227	-0.009742	B01R	43.946	-0.17313	0.015127
B02L	13.593	0.34903	-1.077	-0.022588	B02L	13.592	-0.95099	-0.59117	B02L	-0.13214	-0.51748	0.034074
B03R	-13.308	-27.565	-0.50643	-0.0065231	B03R	-13.384	0.27146	-0.4673	B03R	-21.759	-12.115	-0.0011623
B04L	-40.479	0.64329	-0.48265	0.0036728	B04L	-40.444	-0.56218	-0.21886	B04L	23.129	-20.241	-0.011238
B05R	66.256	-0.34814	-0.67289	0.00013462	B05R	66.092	-0.46154	-0.39498	B05R	-0.57148	-0.43396	0.033115
B06L	-19.348	-19.989	-0.55319	0.017916	B06L	-19.4	0.031653	-0.42228	B06L	-1.173	-14.429	0.020891
B07R	36.093	-0.029168	-0.6597	0.0038575	B07R	36.035	-0.53234	-0.3633	B07R	-0.13214	-0.51748	0.034074
B08L	84.315	46.963	-0.82086	-0.032378	B08L	85.599	-18.158	-0.16925	B08L	43.946	-0.17313	0.015127
B08aR	-11.481	27.622	0.27655	0.05014	B08aR	-11.395	-0.48749	0.37819	B08aR	32.008	0.013023	0.032389
B10R	-25.567	35.848	-0.50108	-0.037954	B10R	-25.454	-12.823	-0.069282	B10R	46.429	-12.621	-0.034975
B11L	12.651	-17.732	-15.913	-0.075282	B11L	12.586	-0.81701	-10.598	B11L	-21.759	-12.115	-0.0011623
B12R	-19.277	-34.158	-0.14406	0.013555	B12R	-19.369	0.71905	-0.2939	B12R	-26.153	-1.128	-0.0021206
B13L	46.183	-0.20756	-0.64543	0.0033183	B13L	46.069	-0.47601	-0.36775	B13L	-0.35181	-0.47572	0.033594
B15R	-30.34	-10.371	0.93994	0.091667	B15R	-30.352	0.97082	0.52808	B15R	0.13327	-0.3188	0.024915
B16L	-13.353	-10.697	-0.058132	0.033928	B16L	-13.379	0.19777	-0.074196	B16L	-0.52182	-0.65175	0.023095
B18L	2.632	-0.68076	-0.66977	-0.00628	B18L	26.077	-0.37386	-0.42045	B18L	-0.74149	-0.60999	0.022616
C05R	-74.048	0.022119	-0.53249	0.0096386	C05R	-74.036	-0.44621	-0.28428	C05R	0.35687	-0.8188	0.025011
C07L	-23.379	-0.58299	0.13514	0.051952	C07L	-23.385	0.22362	0.080314	C07L	0.35687	-0.8188	0.025011
C08R	-20.45	11.057	-0.14512	0.02928	C08R	-20.41	-0.41139	0.018528	C08R	19.403	-0.87068	0.018728
C09L	12.473	10.574	0.36733	-0.049513	C09L	15.553	-22.961	0.86299	C09L	10.468	11.229	-0.049131
C10R	18.277	-53.588	-0.18494	-0.069801	C10R	1.671	12.147	-0.51566	C10R	-54.045	-0.47533	-0.067802
C12R	-16.127	-73.557	-0.23107	-0.06686	C12R	-16.334	16.676	-0.67025	C12R	-6.665	-1.359	-0.081463
D01R	-54.871	12.265	12.118	-0.26835	D01R	-54.484	-19.218	12.625	D01R	14.373	-0.13089	-0.34951
E03R	-89.875	-79.135	23.455	-0.12583	E03R	-92.003	39.399	0.66655	E03R	-76.789	14.475	-0.24064
E02L	53.866	-37.363	0.22133	-0.1798	E02L	53.735	12.103	-0.27765	E02L	-59.213	20.735	-0.14643
F02R	-25.957	-5.869	13.554	-0.051586	F02R	-27.576	25.875	0.31669	F02R	-58.349	0.8522	-0.11743

Sample B - PCA Scores

Variables: Footprint length, windth, area, windth/length ratio x 100					Variables: Footprint length, windth, area				Variables: Footprint length, windth, windth/lengthratio x 100			
Cases	PC 1	PC 2	PC 3	PC4	Cases	PC 1	PC 2	PC 3	Cases	PC 1	PC 2	PC 3
A08R	18.725	0.5224	0.40787	0.0071051	A08R	18.659	0.12983	0.19511	A08R	15.905	0.9838	0.0080705
A17R	11.666	-0.47642	0.42348	0.0072532	A17R	11.663	0.56131	0.10681	A17R	0.24203	0.94469	0.0072624
A18L	17.752	0.93216	0.64454	0.0087328	A18L	17.661	0.16393	0.31518	A18L	19.878	10.942	0.0069881
A21R	27.733	0.27416	0.42605	-0.00054391	A21R	27.665	0.24924	0.17152	A21R	1.831	13.865	0.002933
A22L	-0.41191	-11.909	-0.021457	0.014311	A22L	-0.34886	0.47415	-0.10514	A22L	-11.901	0.21066	0.015647
A23R	46.028	-10.477	-0.068018	0.011647	A23R	46.511	0.37371	-0.10974	A23R	-0.7929	0.32111	0.014565
A24L	44.758	0.47278	-0.0067242	-0.017275	A24L	44.66	-0.20791	0.028601	A24L	28.421	15.524	-0.0057805
A25R	12.813	18.849	12.595	0.014135	A25R	12.668	0.2994	0.61764	A25R	27.823	13.151	0.0048234
A26L	12.611	-10.377	-0.25619	0.0068358	A26L	12.65	0.20599	-0.17667	A26L	-0.39566	0.43155	0.013482
B03R	-20.427	0.12599	-0.68765	0.015192	B03R	-20.386	-0.64847	-0.20877	B03R	-11.048	-14.545	0.015468
B05R	-0.35615	0.70823	-0.62957	-0.0039827	B05R	-0.3793	-0.83998	-0.15132	B05R	0.54405	-0.77541	0.00053437
B07R	-33.309	12.877	-0.50641	-0.014624	B07R	-33.819	-0.97129	-0.065543	B07R	0.97735	-0.88532	-0.012563
B11L	55.184	-1.029	-1.915	-0.0034083	B11L	56.023	-12.315	-0.74899	B11L	-11.048	-14.545	0.015468
B12R	-26.433	-0.053727	-0.38597	0.032272	B12R	-26.379	-0.31534	-0.10755	B12R	-15.381	-13.446	0.028565
B13L	-23.425	10.202	-0.54439	-0.0089454	B13L	-23.803	-0.89442	-0.098043	B13L	0.7607	-0.83036	-0.0060145
B15R	-37.238	30.306	13.336	-0.0052095	B15R	-37.362	-0.097913	0.72846	B15R	12.539	-0.70298	-0.029716
B16L	-20.32	16.776	0.1066	-0.003374	B16L	-20.376	-0.60176	0.18839	B16L	0.58011	-0.99576	-0.011481
B18L	-43.635	0.74371	-0.63944	-0.0084269	B18L	-43.817	-0.86125	-0.15578	B18L	0.36346	-0.94081	-0.0049321
C05R	-14.295	23.035	-0.21353	-0.033241	C05R	-14.387	-11.335	0.11061	C05R	14.467	-12.156	-0.037676
E03R	-16.609	-58.863	0.94973	-0.038384	E03R	-16.296	32.918	-0.26434	E03R	-64.416	15.329	-0.04466
F02R	-10.052	-42.622	0.3229	0.01993	F02R	-98.213	20.539	-0.27045	F02R	-4.634	0.82682	0.019018

Sample A: PCA Loadings				
Variable	**Variables: Fl, Fw, Fa, and Fin**			
	PC 1	**PC 2**	**PC 3**	**PC 4**
Fl	0.10676	0.12917	0.9598	0.22516
Fw	0.0032548	-0.0068518	-0.22785	0.97367
Fa	0.97567	-0.2045	-0.075739	-0.022425
Fin	0.19145	0.97028	-0.14534	-0.027825
Variable	**Variables: Fl, Fw, and Fa**			
	PC 1	**PC 2**	**PC 3**	
Fl	0.10841	0.97801	0.17819	
Fw	0.0033266	-0.1796	0.98373	
Fa	0.9941	-0.10606	-0.022724	
Variable	**Variables: Fl, Fw, and Fin**			
	PC 1	**PC 2**	**PC 3**	
Fl	0.42494	0.90445	0.037466	
Fw	0.0098215	-0.045993	0.99889	
Fin	0.90517	-0.4241	-0.028427	

Sample B: PCA Loadings				
Variable	**Variables: Fl, Fw, Fa, and Fin**			
	PC 1	**PC 2**	**PC 3**	**PC 4**
Fl	0.019596	-0.43242	0.81632	-0.38243
Fw	0.023039	0.037477	0.43959	0.89712
Fin	0.056567	0.89985	0.37169	-0.22117
Fa	0.99794	-0.043381	-0.047247	-0.00066495
Variable	**Variables: Fl, Fw, and Fa**			
	PC 1	**PC 2**	**PC 3**	
Fl	-0.2488	0.88728	-0.38837	
Fw	0.13339	0.42854	0.89362	
Fa	0.95933	0.17053	-0.22497	
Variable	**Variables: Fl, Fw, and Fin**			
	PC 1	**PC 2**	**PC 3**	
Fl	0.019839	0.99098	-0.13256	
Fw	0.023041	0.13209	0.99097	
Fin	0.99954	-0.022714	-0.020212	

Table SI5 – Selected measurements of the human footprints from Cape South Coast (South Africa) ichnosites used for the analysis.
Data from Helm et al. (2018a,b, 2019a,b, 2020a,b)

Ichnosite	Footprint	Measurements		
		Footprint length (Fl)	Footprint width (Fw)	Fw/Fl x 100
Brenton 1 (Cape South Coast - Brenton-on-Sea)	01L	17	7	41.17
	03L	16	7.5	46.87
	06R	16.5	6.5	39.39
	06A	16,5	6,5	39.39
	07R	19.5	7,5	38.46
	08L	23	10	43.47
	09L	20	7	35.00
	10R	15	7	46.66
	11	16	6	37.50
	15L?	17.5	8.5	48.57
	16	17	8	47.05
	17L?	18	9	50.00
	18	18.5	9	48.64
	19	12	7	58.33
	20L?	22	10	45.45
	21L?	20	10	50.00
	22	17	7	41.17
	23	15	6	40.00
	24	20	10	5.00
	25L?	21.5	9.5	44.18
	28	18.5	5.5	13.51
	28A	18	4	22.22
	29	21	3	14.28
	30	16	1.5	9,37
	31L	19	7	36.84
	L03	12	5	41.66
	L05R	16	7	43.75
Garden Route National Park	C	24	11	45.83
	(D)	15	8	53.33
	F	9.5	5.5	57.89
	G	24	10	41.66
Goukamma Tracksite 1	Gouk1-R	21	11	52.38
	Gouk1-IIR	21	8.5	40.47
	Gouk1-IIIL	21	11.5	54.76
Goukamma Tracksite 2 (Nature Reserve)	A1	14	7	50.00
	A3	15	7	46.66
	A7	20	10	50.00
	A8	15	9	60.00
	A9	16	7	43.75
	A11	20	9.5	47.50
	A12	16	10	62.50
	A13	16	8	50.00
	A14	18	8	44.44
	B1	13	6	46.15
	B2	12	5.5	45.83
	B5	16	8	50.00
	B6	13	7	53.84
	C1	13	8	61.53
	C2	14	8	57.141
	C4	15	8	53.33